MCM-41 AS AN ADSORBENT, CATALYST AND/OR CATALYST SUPPORT

A THESIS
SUBMITTED TO
THE UNIVERSITY OF PUNE
FOR THE DEGREE OF
DOCTOR OF PHYLOSOPHY
IN CHEMISTRY

BY

KSHUDIRAM MANTRI, M.Sc.

CHEMICAL ENGINEERING DIVISION
NATIONAL CHEMICAL LABORATORY
PUNE – 411 008
INDIA

AUGUST, 2001

DEDICATED
TO
MY PARENTS
BROTHER AND SISTERS

CERTIFICATE

Certified that the work incorporated in the thesis **"MCM-41 As Adsorbent, Catalyst and / or Catalyst Support"** submitted by Mr. Kshudiram Mantri for the degree of ***Doctor of Philosophy***, was carried out by the candidate under my supervision in the Chemical Engineering Division, National Chemical Laboratory, Pune, INDIA. Such material as has been obtained from other sources has been duly acknowledged in the thesis.

(Dr. Vasant R. Choudhary)
Research Guide

ACKNOWLEDGEMENT

I take this opportunity to express my deepest sense of gratitude to my research supervisor, Dr. Vasant R. Choudhary, for his invaluable guidance, teaching, support and advice through out the course of this investigation. He has taught me to concise and corrects my approach to science from the formulation to the presentation of results. I am expressing my reverence towards him and my sincere regards for him forever.

My sincere thanks are due to Dr. S. G. Pataskar, Dr. S. D. Sansare for the helpful discussions, encouragement and co-operation. I wish to thank Dr. A. G. Gaikwad, Dr. A. S. Mamman, Dr. A. M. Rajput, Dr. (Mrs.) S. Mayadevi and Dr. V. H. Rane for helpful discussions, friendship and a cheerful company over these past years.

I appreciate and acknowledge the help and co-operation of my seniors, Dr. Mulla, Dr. Sivadinarayana, Dr. Uphade, Dr. Kinage and Dr. Devadas. The help and co-operation extended by Mr. V. L. Rajput, Mr. V. L. Chandekar and Mr. B. G. Pingale is also duly acknowledged.

Association with my colleagues Subho and Sumanda are greatly appreciated and I am indebted to them for their company, discussions and help throughout the research work. They have been a constant source of information and inspiration. Many thanks are also due to Nilesh, Joshi, Rajamani, Narkhede, Jayant, Sachin, Deepa, Kailash and Pankaj.

The invaluable help I received from Mr. Mandale for XPS, Mr. Sainkar for SEM (SIL), Dr. Ganpathy and Dr. Rajmohanan for NMR (NMR group), Mr. Bhujang for drawing/tracing of figures (PD), and staff of electrical section (CE) is also appreciated. To them my thanks are due no small amounts.

I am indebted to Dr. B. D. Kulkarni, Head, Chemical Engineering Division for allowing me to use the facilities in the division. I would like to thank all other scientific and nonscientific staff in the Chemical Engineering Division, NCL, for their help and cooperation given to me in completing my research work successfully.

I would like to thank my friends Raja, Babu, Chitta, Annyt, Karuna, Tapanda, Somnath, Bikash, Tapasda, Anilda, Priyada, Laha, Dinu, Aditya, Koushik, Bivas, Debdut, Ananda, Abhijeet, Kiran, Tushar, Mannada and Boudi, Manasda, Subarnada, Saptarshida, Gourda, Lahada, Majida, Hazra, Tarun, Anuradha, Mahuadi, Sumit, Samantabhai, Arindam, Smritilekha, Ghota, Prabal, Utpal, Dilip and all my friends in NCL who are not mentioned. I will be failing in my duties if I do not recall my friends outside NCL namely, Pradip, Partha, Amiya, Sankarda, Kakali, Subhas, Sukumar, Achintya, Sadhan, Sanatan as well as my high school friends and college friends. I owe special thanks to Ms. Smritirekha Jana for her support, inspiration, and encouragement from the beginning of my academic life.

It gives me great pleasure to thank my parents, brother, sisters and my brother-in-law, for their love, tremendous patience, trust and encouragement during many years of studies. They have been my constant source of strength and have brought a great deal of happiness to my life.

Finally, my thanks are due to the Council of Scientific & Industrial Research, New Delhi, for awarding me research fellowship and to Dr. P. Ratnasamy, Director, National Chemical Laboratory, Pune, for allowing me to carry out my research and extending all the possible infrastructure facilities.

(Kshudiram Mantri)

PUNE
July, 2001

LIST OF CONTENTS

SUMMARY AND CONCLUSIONS

SUMMARY AND CONCLUSIONS

MCM-41 is a member of a new family of silicate mesoporous material, designated as M41S, containing hexagonal arrays of uniform channels with 2 to 10 nm in diameter. It can be synthesized in its high silica form (Si-MCM-41) and also in its high alumina form (Al-MCM-41). Because of its high surface area ($\geq$ 1100 $m^2 g^{-1}$) and adsorption capacity, thermal/hydrothermal stability, and mesoporous channels, MCM-41 has high potential for practical use as an adsorbent both for small and bulky adsorbate molecules. The AlSi-MCM-41 has a capacity of cation exchange similar to that of zeolites and it can be modified by exchanging its cations with other cations. Because of the presence of tetrahedral Al, H-AlSi-MCM-41 has acid sites with high strength. Its acidity can be reduced or it can be made basic by exchanging its protons with alkali metal cations. Microporous zeolites can not be used for the acid or base catalyzed reactions involving large molecular size or bulky reactants and/or products. However, since H-AlSi-MCM-41 is mesoporous, its different cation exchanged forms can be used for the reaction involving bulky molecules, particularly in the synthesis of fine chemicals.

Presence of at least four types of different terminal Si-OH groups (which are poorly acidic or non acidic in nature) in the channels of MCM-41 has been detected earlier. In addition to the terminal Si-OH groups, the H^+ form of AlSi-MCM-41 contains acidic surface hydroxyl groups and the Na^+ form of AlSi-MCM-41 contains Na^+ cations in the channels. It is interesting to study the interaction of different aromatic substrates, which are used in the synthesis of fine chemicals, with the acidic hydroxyl groups or Na^+ cations and also with the terminal Si-OH groups of these mesoporous materials.

Pure siliceous MCM-41 (Si-MCM-41) mesoporous materials are electrically neutral, which limits their catalytic applications. In order to provide a specific catalytic activity to the chemically inert silicate framework, researchers have incorporated, in addition to Al, a variety of metals into the walls of nanostructures by either direct synthesis, ion exchange, impregnation or grafting. It is therefore also interesting to study the impregnation, grafting or immobilization of metal chloride on Si-MCM-41.

The present Ph.D. work was undertaken with the following objectives:

1. To measure the adsorption isotherms and study the thermodynamics of adsorption (viz. heat of adsorption, entropy change associated with the adsorption, etc.) for different aromatic hydrocarbons (viz. benzene, toluene, p-xylene and mesitylene) on Si-MCM-41.
2. To study the interaction of aromatic hydrocarbons (viz. benzene, toluene, p-xylene, mesitylene and naphthalene) with the terminal silanol groups, acidic hydroxyl groups and Na present in the channels of MCM-41 by carrying out TPD of aromatic hydrocarbons over Si-MCM-41, H-AlSi-MCM-41 and Na-AlSi-MCM-41 from 323 K to 673 K at different heating rates and adsorbate loadings by using gas chromatography technique.
3. To study the esterification of tert-butanol with acetic anhydride and dehydration of tert-butanol over Si-MCM-41 supported $InCl_3$, $GaCl_3$, $FeCl_3$ and $ZnCl_2$ catalysts.
4. To modify Si-MCM-41 by grafting of anhydrous $AlCl_3$ by a liquid phase reaction between anhydrous $AlCl_3$ and terminal Si-OH groups of Si-MCM-41 and study of kinetics of the grafting reaction, to evaluate the catalytic activity of the modified MCM-41 for the Friedel-Crafts type reaction and also to study

the influence of thermal treatment at different conditions on surface properties and incorporation of Al in the structure of MCM-41

The thesis has been divided into two parts, as follows.

PART-I: MESOPOROUS MCM-41 MATERIALS AS AN ADSORBENT

This part of the thesis is divided into three chapters.

1.1 GENERAL INTRODUCTION – LITERATURE SURVEY, OBJECTIVES AND SCOPE

This section presents the general background and also provides a summary of the available literature on mesoporous MCM-41 materials as adsorbent, along with the objectives and scope of the present work.

1.2 EXPERIMENTAL

This section deals with the following:

- Hydrothermal synthesis of Si-MCM-41and AlSi-MCM-41
- Techniques used for characterization of adsorbents/catalysts by XRD, TEM, SEM, EDAX, FTIR, ^{29}Si and ^{27}Al MAS NMR, XPS, N_2 adsorption at liquid N_2 temperature, and TPD of pyridine (for the measurement of acidity of MCM-41)
- Adsorption isotherms of aromatic hydrocarbons by "GC peak maxima method"
- Temperature programmed desorption (TPD) of aromatic hydrocarbons by "GC technique"

1.3 RESULTS AND DISCUSSION

This chapter of Part-I of the thesis has been divided into following four sections:

1.3.1 Adsorption of Aromatic Hydrocarbons on Highly Siliceous MCM-41.

Adsorption isotherms of benzene, toluene, p-xylene and mesitylene on high silica MCM-41 (Si-MCM-41) at different temperatures (348 – 498K) have been studied using gas chromatographic technique (GC peak maxima method). Freundlich adsorption model fits the adsorption data for the aromatic hydrocarbons at all the temperatures. The isosteric heats of adsorption of the aromatic hydrocarbons at different loading, obtained from the adsorption isotherms, is found to be in the following order: $Q_{a\ (benzene)} < Q_{a\ (toluene)} < Q_{a\ (p\text{-}xylene)} < Q_{a\ (mesitylene)}$. The heat of adsorption of all the aromatic hydrocarbons is decreased with increasing the adsorbate loading; the decrease for the benzene adsorption at intermediate adsorbate loading is found to be more pronounced, indicating induced surface heterogeneity due to the presence of adsorbed benzene. Entropy analysis of the adsorption indicated that the adsorbed aromatic hydrocarbons (except benzene at very low adsorbate loading) are neither completely mobile nor localized; only the benzene adsorbed at very low adsorbate loading ($\leq 1.04 \times 10^{16}$ molecules m^{-2}) is completely mobile or even supermobile. The mobility of the adsorbed toluene, p-xylene and mesitylene is decreased (or increasingly restricted), but that of the adsorbed benzene is passed first through a minimum and then through a maximum, with increasing the adsorbate loading.

1.3.2 Temperature Programmed Desorption of Benzene on Mesoporous Si-MCM-41, Na-AlSi-MCM-41 and H-AlSi-MCM-41.

Temperature programmed desorption (TPD) of benzene on Si-MCM-41, Na-Al Si-MCM-41 and H-AlSi-MCM-41 mesoporous materials from 323 K to 673 K at

different linear heating rates (5, 10, 20 and 25 K min^{-1}) and that on Si-MCM-41 at different adsorbate loading (0.45 – 10.7 μmol g^{1}) has been investigated. ^{1}H – ^{29}Si CP MAS NMR and IR of the Si-MCM-41 showed presence of a large number of terminal Si–OH groups. All the TPD spectra have multiple peaks (four for Si-MCM-41 and five for H (or Na)- AlSi-MCM-41), indicating presence of different types of benzene adsorption sites on these mesoporous materials. Heat of adsorption of benzene corresponding to the different TPD peaks, estimated from the TPD peak maximum temperatures measured at the different heating rates, was found to be in the following order: Si-MCM-41 < H-AlSi-MCM-41 < Na-AlSi-MCM-41. The TPD peak multiplicity for Si-MCM-41 is reduced with decreasing the adsorbate loading, indicating induced surface heterogeneity due to the adsorbate at its higher loading.

1.3.3 Temperature Programmed Desorption of Toluene, P-Xylene, Mesitylene and Naphthalene on Mesoporous High Silica MCM-41

Temperature programmed desorption of aromatic hydrocarbons (viz. toluene, p-xylene, mesitylene and naphthalene) on mesoporous high silica MCM-41 from 323 K to 673 K at different linear heating rates (5, 10, 15, 25 K min^{-1}) has been investigated. TPD of toluene at different adsorbate loading (0.5 to 16.3 μmol g^{-1}) has also been investigated. All the TPD curves have a single asymmetric peak. The heats of adsorption of aromatic hydrocarbons on the mesoporous material, estimated from the TPD peak maximum temperatures measured at different heating rates, was found to occur in the following order: toluene < p-xylene < mesitylene < naphthalene. This ΔH_a increases with the decrease in the ionization potential of the hydrocarbons. The adsorption results from weak interactions between the π-electrons of aromatic hydrocarbons and the terminal poorly acidic silanol (Si–OH) groups. In the case of

toluene TPD, the TPD peak maximum temperature increases with decreasing the adsorbate loading, indicating the presence of site energy distribution on the high silica MCM-41.

1.3.4 Temperature Programmed Desorption of Toluene, p-Xylene, Mesitylene and Naphthalene on Na-AlSi-MCM -41 and H-AlSi-MCM -41

Adsorption properties of the mesoporous H-AlSi-MCM-41 and Na-AlSi-MCM-41 materials for aromatic hydrocarbons have been investigated by studying the temperature programmed desorption of toluene, p-xylene, mesitylene and naphthalene over the mesoporous materials from 323 K to 673 K at different linear heating rates (5 - 25 K min^{-1}). The toluene TPD spectra show three distinct peaks for the H-AlSi-MCM-41 but a single asymmetric peak with humps for the Na-AlSi-MCM-41. The TPD spectra of all the other aromatic hydrocarbons for both the adsorbents show a single asymmetric peak with humps. The order of the heat of adsorption for the aromatic hydrocarbons, estimated from the temperature dependence of their peak (first one) maximum temperature was found as follows: Toluene < p-xylene < mesitylene < naphthalene. The heat of adsorption was found to decrease exponentially with increasing the ionization potential of the aromatic hydrocarbons. For the TPD of toluene, the heat of adsorption obtained from the three peaks was in the following order: 1^{st} < 2^{nd} < 3^{rd} peak. The heat of adsorption for each of the aromatic hydrocarbons was found to be higher for the Na-AlSi-MCM-41, indicating that the interaction of aromatic hydrocarbons with the Na^{+} cations are stronger than that with the protons in the mesoporous materials.

PART-II: MESOPOROUS MCM-41 AS CATALYST AND/OR CATALYST SUPPORT

This part of the thesis has been divided into three chapters:

2.1 GENERAL INTRODUCTION – LITERATURE SURVEY, OBJECTIVES AND SCOPES

This chapter presents general introduction and also summarizes the available literature on mesoporous MCM-41 materials as catalyst and/or catalyst support, along with the objectives and scope of the present work.

2.2 EXPERIMENTAL

This chapter deals with the following:

- Preparation of Si-MCM-41 supported $InCl_3$, $GaCl_3$, $FeCl_3$ and $ZnCl_2$ catalysts by incipient wetness technique
- Procedure for the esterification of tert-butanol by acetic anhydride over metal chloride supported catalysts
- Grafting of anhydrous $AlCl_3$ on Si-MCM-41
- Procedure for the Friedel-Crafts type benzylation and acylation reactions.

2.3 RESULTS AND DISCUSSION

Results and discussion chapter of the Part-II of the thesis has also been divided into following three sections:

2.3.1 Highly Selective Si-MCM-41 Supported $InCl_3$, $GaCl_3$, $FeCl_3$ and $ZnCl_2$ Catalysts for Low Temperature Esterification of tert-Butanol by Acetic Anhydride

Liquid phase reaction for the esterification of tert-butanol by acetic anhydride and dehydration of tert-butanol over Si-MCM-41 supported $InCl_3$, $GaCl_3$, $FeCl_3$ and

$ZnCl_2$ catalysts in a magnetically stirred glass reactor at 26°C have been thoroughly investigated. Si-MCM-41 supported $InCl_3$, $GaCl_3$, $FeCl_3$ and $ZnCl_2$ catalysts (metal chloride loading = 1.1 mmol g^{-1}) have very small activity for the dehydration of tert-butanol and hence show very high selectivity (>99%) for the esterification of tert-butanol by acetic anhydride, producing acetic acid as a by-product, at ≤ 50°C. The esterification activity of the supported metal chloride catalysts is in the following order: $InCl_3$ > $GaCl_3$ > $ZnCl_2$ > $FeCl_3$. The effect of $InCl_3$ loading (0.45 to 2.2 mmol g^{-1}) on Si-MCM-41 in the esterification has also been studied.

2.3.2 $AlCl_x$-Grafted Si-MCM-41 Prepared by Reacting Anhydrous $AlCl_3$ with Terminal Si-OH Groups: An Active Solid Catalyst for Benzylation and Acylation Reactions

A liquid phase reaction between anhydrous $AlCl_3$ and terminal Si-OH groups of mesoporous Si-MCM-41 in dry CCl_4 results in a $AlCl_x$ -grafted Si-MCM-41 (with Cl/Al ratio = 1.43, $Al_{(tetrahedral)}$ / $Al_{(octahedral)}$ = ratio = 0.84 and Al/Si ratio = 0.17). This catalyst shows high catalytic activity in Friedel-Crafts type benzylation (by benzyl chloride) and acylation (by benzoyl chloride) of benzene and toluene.

2.3.3 $AlCl_3$-Grafted Si-MCM-41: Influence of Thermal Treatment Conditions on Surface Properties and Incorporation of Al in The Structure of MCM-41

Grafting of $AlCl_3$ on Si-MCM-41 by the reaction of anhydrous $AlCl_3$ from its CCl_4 solution with terminal Si–OH groups of Si-MCM-41 under reflux at two different concentrations of $AlCl_3$ relative to Si-MCM-41 has been studied. The influence of thermal treatment conditions (viz., temperature and gas atmosphere, such as vacuum, static or flowing air and flowing N_2) on the bulk and surface properties of the $AlCl_3$-grafted Si-MCM-41 has also been investigated. The $AlCl_3$-grafted Si-

MCM-41 samples with or without thermal treatment were characterized by FTIR, ^{27}Al MAS NMR, XPS, and EDAX analysis and also for their surface area and strong acid sites (measured in terms of the pyridine chemisorbed at 673 K). The incorporation of tetrahedral Al in the MCM-41 structure with the creation of strong acid sites could be accomplished by thermally treating the $AlCl_3$-grafted Si-MCM-41, particularly in a flow of N_2 at 673 K.

PART–I

MESOPOROUS MCM-41 AS AN ADSORBENT

Chapter 1.1

GENERAL INTRODUCTION– LITERATURE SURVEY, OBJECTIVES AND SCOPE

Chapter – 1.1

GENERAL INTRODUCTION – LITERATURE SURVEY, OBJECTIVES AND SCOPE

1.1.1 GENERAL BACKGROUND

Crystalline porous solids are very important materials because of their wide applications in various adsorption/separation, purification and catalytic processes. According to IUPAC definition[1], based on pore width, three types of pore can be present in a porous solid: micropore (<2 nm), mesopore (2 - 50 nm) and macropore (>50 nm). The classification of porous materials is shown in Table 1.1.1.

Table 1.1.1 Classification of porous materials[2].

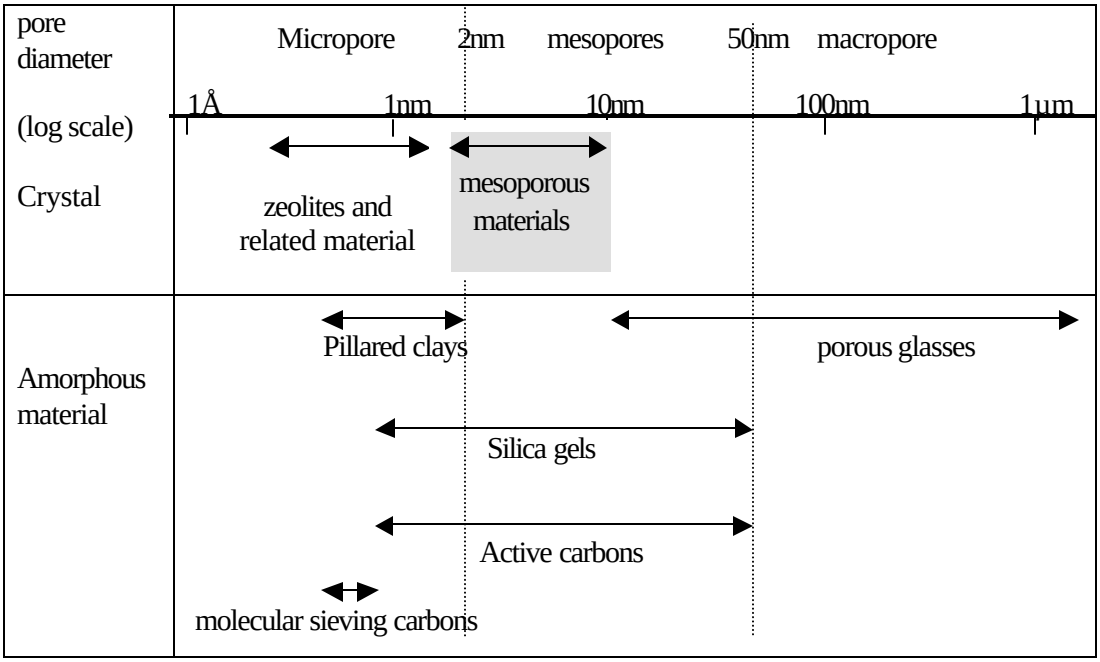

Well known microporous materials are zeolites[3] and zeolite-like materials, such as aluminophosphate molecular sieves[4] which are inorganic composites, having a crystalline three-dimensional framework with tetrahedral atoms (T atoms) like Al, Si,

P etc. bridged by oxygen atoms. These materials possess uniform channels or cavities circumscribed by rings of a definite number of T atoms. The architectural features of zeolites resulting with different acid sites and acid strengths, exchangeable cations, shape and size selective channels and pores has been well established by now. Most of the shape-selective reactions used in the chemical industries today involve catalysts containing zeolites having pore diameters between 0.5 and 0.6 nm. This size is sufficient to accommodate a broad spectrum of small molecules of technological interest. However, the usefulness of present day heterogeneous catalysts in processing high-molecular-weight hydrocarbons, which are of increasing importance, is limited by the pore size of the zeolite used and/or by the pore geometry of the metal support. The largest-pore zeolites commercially used (i.e., faujasites) have micropores with a free diameter of only 0.72 nm. Hence there has been an ever-growing interest in expanding the pore sizes of the zeotype materials from the micropore region to mesopore region. The requirement of larger pore materials having adsorption capacity of larger molecules at their catalytic sites has triggered major synthetic efforts in academic and industrial laboratories.

In order to preserve the remarkable adsorptive and catalytic properties of the zeolites, while expanding their use to process bulkier molecules, new synthesis routes have been undertaken to increase their pore diameters. This approach has led to synthesis of ultra large pore molecular sieves. A significant breakthrough in zeolite science occurred in 1982 when Wilson and co-workers[5] disclosed the synthesis of a novel crystalline, microporous aluminophosphate ($AlPO_4$) materials with pores formed by more than 12 tetrahedral atoms about 0.8 nm in diameter. Later, in 1988, Davis et. al.[6], reported the synthesis of VPI-5, an $AlPO_4$ molecular sieve with 18 tetrahedral atom rings that could sorb molecule about 1.3 nm in size. Since then,

microporous materials with pore openings containing 20 tetrahedral atoms have been synthesized. They include cloverite[7] (gallophosphate) and JDF-20 ($AlPO_4$)[8]. Recently, UTD-1, a unidirectional 14 membered ring zeolite was synthesized using cobalt organometallic complex as the template.[9] However, these materials suffer from limited thermal stability and negligible catalytic activity because of the electrical neutrality of the framework. Table 1.1.2 typically lists some zeolites and molecular sieves with variable pore sizes, mostly in the microporous range.

Table1.1.2 Examples of zeolites and molecular sieves[10]

Definition	Materials	Ring size	Pore diameter (Å)	Reference
Small pore	CaA	8	4.2	11
	SAPO-34	8	4.3	12
Medium pore	ZSM-5	10	5.3 x 5.6 5.1 x 5.5	13
	ZSM-48	10	5.3 x 5.6	14
Large pore	ZSM-12	12	5.5 x 5.9	15
	$AlPO_4$-5	12	7.3	16
	Faujasite	12	7.4	17
Ultralarge pore	Cloverite	20	6.0 x 13.2	7
	JDF-20	20	6.2 x 14.5	8
	VPI-5	18	12.1	6
	$AlPO_4$-8	14	7.9 x 8.7	18
	UTD-1	14	7.5 x 10	9

Researchers had taken great efforts to synthesize mesoporous materials such as silicas,[19] transitional aluminas[20] and pillard clays. In fact, in 1990, Yanagisawa and

co-workers,[21,22] described the preparation of mesoporous silicas with uniform pore size. However, the pores in these materials are generally irregularly spaced and broadly distributed in size. Thus, a gap has been bridged by the discovery of M41S family, which have opened up new possibilities for preparing catalysts with uniform pores in the mesoporous region that can be easily accessed by bulky molecules that are present in crude oils and fine chemical productions.

1.1.2 MESOPOROUS MCM-41

In 1992 researchers at Mobil Research and Development Corporation reported the synthesis of a new family of silicate/aluminosilicate mesoporous materials (M41S)[23-27], possesses a regular hexagonal array of uniform pore openings with a broad spectrum of pore diameters between 1.5 and 10 nm. M41S can be divided into three main sub-groups[23,26]: MCM-41 with a hexagonal array, MCM-48 has a cubic pore structure, and MCM-50, which has a lamellar structure. The main characteristics of MCM-41 materials are their high thermal stability, large surface area and narrow pore size distribution. Si-MCM-41 is structurally stable towards thermal treatment, hydrothermal treatment with steam at mild conditions, mechanical grinding and also towards acid treatment at mild condition.[28-34] However, the structural Al in AlSi-MCM-41 is unstable even to mild thermochemical treatment. Si-MCM-41 has high potential for practical use as an adsorbent or a mesoporous support for depositing active catalyst components, particularly useful in the synthesis of fine chemicals involving bulky molecules. The wide spectrum of pore diameter makes these materials readily accessible to large molecules, and has major significance in the processing of those. The understanding about the synthesis of these materials and the corresponding mechanism has opened up a new era of molecular engineering. The most outstanding feature of the preparation of these materials is the role of the

templating agents. The formation of mesoporous materials with a variety of crystallographically well-defined frameworks[35] has been made possible via a generalized "liquid-crystal templating" (LCT) mechanism.[36,37] The surfactants (act as templates) are large organic molecules (amines) having a long hydrophobic tail of variable length (e.g. alkyltrimethylammonium cations with formula $C_nH_{2n+1}(CH_3)_3N^+$, where n > 8) and a hydrophilic head.

1.1.2.1 Synthesis of Mesoporous MCM-41

Different synthesis strategies have been proposed and successfully used to prepare nanostructures with a unique pore size distribution. Similar to zeolite and molecular sieve synthesis, mesoporous molecular sieves can be synthesized hydrothermaly by mixing surfactants, silica, and/or silica-alumina source to form a gel while maintaining the mixture at a temperature between 70 and 150°C for a fixed period of time. It is interesting to note that mesoporous siliceous[38-40] MCM-41 as well as metallosilicate[41-43] MCM-41 can also be synthesized at room temperature. Chatterjee et al.[41] synthesized high Al containing (Si/Al = 1.5) MCM-41 mesoporous materials in a very short time (a minute) at room temperature. The compound showed similar characteristics to hydrothermally synthesized materials. They have also reported the characterization of V-MCM-41[42] and Ga-MCM-41[43] synthesized at room temperature. The product obtained after crystallization is filtered, washed with distilled water, dried at ambient temperature. To get mesoporous silicate / alumino-silicate network, surfactant molecules are removed by calcination or extraction by solvent. The structure and pore diameter of mesoporous materials can be altered by varying the surfactant/SiO_2 ratio.[27] It has been found that as the surfactant/silica molar ratio increased, the siliceous products obtained could be grouped into four categories[44]:

Surfactant/Silica	Typical phase
< 1.0	Hexagonal phase (MCM-41)
= 1.0 - 1.5	Cubic phases (MCM-48)
= 1.2 - 2.0	Thermally unstable materials
= 2.0	Cubic octamer $[(CTMA)SiO_{2.5}]_8$

The pore diameter (2 to 10 nm) of MCM-41 materials can be controlled by three different methods: (i) by varying the chain length of alkyl groups (8 to 22 C-atoms) of surfactants,[24,27] (ii) by adding auxiliary chemicals (viz. 1,3,5 trimethylbenzene) which dissolve in the hydrophobic region of the micelles, thus increasing their size, or (iii) by varying aging conditions[45] (viz. temperature and aging periods). The pore diameter of MCM-41 also depends on other factors such as temperature, pH and crystallization time.[10,46]

Since the first report of MCM-41 synthesis in alkaline medium appeared,[23-27] a number of patents and publications on the synthesis of MCM-41 have been reported.[47-51] Huo et al.[36,52] reported the synthesis of mesoporous silica under acidic conditions, while Tanev and Pinnavaia[53] proposed a neutral templating synthesis mechanism based on hydrogen bonding between primary amines and neutral inorganic species (Table1.1.3). Mesoporous materials obtained from neutral templating mechanism are named as 'hexagonal mesoporous silica' (HMS). Casci[54] and Antonelli and Ying[55] have reviewed the synthesis of mesoporous materials.

Pure siliceous MCM-41 (Si-MCM-41) mesoporous materials are electrically neutral, which limits their catalytic applications. In order to provide a specific catalytic activity to the chemically inert silicate framework, researchers have incorporated, in addition to Al, a variety of metals into the walls of nanostructures by either direct synthesis, ion exchange, impregnation or grafting. The modification of

mesoporous siliceous MCM-41 materials would be discussed in the second part of the thesis.

Table 1.1.3 Routes for synthesis of mesoporous materials

Surfactant	pH	Example	Phase	Reference
S^+I^-	10 - 13	Cetyltrimethyl ammonium ions + silicate species	Hexaggonal, cubic and lamella r	23
S^0I^0	< 7	$C_{12}H_{25}NH_2 + (C_2H_5O)_4Si$	Hexagonal	53
S^+XT^+	<2	Cetyltrimethyl ammonium ions + silicate species	Hexagonal	52

1.1.2.2 Characterization of MCM-41

Different techniques are used to characterize mesoporous materials. X-ray powder diffraction, N_2 adsorption/desorption isotherms and transmission electron microscopy (TEM) are the essential characterization techniques to identify the mesostructure of MCM-41 materials. Other techniques such as infrared (IR) spectroscopy, magic angle spinning nuclear magnetic resonance (MAS NMR), X-ray photoelectron spectroscopy (XPS), etc. have also been applied to obtain additional structural information on MCM-41 mesoporous materials. Detailed characterization (by XRD, N_2 adsorption, IR, Raman, thermal analysis, TEM, ^{29}Si, and ^{27}Al MAS NMR, and NH_3-TPD for acidity measurement) of MCM-41 have been reported by Davis and co-workers[56].

X-ray diffraction pattern of MCM-41 structures show a typical four-peak pattern with a very strong peak at a low angle (d_{100} reflection line) and three weaker peaks at a higher angle (110, 200, and 210 reflection lines).[23,57] Powder X-ray diffraction technique is used to identify the structure, phase purity, degree of

crystallinity, unit cell parameters and crystallite size. In the case of MCM-41 the wall thickness of hexagonal channels is usually calculated by subtraction of the inside pore diameters obtained by gas adsorption from the unit cell dimensions determined by XRD.

Sorption capacities for probe molecules such as n-hexane, water, benzene, nitrogen, argon, etc. yield information about the hydrophilicity/hydrophobicity[58,59], pore volume and pore size distribution of the molecular sieves. The BET volumetric gas adsorption technique using nitrogen, argon, etc. is a standard method for the determination of the surface areas and pore size distribution of finely divided porous samples. For MCM-41, three well-defined stages may be identified in a nitrogen adsorption-desorption isotherm at 77 K: (i) a slow increase in nitrogen uptake at low relative pressures, corresponding to monolayer-multilayer adsorption on the pore walls, (ii) a steep increase in N_2 adsorption at intermediate relative pressures (P/P_0 range between 0.2 to 0.4) indicate the capillary condensation in mesopores, and (iii) a plateau at high relative pressures associated with multilayer adsorption on the external surface of the crystals.[60] According to IUPAC,[61] N_2 adsorption-desorption isotherms of MCM-41 is of the type IV isotherm.

TEM is used to elucidate the image of mesostructured channels.[24,27,36,37] However, the quantitative analysis of pore sizes and thickness of the pore walls is very difficult and not possible without additional simulation because of the 'focus' problem. HRTEM can be used successfully to examine the microstructural feature of mesoporous molecular sieves.[62,63] This technique can also be used to detect the location of metal clusters and heavy cations in the framework.[63]

IR spectroscopy can be used to confirm acidic nature, presence of surface hydroxyl groups[64,65] and isomorphous substitution in mesoporous materials. The IR

spectrum in the range 200-1300 cm^{-1} is used to characterize and to differentiate framework structures of different molecular sieves.

Lippamaa et al.[66] reported the use of ^{29}Si MAS NMR spectra in determining the nature and chemical environment of the atoms. ^{29}Si and ^{27}Al MAS NMR spectra provide information on Si/Al ordering,[67] crystallographically equivalent or non-equivalent Si and Al ions in various sites,[68,69] framework silica to alumina ratio,[70] co-ordination of Si and Al,[71,72] spectral correlation with Si-O-T bond angles[73] and Si-O bond lengths.[74] Solid state MAS NMR spectroscopy of ^{27}Al can prove the presence of tetrahedrally and octahedrally co-ordinated Al in the MCM lattice.[67,68] The broad ^{29}Si NMR spectra of mesoporous materials show a close resemblance to that of amorphous silica.

1.1.2.3 Mechanism of Formation of Mesoporous MCM-41

Various synthesis mechanisms have been proposed in the literature to explain the formation of mesoporus materials. A few review articles are available on the mechanism of mesoporous MCM-41 formation.[10,75,76] A few of the proposed mechanism are described below.

1.1.2.3.1 Liquid Crystal Templating Mechanism

A "liquid crystal templating" (LCT) mechanism was proposed by the Mobil researchers. It is based on the similarity between liquid crystalline surfactant assemblies (i.e., lyotropic phase) and M41S.[23-27] Two mechanistic pathways were postulated for the synthesis of MCM-41 as the representative M41S material:

1) The aluminosilicate precursor species occupied the space between a pre-existing hexagonal lyotropic liquid crystal (LC) phase and deposited on the micellar rods of the LC phase.

2) The inorganic mediated, in some manner, the ordering of the surfactants into the hexagonal arrangement.

Initially three different mesophases in M41S family were reported, viz.; lamellar,[77] hexagonal,[27] and cubic,[44] in which the hexagonal mesophase MCM-41 possessed highly regular arrays of uniform-sized channels. Later additional phases such as SBA-1 (cubic phase with the space group, Pm3n),[36,52] SBA-2[78] (three dimensional hexagonal symmetry, P63/mmc) with super cages instead of unidimensional channels and MSU-n having highly disordered hexagonal like array of channels with diameters in the nanometer range[79] were reported

1.1.2.3.2 Silicate Rod Assembly

Davis et al.[37] reported that under the synthesis conditions reported by Mobil researchers, the formation of MCM-41 began with the deposition of two to three monolayers of silicate precursor onto isolated surfactant micellar rods. The silicate-encapsulated rods were randomly ordered, eventually packing into a hexagonal mesostructure. Heating and aging then completed the condensation of the silicates into the as-synthesized MCM-41 mesostructure.

1.1.2.3.3 Folded Sheet Mechanism

Yanagisawa et al.[21] and Inagaki et al.[80,81] have proposed a folded sheet mechanism for the synthesis of mesostructures derived from kanemite (layered silicate). They synthesized mesoporous silicate and aluminosilicate materials designated as FSM-16 (Folded Sheet Mesoporous Materials). The surfactant cations

intercalate into the bilayers of kanemite by ion-exchange process. MCM-41 and FSM-16 are similar but show slightly different properties in adsorption[82] and surface chemistry[83].

1.1.2.3.4 Mechanism of Transformation from Lamellar to Hexagonal Phase

The transformation from lamellar to hexagonal phase has been proposed by Stucky and co-workers.[52,84,85] They have proposed that in a surfactant/silicate aqueous mixture with relatively low pH, low degree of polymerization of silica, and low temperatures, small silica oligomers (3 - 8 silicon atoms) interact with surfactant cations by coulombic interactions at the interfaces forming multidentate binding between them. These subsequently polymerize to form larger ligands, enhancing the binding between the surfactant and silicate species. These surfactant silicate multidentate ligands lead to a lamellar biphase governed by the optimal surfactant average head group area. During polymerization of silicate species, the average head group area of surfactant assembly increases due to the decrease in charge density of larger silicate layers and ultimately results in the hexagonal mesophase precipitation.

1.1.2.4 Adsorption Properties of MCM-41

Since the mesoporous materials are good adsorbents because of their narrow pore size distribution and high surface area, a number of investigations have focused on adsorption-desorption behavior of gases and vapors on those mesoporous materials. Ever since the first report of MCM-41, a number of studies on the synthesis and adsorptions studies on this mesoporous material have been reported. Molecular sieves have the ability to adsorb probe molecules of different sizes. Sorption capacities for probe molecules such as n-hexane, water, benzene, nitrogen, argon, etc. yield information about the hydrophilicity/hydrophobicity, pore volume

and pore size distribution of MCM-41. The important adsorptions studied on different MCM-41 materials are summarized in Table1.1.4. The modification of Si-MCM-41 and their catalytic properties would be described in the second part of the thesis.

Table 1.1.4 Summary of important studies reported for the adsorption on MCM-41

No.	Adsorbent	Adsorbate(s) and adsorption conditions	Information obtained	Ref
1.	Si-MCM-41 and AlSi-MCM-41	Benzene at 298 K, P = 0 to 60 torr	Adsorption isotherm	27
2.	MCM-41	CO_2 at 195, H_2O vapor at 303 K, SO_2 at 254 and 273 K	Adsorption isotherm, isosteric heat of adsorption, surface heterogeneity and adsorbent -adsorbate interaction	86
3.	AlSi-MCM-41	Cyclopentane at 243 to 333 K	Determined pore size, adsorption isotherms, isosters, isosteric enthalpy	87
4.	Si- and AlSi-MCM-41	N_2 at 70.6, 77.4 and 82 K	Adsorption-desorption isotherm	88
5.	MCM-41 derived from kanemite	N_2 at 77 K, H_2O and cyclohexane at 298 K	Adsorption-desorption isotherm	28
6.	Si- and AlSi-MCM-41	N_2 and O_2	Adsorption isotherm	89
7.	Si- and AlSi-MCM-41	Three adsorbed fluids; CH_4, N_2 and propane	Adsorption isotherm	90
8.	MCM-41	N_2 at 77 K and cyclopentane at 273, 293, 313 and 333 K	Adsorption isotherm and adsorption capacity	91
9.	Ga-MCM-41 (Si/Ga = 12, 19, 28, 50, 97)	N_2 at 77 K	Adsorption isotherm, BET surface area, pore size and avg. pore volume	92
10.	MCM-41 and MCM-48	N_2 at 77 K	Adsorption isotherm, BET surface area, pore size and avg. pore volume	93

11.	Si- and AlSi-MCM-41	Methanol, ethanol, propane-1-ol, butane-1-ol and water vapor	Adsorption isotherm and isosters	58
12.	TiSi-MCM-41	N_2 at 77 K	Adsorption isotherm	94
13.	AlSi-MCM-41	Ar, N_2, O_2 at 77 K	Adsorption isotherms	95
14.	MCM-41	N_2 at 77 K	Adsorption isotherms	96
15.	Si-MCM-41, MgO and Cr_2O_3 modified MCM-41 (Si/Al = 15)	CH_4 at 298 K and upto 6.9 Mpa	Adsorptive storage of CH_4 (0.06 g/g)	97
16.	Si-MCM-41	N_2 at 77 K	Mechanical stability measured by N_2 adsorption, adsorption isotherm	98
17.	Si-MCM-41	N_2 at 77 K	Adsorption isotherm	99
18.	MCM-41 **(Review)**	N_2 at 77 K	BET surface area, pore diameter, pore volume and adsorption isotherm	100
19.	Si-, Na^+, H^+-MCM-41 (Si/Al = 34, 71)	N_2 at 77 K	Adsorption/desorption isotherm	28
20.	Si-MCM-41, VMCM-41	N_2 and Ar at 77 K	Adsorption isotherm	101
21.	Si-MCM-41	N_2 at 77 K	Adsorption isotherm, BET surface area, pore diameter and adsorption energy distribution	102
22.	AlSi-MCM-41	N_2 at 77 K and cationic surfactant from aq. solution	Adsorption of a cationic surfactant as a function of pore size and Al content; and N_2 adsorption isotherm	103
23.	Si-MCM-41, $AlPO_4$ –5	Alcohols from water solution	Comparative study of alcohols adsorption from H_2O	104
24.	Large pore Si-MCM-41	N_2 at 77 K	Adsorption isotherm	105
25.	Si-MCM-41	N_2 at 77 K and CCl_4 at 273 to 323 K	Adsorption isotherm	106
26.	MCM-41	Pyridine TPD	Acidity and active sites for adsorption pyridine	107

27.	MCM-41	H_2 adsorption at temperatures ranging from 20 to 77 K	Adsorption isotherm and isosteric heats of adsorption	108
28.	AlSi-MCM-41	N_2 at 77 K and TPD of NH_3 with in situ FTIR	N_2 adsorption isotherm and acidity	109
29.	AlSi-MCM-41	Ar, N_2, O_2, C_2H_4 and CO_2	Adsorption isotherm and capillary critical point	110
30.	Room temperature synthesized Si-MCM-41	N_2 and Ar at 77 K	Adsorption isotherm	111
31.	Al-, Ga-, Fe-MCM-41	NH_3 loaded samples are characterized by FTIR	Acidity	112
32.	AlSi-MCM-41	N_2 adsorption at 77 K	Adsorption isotherm, BET surface area, pore diameter, pore volume	113
33.	Ti-MCM-41 and Ti-HMS **(Review)**	N_2 at 77 K	Adsorption isotherm, BET surface area, pore size and avg. pore volume	114
34.	Si-MCM-41 and AlSi-MCM-41	N_2 at 77 K, H_2O, toluene at 303, 333, 353 K and alcohols (methanol & butanol) at 333 K	Influence of Al content on adsorptive properties and adsorption isotherms	115
35.	Ti-grfted Si-MCM-41	N_2 at 77 K	Adsorption isotherm	116
36.	Si-MCM-41, Al-Si-MCM-41, TMS modified MCM-41	H_2O, benzene, N_2	Adsorption isotherm	117
37.	MCM-41 samples of different pore diameters	N_2 at 77 K, benzene and ethanol at various temperatures	Adsorption and effect of temperature on the capillary condensation	118
38.	Si-MCM-41 and TMS-MCM-41	N_2, H_2O, NH_3, Pyridine, n-hexane and cyclohexane	Adsorption isotherm, BET surface area and acidity	119

39.	MCM-41 of six different pore diameters	Ar at 77.4 and 87.4 K, N_2 and O_2 at 77.4 K and CO_2 at 194.6 K	Adsorption isotherm	120
40.	MCM-41	Benzene, carbon tetrachloride and n-hexane	Adsorption isotherm and adsorption capacity	121
41.	MCM-41	H_2O	Adsorption by gravimetric technique	122
42.	MCM-41 of different pore diameters	N_2 at 77.4 K	Adsorption isotherm	123
43.	Si-MCM-41, AlSi-MCM-41, NbMCM-41 and Ni/MCM-41	N_2 at 77 K	Adsorption-desorption isotherm	124
44.	MCM-41	Acetonitrile adsorbed at 303 K	Adsorption isotherm and adsorption capacity	125
45.	Mo-MCM-41	N_2 at 77 K	Adsorption isotherm	126
46.	Si-MCM-41 modified by disilagen agents	Competitive H_2O/toluene adsorption	Sorption capacity and hydrophobicity	127
47.	Si-MCM-41 prepared in presence of octyltrimethylammonium bromide	N_2 at 77 K in a wide relative pressure from 10-6 to 1	Adsorption isotherm	128
48.	Si-MCM-41, AlSi-MCM-41 and ZrSi-MCM-41	[60] fullerene from toluene	Differences in the amount adsorbed between three samples	129
49.	MCM-41	N_2 and Ar adsorption at low temperature	Adsorption isotherms	130
50.	Al-Si-MCM-41	N_2 adsorption and NH_3 TPD	N_2 adsorption isotherm and acid strength by NH_3 TPD	131
51.	Rh-MCM-41	N_2 at 77 K	N_2 adsorption-desorption isotherm	132

52.	MCM-41 with different pore radius	Ar, N_2, O_2, C_2H_4 and CO_2	The effect of temperature on adsorption isotherms	133
53.	MCM-41	Ar, N_2, O_2, CO_2, SO_2, lower alcohols and water vapor	Adsorption isotherm and adsorption capacity.	134
54.	MCM-41	Benzene	Adsorption isotherm	135
55.	Pheny-modified MCM-41	N_2, water vapor and benzene	Adsorption isotherm and hydrophobicity & hydrophilicity	136
56.	Ti-MCM-41	N_2	N_2 adsorption-desorption isotherm	137
57.	MCM-41 and MCM-48	N_2 at 77 K	N_2 adsorption-desorption isotherm	138
58.	AlSi-MCM-41	H_2O, CO and NH_3	Lewis and Bronsted acid sites	139
59.	MCM-41	N_2 at 77 K	N_2 adsorption isotherm and Capillary coexistence and criticality in mesopores	140
60.	Si-MCM-41	N_2 adsorption at 77 K	Pore size uniformity and distributions	141
61.	Porous adsorbents including MCM-41	Natural gas storage at 500 psig and ambient temperature	Adsorption capacity	142
62.	FeSi-MCM-41 and LaSi-MCM-41	N_2 and benzene	Adsorption isotherm	143
63.	Ga-MCM-41	TPD of NH_3	Acid strength	144
64.	MCM-41 of different pore diameter	N_2 adsorption at 77 K and Ar at 77 and 87 K	Adsorption isotherm	145
65.	Si-MCM-41	N_2 adsorption at 77 K	Adsorption isotherm	146

66.	Si-MCM-41	Carbon tetrachloride at the temperatures between 273 to 323 K	Adsorption capacity at different temperatures and adsorption isotherms	147
67.	Si-MCM-41	N_2 at 77K over a wide range of relative pressure	Adsorption isotherm and surface heterogeneity	148
68.	Sn-MCM-41	N_2 adsorption at 77 K	Adsorption isotherm	149
69.	MFI zeolites and MCM-41	Adsorption of n-hexane, trichloroeth-ylene, tetrachloro-ethylene, CO_2 and nitrogen oxides at room temperature	MCM-41 showed largest adsorption capacity for hydrocarbons	150
70.	Rh-MCM-41	N_2 adsorption at 77 K	Adsorption isotherm	151
71.	AlPO4-5 and MCM-41	Selective adsorption of CO_2-CH_4 mixture	Materials are selective for CO_2 under all conditions studied	152
72.	Cu- and Zn-MCM-41	N_2 and CO adsorption and TPR	N_2 adsorption isotherm, reducibility of Cu and confirmation of position of Zn^{2+} by CO adsorption	153
73.	Sulfated-Al-MCM-41	N_2 adsorption at 77 K and TPD of NH_3	N_2 adsorption isotherm and Acidity by NH_3 TPD	154
74.	Ti-MCM-41	Pb^{2+} ions adsorption from aqueous solution	Removal of Pb^{2+} ions from aq. solution and adsorption of Pb^{2+} ions was fitted to a Freundlich isotherm	155
75.	Al-MCM-41	NH_3 TPD	Acidity and active sites of Al-MCM-41	156
76.	Activated carbon, MCM-41 and zeolite Y	Benzene and EtOH at 0.15 and 30°C	Adsorption isotherm of benzene and EtOH	157
77.	Microporous and mesoporous materials	N_2, CO	Review on the adsorption of CO and N_2 on microporous and mesoporous materials at different conditions	158
78.	Uncalcined MCM-41	Adsorption of 3-chlorophenol from aq. solution	Adsorption isotherm	159

79.	Phys. coated MCM-41 and Chem. modified MCM-41	N_2 adsorption at 77 K over wide pressure range	Adsorption isotherm	160
80.	AlSi-MCM-41 of different Si/Al ratio	Pyridine adsorption	Adsorption isotherm and Surface acidity	161
81.	MCM-41	Methylaluminoxane	Adsorptive separation	162
82.	AlSi-MCM-41	Ammonia adsorption	Acidity by NH_3 TPD	163
83.	MCM-41	N_2 adsorption	Analysis of isotherm reversibility	164
84.	Activated carbon or Y zeolites having adsorbent coatings e.g., ZSM-5, MCM-41 or SAPO	Adsorption of alcohols	To lower the alcohol content of alcoholic beverages	165
85.	Si-MCM-41 and Cr-MCM-41	N_2 at 77 K	Adsorption isotherm	166
86.	Si-MCM-41	N_2 at 77 K	Adsorption isotherm, BET surface area, pore volume and pore diameter	167
87.	AlSi-MCM-41 and H-AlSi-MCM-41	NH_3 adsorption, TPD of primary, secondary and tertiary amines	Concentration of surface acid sites	168
88.	Mo catalysts over AlMCM-41/γ-Al2O3 extruded supports	N_2 at 77 K	Adsorption isotherm	169
89.	Silylated MCM-41	N_2 at 77 K	Adsorption isotherm, pore vol. and avg. pore diameter	170
90.	MCM-41	N_2 at 77 K	Adsorption isotherm, determination of pore size and pore wall structure	171
91.	MCM-41	N_2 at 77 K	Determination of lamellar phase in MCM-41	172

92.	Organically modified Ti-MCM-41	N_2 and H_2O	Adsorption isotherm and hydrophobicity	173
93.	AlSi-MCM-41	Adsorption of CTAB surfactant from aq. solution	Adsorption isotherm, adsorption capacity and adsorption mechanism	174
94.	Al-, Fe- and Ga-Si-MCM-41	CH_4 adsorption at various pressure	IR study on methane adsorption sites	175
95.	Si- and AlSi-MCM-41	N_2 at 77K	Adsorption isotherm, avg. pore size and pore volume	176
96.	Post synthesized AlSi-MCM-41	NH_3 TPD and N_2 adsorption	N_2 Adsorption isotherm and Acidity	177
97.	Silica and Si-MCM-41	N_2 at 77 K and Ar at 87 K	Adsorption isotherm	178
98.	NiAl-MCM-41	N_2, D_2O, CO and ethylene	Adsorption isotherm and ESR study	179
99.	Si-MCM-41	N_2 at 77 K, 1-butanol adsorption from n-heptane at 298 K and [60] fullerene from toluene solutions	Adsorption isotherm, adsorption capacity, enthalpy of fullerene adsorption	180
100.	AlSi-MCM-41	N_2 at 77 K	Adsorption isotherm	181
101.	MCM-41	N_2 at 77 K	Determination of lamellar phase in MCM-41	182
102.	Si- and AlSi-MCM-41	N_2 adsorption and NH_3 TPD	Adsorption isotherm and acidity	183
103.	Si-MCM-41	N_2 at 77 K and water vapor at 298 K	Adsorption-desorption isotherm and stability	184
104.	AlSi-MCM-41	N_2 at 77 K	Adsorption isotherms	185
105.	NaY and AlSi-MCM-41 (Si/Al = 2.6/1)	Lindane and toluene adsorption	Adsorption capacity and competitive adsorption	186

106.	Si-MCM-41	Butane and butanone adsorption at 30°C with a high partial pressure (27.2 torr)	Removal/recovery of butane and butanone vapor by pressure swing adsorption	187
107.	CeMCM-41	N_2 at 77 K	Adsorption isotherm	188
108.	Room temperature synthesized Ga-MCM-41	N_2 adsorption	Adsorption isotherm, pore diameter, pore volume, etc.	189
109.	AlSi-MCM-41 (Si/Al = 37)	Xe at different temperatures (140 340 K)	^{129}Xe NMR of adsorbed Xe on MCM-41 and adsorption isotherm	190
110.	Si-MCM-41	Adsorption hysteresis of N_2, O_2 and Ar at 77 K	Adsorption isotherm	191
111.	Ti-MCM-41 of different Si/Ti ratios	N_2 at 77 K	Adsorption-desorption isotherm	192
112.	Si-MCM-41	N_2 at 77 K and water vapor at 298 K	Adsorption isotherm	193
113.	Post synthesized AlSi-MCM-41	N_2 at 77 K	Adsorption isotherm, pore diameter, pore volume and BET surface area	194
114.	Ti grafted M41S type hosts	N_2 at 77 K and methyl iso-butyl ketone	Adsorption isotherm and adsorption capacity	195
115.	LaMCM-41	N_2 at 77 K and thermodesorption of n-butanol	Adsorption-desorption isotherm	196
116.	AlSi-MCM-41	N_2 at 77 K and NH_3 at 353 K	Adsorption isotherm and surface acidity	197
117.	Si-MCM-41	Kr at 80 to 130 K	Adsorption isotherm, isosteric heat of adsorption and desorption, etc.	198
118.	MCM-41-supported dimolybdenum complexes	N_2 at 77 K	Adsorption isotherm, BET surface area, pore diameter, etc	199

119.	AlSi-MCM-41	N_2 at 77 K and Xe, coadsorption of benzene and cyclohexane	Roughness of internal surface	200
120.	MCM-41 and MCM-48	N_2, O_2 and Ar	Adsorption isotherm	201
121.	Si-MCM-41, SiO_2	Ar at the temperature between 77 and 99 K	Adsorption isotherm and isosteres	202
122.	Rare earth metal complex grafted-Si-MCM-41	N_2 at 77.4 K	Adsorption-desorption isotherm	203
123.	AlSi-MCM-41	N_2 at 77 K	Adsorption-desorption isotherm	204
124.	CoMo/AlSi-MCM-41	N_2 at 77 K and NH_3 TPD	N_2 adsorption isotherm and acidity by NH_3 TPD	205
125.	AlSi-MCM-41	N_2 and Ar at 77 K	Adsorption-desorption isotherm	206
126.	Cu-, Zn- and Al-MCM-41	N_2 and CO adsorption and TPR study	N_2 adsorption isotherm and position of Cu^+ and Zn^{2+} in the MCM-41 by TPR	207
127.	Ag/MCM-41, Ag/SiO_2 and $Ag/\gamma\text{-}Al_2O_3$	Olefin/paraffin (ethane/ethylene or propane/propylene) adsorption /separation	Adsorption/separation of olefin from olefin/paraffin mixture	208
128.	Si-MCM-41	Low pressure N_2 adsorption isotherm	Chemical modification of silica, presence of surface heterogeneity	209
129.	MCM-41 **(Review)**	N_2 at 77 K and Ar at 87 K	Adsorption isotherm and adsorption characterization	210
130.	La-, Ce-MCM-41	N_2 at 77 K and n-butylamine adsorption	Adsorption isotherm, total acidity, low pressure isotherm, adsorption energy distribution	211
131.	Mo-MCM-41	N_2 at 77 K	Adsorption-desorption isotherm	212
132.	Si-, AlSi-MCM-41	Thermodesorption of water at temperature between 163 and 473 K	Thermodesorption	213

133.	Cobalt complex immobilized MCM-41	N_2 and O_2	Adsorption isotherm	214
134.	Si-MCM-41	N_2 at 77 K	Surface area analysis, pore volume, avg. pore size, adsorption isotherm	215
135.	Nb-, Ta-MCM-41 and silicalite	N_2 at 77 K	Adsorption isotherm and surface area analysis	216
136.	MCM-41	Benzene, methanol and pyridine adsorption	Acidity, physisorption of benzene and chemisorption of MeOH concluded from in situ adsorption measurement by IR	217
137.	Phenyl-modified MCM-41	n-butyl and tert-butyl alcohol, N_2, H_2O and benzene	Comparison of butanol sorption with N_2, H_2O, benzene and adsorption isotherm	218
138.	Si-,HAl-,Al-, Fe-, La- MCM-41	NH_3 adsorption and NH_3 TPD	Acidity	219
139.	AlSBA, AlSi-MCM-41	N_2 at 77 K and NH_3 chemisorption	Acidity by NH_3 TPD and N_2 adsorption isotherm	220
140.	Si-MCM-41	Low temperature N_2 adsorption, H_2O vapor adsorption	Surface properties and adsorption isotherm	221
141.	Zr-MCM-41 (Si/Zr = 96, 55, 39, 23)	N_2 at 77 K	Adsorption isotherm, BET surface area, avg. pore diameter, pore size distribution	222
142.	Chemically modified MCM-41	N_2,VOCs (n-hexane, benzene, acetone and methanol) and H_2O vapor	Surface properties, pore structure and avg., pore diameter	223
143.	Microporous and mesoporous materials	CO, CO_2, C_4H_4NH, N_2, H_2O, NH_3 adsorption	IR, UV-visible analysis and spectra of molecules (CO, CO_2, C_4H_4NH, N_2, H_2O, NH_3) adsorbed on catalysts containing acid, base and redox centers	224
144.	$ZrCl_4$ grafted MCM-41	N_2 at 77 K	Adsorption-desorption isotherm	225
145.	MCM-41	N_2 and benzene	Adsorption isotherm	226

146.	Ink-Bottle-Like MCM-41	N_2 at 77 K, benzene at 298, 310, 320 and 330 K	Adsorption isotherm of N_2 and benzene, adsorption kinetics of benzene at different temperatures	227
147.	SiMCM-41, NaMCM-41 and CsMCM-41	N_2 at 77 K	Adsorption/desorption isotherm	34
148.	Si-MCM-41, AlSi-MCM-41, Ti-MCM-41, TMS-MCM-41	Volumetric adsorption of hexane, benzene, acetone, and methanol and gravimetric adsorption of water vapor at 24 °C	Adsorption isotherm	228

1.1.3 OBJECTIVES AND SCOPE OF THE PRESENT STUDIES

Because of its high surface area and pore volume, MCM-41 has a high adsorption capacity. Its mesopore size distribution is also narrow. All these characteristics make MCM-41 as an ideal adsorbent and, therefore, it is of great scientific and practical interest to explore its adsorption properties for different adsorbates.

The literature survey (Table 1.1.4) indicated that no detailed investigation on the adsorption and thermodynamics of adsorption of aromatic hydrocarbons on the different forms of MCM-41, particularly above the room temperature, has been reported earlier.

The present Ph.D. work for this part of the thesis was undertaken with the following objectives:

5. To measure the adsorption isotherms and study the thermodynamics of adsorption (viz. heat of adsorption, entropy change associated with the

adsorption, etc.) for different aromatic hydrocarbons (viz. benzene, toluene, p-xylene and mesitylene) on Si-MCM-41 (348 – 498 K).

6. To study the interaction of aromatic hydrocarbons (viz. benzene, toluene, p-xylene, mesitylene and naphthalene) with the terminal silanol groups, acidic hydroxyl groups and Na present in the channels of MCM-41 by carrying out temperature programmed desorption (TPD) of aromatic hydrocarbons over Si-MCM-41, H-AlSi-MCM-41 and Na-AlSi-MCM-41 from 323 K to 673 K at different heating rates and adsorbate loading by using gas chromatography technique.

1.1.4 REFERENCES

1. Sing, K. S. W.; Everett, D. H.; Haul, R. H. W.; Moscou, L.; Pierotti, R. A.; Rouquerol, J.; Siemieniwska, T., *Pure Appl. Chem.*, **57** (1985) 603
2. Inagaki, S.; Ogata, S.; Goto, Y.; Fukushima, Y., *Stud. Surf. Sci. Catal.*, **117** (1998) 65.
3. Breck, D. W., *"Zeolites Molecularsieves"* Wiley, New York (1974)
4. Szostak, R., *"Molecular Sieves: Principles of Synthesis and Identification"* Van-Nostrand Reinfold, New York (1989).
5. Wilson, S. T.; Lok, B. M.; Flanigen, E. M.; *U.S. Pat*, **US 4,310,440** (1982); Wilson, S.T.; Lok, B. M., Messina, C. A.; Cannon, T. R.; Flanigen, E. M., *J. Am. Chem. Soc.*, **104** (1982) 1146.
6. Davis, M. E.; Saldarriaga, C.; Montes, C.; Graces, J. M.; Crowder, J. A., *Nature*, **331** (1988) 698
7. Estermann, M.; McCusker, L. B.; Baerlocher, C.; Merrouche, A.; Kessler, H., *Nature*, **352** (1991) 320
8. Jones, R. H.; Thomas, J. M.; Chen, J.; Xu, R.; Huo, Q.; Li, S.; Ma, Z.; Chippindale, A. M., *J. Solid State Chem.*, **102** (193) 204.
9. Freyhardt, C. C.; Tsapatsis, M.; Lobo, R. F.; Balkus Jr., K. J.; Davis, M. E., *Nature*, **381** (1995) 369.
10. Zhao, S. X.; (Max) Lu, G. Q.; Millar, G. J., *Ind. Eng. Chem. Res.*, **35** (1996) 2075
11. Meier, W. E.; Olson, D. H., *"Atlas of Zeolite Structure Types"*; Butterworth-Heinemann, London, (1987).
12. Lok, B. M.; Messina, C. A.; Lyle, Patton, R.; Gajec, R. T.; Cannon, T. R.; Wilson, S. T.; Flanigen, E. M, *J. Am. Chem. Soc.*, **106** (1984) 6092.
13. Van Koningsveid, H.; Jansen, J. C.; Van Bakkum, H., *Zeolite*, **11** (1990) 235.
14. Schlenker, J. L; Rohrbaugh, W. J.; Chu, P.; Valyocsik, E. W.; Kokotalio, G. T., *Zeolite*, **5** (1985) 355.
15. Fyte, C. A.; Gies, H.; Kokotalio, G. T.; Marler, B.; Cox, D. E.; *J. Phys. Chem.*, **94** (1990) 3718.
16. Bialek, R.; Meier, W. M.; Davis, M. E., *Zeolite*, **11** (1991) 438.
17. Olson, D. H., *J. Phys. Chem.*, **74** (1970) 2758.
18. Dessau, R. M.; Schlenkar, J. L.; Higgins, J. B., *Zeolite*, **10** (1990) 522.

19. Iler, R. K., *"The Chemistry of silica"*, J. Wiley and Sons Inc., 1979.
20. Wefers, K.; Misra, C., *"Oxides and Hydroxides of Alumina"*; Alcoa Technical Paper No. 19, Revised, Alcoa Laboratories, 1987.
21. Yanagisawa, T.; Schimizu, T.; Kuroda, K21.; Kato, C.; *Bull. Chem. Soc. Japan.*, (1990) 988.
22. Pinnavia, T. J., *Science*, **220** (1983) 365
23. Kresge, C. T., Leonowicz, M. E.; Roth, W. J.; Vartuli, J. C.; Beck, J. S., *Nature*, **359** (1992) 710.
24. Kresge, C. T., Leonowicz, M. E.; Roth, W. J.; Vartuli, J. C., *U. S. Patent*, **US 5,098,684** (1992).
25. Beck, J. S.; Chu, C. T.; Johnson, I. D.; Kresge, C. T.; Leonowicz, M. E.; Roth, W. J.; Vartuli, J. C., U. S. Patent, 5,145,816 (1992).
26. Beck, J. S.; Calabro, D. C.; McCullen, S. B.; Pelrine, B. P.; Schmitt, J. D.; Vertuli, J. C., *U. S. Patent*, **US 5,145,816** (1992).
27. Beck, J. S.; Vertuli, J. C.; Roth, W. J.; Leonowicz, M. E.; Kresge, C. T.; Schmitt, K. D.; Chu, C. T-W.; Olson, D. H.; Sheppard, E. W.; McCullen, S. B.; Higgins, J. B.; Schlenker, J. L., *J. Am. Chem. Soc*., **114** (1992) 10834.
28. Luan, Z.; He, H.; Zhou, W.; Cheng, G-F.; Klinowski, J., *J. Chem. Soc., Faraday Trans*., **91** (1995) 2955.
29. Chen, C-Y.; Xiao, Si-Q.; Davis, M. E., *Microporous Mater.*, **4** (1995) 1
30. Choudhary, V. R.; Sansare, S. D., *Proc. Indian Acad. Sci., Chem. Sci.*, **109** (1997) 229.
31. On, D. T.; Zaidi, S. M. J.; Kaliaguine, S., *Microporous and Mesoporous Mater*., **22** (1998) 211.
32. Landau, M. V.; Varkey, S. P.; Herkowitz, M.; Regev, O.; Pevzner, S.; Sen, T.; Luz, Z., *Microporous Mesoporous Mater*., **33** (1999) 149.
33. Lin, W.; Cai, Q.; Pang, W.; Yue, Y.; Zou, B., *Microporous Mesoporous Mater*., **33** (1999) 187.
34. Perez, C. N.; Moreno, E.; Henriques, C. A.; Valange, S.; Gabelica, Z.; Montero, J. L. F., *Microporous Mesoporous Mater*., **41** (2000) 137.
35. Huo, Q.; Margolese, D. I.; Stucky, G. D., *Chem. Mater*., **8** (1996) 1147.
36. Huo, Q.; Margolese, D. I.; Ciesla, U.; Feng, P.; Gier, T. E.; Sieger, P.; Leon, R.; Petroff, P. M.; Schuth, F.; Stucky, G. D., *Nature*, **368** (1994) 317.

37. Chen, C.-Y.; Brukett, S. L.; Li, H. -X. Davis, M. E., *Microporous Mater*., **2** (1993) 27.

38. Edler, K.; White, J. W., J. Chem. Soc., *Chem. Commun*., (1995) 155.

39. Setoguchi, Y. M.; Teraoka, Y.; Moriguchi, I.; Kagawa, S.; Tomonaga, N.; Yasutake, A.; Izumi, J., *J. Porous Mater*., **4** (1997) 129.

40. Voegtlin, A. C.; Matijasic, A.; Patarin, J.; Sauerland, C.; Grillet, Y.; Huve, L., *Microporous Mater.*, **10** (1997) 137.

41. Chatterjee, M.; Iwasaki, T.; Hayashi, H.; Onodera, Y.; Ebina, T.; Nagase, T., *Catal. Lett.*, **52** (1998) 21.

42. Chatterjee, M.; Iwasaki, T.; Hayashi, H.; Onodera, Y.; Ebina, T.; Nagase, T., *Chem. Mater*., **11** (1999) 1368.

43. Chatterjee, M.; Iwasaki, T.; Onodera, Y.; Nagase, T.; Hayashi, H. ; Ebina, T., *Chem. Mater.*, **12** (2000) 1654.

44. Vartuli, J. C.; Schmitt, K. D.; Kresge, C. T.; Roth, W. J.; Leonowicz, M. E.; McCullen, S. B.; Hellring, S. D.; Beck, J. S.; Schlenker, J. L.; Olson, D. H.; Sheppard, E. W., *Chem. Matter*., **6** (1994) 2317.

45. Khushalani, D.; Kuperman, A.; Ozin, G. A.; Tanaka, K.; Garces, J.; Olken, M. M.; Coombs, N., *Adv. Mater*., **7** (1995) 842.

46. Chen, X.; Huang, L.; Li, Q., *J. Phys. Chem. B*, **101** (1997) 8460.

47. Schmidt, R.; Akporiaye, D.; Stocker, M.; Ellestad, O. H., *J. Chem. Soc. Chem. Commun*., (1994) 1493.

48. Stucky, G. D.; Monnier, A.; Schuth, F.; Huo, Q.; Margolese, D. I.; Kumar, D.; Krishnamurthy, M.; Petroff, P.; Firouzi, A.; Janicke, M.; Chmelka, B. F., Mol. *Cryst. Liq. Cryst.*, **240** (1996) 187.

49. Koyona, K. A.; Tatsumi, T., *Chem. Commun*., (1996) 145.

50. Ulagappan, N.; Neeraj, B. V. N. R.; Rao, C. N. R., *Chem. Commun*., (1996) 2243.

51. Zhao, D.; Goldfarb, D., J44. Chem. Soc., *Chem. Commun.*, (1995) 875.

52. Huo, Q.; Margolese, D. I.; Ciesla, U.; Demuth, D. G. Feng, P.; Gier, T. E.; Sieger, P.; Firouzi, A.; Chmelka, B. F.; Schuth, F.; Stuky, G. D., *Chem. Mater*., **6** (1994) 1176.

53. Tanev, P. T.; Pinnavaia, T. J., *Science*, **267** (1995) 865.

54. Casci, J. L., Advanced Zeolite Science and Applications, *Stud. Surf. Sci. Catal*., **85** (1994) 325.

55. Antonelli, D. M.; Ying, J. Y., *Curr. Opin. Collid. Interface Sci.*, **1** (1996) 523.

56. Chen, C.-Y.; Li, H.-X.; Davis, M. E., *Microporous Mater.*, **2** (1993) 17.

57. Vartuli, J. C.; Kresge, C. T.; Roth, W. J.; McCullen, S. B.; Beck, J. S.; Schmitt, M. E.; Leonowicz, J. D.; Lutner, J. D.; Sheppard, E. W., *American Chemical Society Meeting in Anaheim*, CA, 1995.

58. Branton, P. J.; Hall, P. G.; Sing, K. S. W., *Adsorption*, **1** (1995) 77.

59. Llewellyn, P. L.; Schuth, F.; Grillet, Y.; Rouquerol, F.; Rouquerol, J.; Unger, K. K., *Langmuir*, **11** (1995) 574.

60. Branton, P. J.; Hall, P. G.; Sing, K. S. W., *J. Chem. Soc., Chem. Commun*., (1993) 1257.

61. Gregg, S. J.; Sing, K. S. W., *Adsorption, Surface Area and Porosity*, 2nd ed., Academic Press, New York, Ch. 4, (1982).

62. Alfredsson, V.; Keung, M.; Monnier, A.; Stucky, G. D.; Unger, K. K.; Schuth, F., *J. Chem. Soc., Chem. Commun.*, (1994) 921.

63. Chenite, A.; Page, Y. L.; Sayari, A., *Chem. Mater*., **7** (1995) 1015.

64. Chen, J.; Li, Q.; Xu, R.; Xiao, F., *Angew. Chem. Int. Ed. Engl.*, **34** (1995) 2694.

65. Jentys, A.; Pham, N. H.; Vinek, H., *J. Chem. Soc., Faraday Trans.*, **92** (1996) 3287.

66. Lippamaa, E.; Magi, M.; Samson, A.; Engelhardt, G.; Gummer, A. R., *J. Am. Chem. Soc*., **102** (1980) 4889.

67. Lippamaa, E.; Magi, M.; Samson, A.;Tarmak, M.; Engelhardt, G., *J. Am. Chem. Soc*., **103** (1981) 4992.

68. Fyfe, C. A. Gobbi, G. C.; Klinowski, J.; Thomas, J. M.; Ramdas, S., *Nature*, **296** (1982) 530.

69. Fyfe, C. A. Gobbi, G. C.; Klinowski, J.; Thomas, J. M., *J. Phys. Chem.*, **482** (1981) 49.

70. Engelhardt, G.; Lohose, U.; Lippmaa, E.; Tarmak, M.; Magi, M., *Anarg. Allg. Chem*., **482** (1981) 49.

71. Mastikim, V. M.; Zamarev, K. I., *J. Phys. Chemie*., **152** (1987) 332.

72. Muller, D.; Gessnev, W.; Behrens, H. S.; Schelev, G., *Chem. Phys. Lett*., **79** (1981) 159.

73. Thomas, J. M.; Fyfe, C. A.; Ramdas, S.; Klinowski, J.; Gobbi, G. C. *J. Phys. Chem*., **86** (1982) 3061.
74. Ramdas, S.; Klinowski, J., *Nature*, **308** (1984) 521.
75. Biz, S.; Occelli, M. L., *Catal. Rev. Sci. Eng.*, **40** (1998) 329.
76. Ying, J. Y.; Mehnert, C. P.; Wong, M. S., *Angew. Chem. Int. Ed*., **38** (1999) 56.
77. Dubois, M.; Gulik-krzywicki, Th.; Cabane, B., *Langmuir*, **9** (1993) 673.
78. Huo, Q.; Leon, R.; Petroff, P. M.; Stucky, G. D., *Science*, **268** (1995) 1324.
79. Bagshaw, S. A.; Pouzet, E.; Pinnavaia, T. J., *Science*, **269** (1995) 1242.
80. Inagaki, S.; Fukushima, Y.; Kuroda, K., *J. Chem. Soc., Chem. Commun.* (1993) 680.
81. Inagaki, S.; Fukushima, Y.; Kuroda, K., *Stud. Surf. Sci. Catal*., **84** (1994) 125.
82. Vartuli, J. C.; Kresge, C. T.; Leonowicz, M. E.; Chu, A. S.; McCullen, S. B.; Johnson, I. D.; Sheppard, E. W., *Chem. Matter*., **6** (1994) 2070.
83. Ishikawa, T.; Matsuda, M.; Yasukawa, A.; Kandori, K.; Inagaki, S.; Fukushima, T.; Kondo, S., *J. Chem. Soc., Faraday Trans.*, **92** (1996) 1985.
84. Monnier, A.; Schuth, F.; Huo, Q.; Kumar, D.; Margolese, D. I.; Maxwell, R. S.; Stucky, G. D.; Krishnamurthy, M.; Petroff, P.; Firouzi, A.; Janicke, M.; Chmelka, B. F., *Science*, **261** (1993) 1299.
85. Firouzi, A.; Kumar, D.; Bull, L. M.; Besier, T.; Sieger, P.; Huo, Q.; Walker, S. A.; Zasadzinski, J. A.; Glinka, C.; Nicol, J.; Margolese, D. I.; Stuky, G. D.; Chmelka, B. F., *Science*, **267** (1995) 1138.
86. Branton, P. J.; Hall, P. G.; Treguer, M.; Sing, K. S. W., *J. Chem. Soc., Faraday Trans*., **91** (1995) 2041.
87. Rathousky, J.; Zukal, A.; Franke, O.; Schulz-Ekloff, G., *J. Chem. Soc., Faraday Trans*., **91** (1995) 937.
88. Ravikovitch, P. I.; Domhnaill, S. C. O.; Neimark, A. V.; Schueth, F.; Unger, K. K., *Langmuir*, **11** (1995) 4765.
89. Branton, P. J.; Hall, P. G.; Sing, K. SS. W., *J. Chem. Soc., Chem. Commun.*, (1993) 1257
90. Maddox, M. W.; Sowers, S. L.; Gubbins, K. E., *Adsorption*, **2** (1996) 23.
91. Franke, O.; Schulz-Ekloff, G.; Rathousky, J.; Starek, J.; Zukal, A., *J. Chem. Soc., Chem. Commun*., (1993) 724.

92. Cheng, C-F.; He, H.; Zhou, W.; Klinowski, J.; Gonclaves, J. A. S.; Gladden, L. F., *J. Phys. Chem. B*, **100** (1996) 390.

93. Schmidt, R.; Stocker, M.; Ellestad, O. H., *Stud. Surf. Sci. Catal.* **97** (1995) 149.

94. Rathouski, J.; Zukal, A.; Franke, O.; Schulz-E.; G., *J. Chem. Soc., Faraday Trans*. **90** (1994) 2821.

95. Branton, P. J.; Hall, P. G.; Sing, K. S. W.; Reichert, H.; Schueth, F.; Unger, K. K., *J. Chem. Soc., Faraday Trans.*, **90** (1994) 2965.

96. Schmidt, R.; Hansen, E. W.; Stoecker, M.; Akporiaye, D.; Ellestad, O. H., *J. Am. Chem. Soc*., **117** (1995) 4049.

97. Ioneva, M. A.; Newman, G. K.; Harwell, J. H., *AIChE Symp. Ser.*, **309** (1995) 40.

98. Gusev, V. Y.; Feng, X.; Bu, Z.; Haller, G. L.; O'Brien, J. A.; *J. Phys. Chem. B*, **100** (1996) 1985.

99. Schmidt, R.; Stocker, M.; Hansen, E.; Akporiaye, D.; Ellestad, O. H.; *Microporous Mater.*, **3** (1995) 443.

100. Sing, K. S. W., *J. Porous Mater*., **2** (1995) 5.

101. Ravikovitch, P. I.; Wei, D.; Chueh, W. T.; Haller, G. L.; Neimark, A. V., *J. Phys. Chem. B*, **101** (1997) 3671.

102. Kruk, M.; Jaroniec, M.; Sayari, A., *J. Phys. Chem. B*, **101** (1997) 583.

103. Meziani, M. J.; Zajac, J.; Jones, D. J.; Roziere, J.; Partyka, S., *Langmuir*, **13** (1997) 5409.

104. Dahl, I. M.; Myhrvold, E.; Slagtern, A.; Stocker, M., *Adsorpt. Sci. Technol.*, **15** (1997) 289.

105. Kruk, M.; Jaroniec, M.; Sayari, A., *Langmuir*, **13** (1997) 6267.

106. Branton P. J.; Sing, K. S. W.; White, J. W., *J. Chem. Soc., Faraday Trans.*, **93** (1997) 2337.

107. Zhao, X. S.; Lu, G. Q.; Whittaker, A. K.; Millar, G. J.; Zhu, H. Y., *J. Phys. Chem. B*, **101** (1997) 6525.

108. Edler, K. J.; Reynolds, P. A.; Branton, P. J.; Trouw, F. R.; White, J. W., *J. Chem. Soc., Faraday Trans*., **93** (1997) 1667.

109. Liepold, A.; Roos, K.; Reschetilowski, W.; Esculcas, A. P.; Rocha, J.; Philippou, A.; Anderson, M. W., *J. Chem. Soc., Faraday Trans.*, **92** (1996) 4623.

110. Morishige, K.; Fujii, H.; Uga, M.; Kinukawa, D., *Langmuir*, **13** (1997) 3494.

111. Voegtlin, A. C.; Matijasic, A.; Patarin, J.; Sauerland, C.; Grillet, Y.: Huve, L., *Microporous Mater*., **10** (1997) 137.
112. Kosslick, H.; Landmesser, H.; Fricke, R., *J. Chem. Soc., Faraday Trans*., **93** (1997) 1849.
113. Sun, Y.; Yue, Y.; Gao, Z., *Appl. Catal., A*, **161** (1997) 121.
114. Reddy, J. S.; Dicko, A.; Sayari, A., *Chem. Ind.* **69** (1997) 405.
115. Boger, T.; Roesky, R.; Glaeser, R.; Ernst, S.; Eigenberger, G.; Weitkemp, J., *Microporous Mater.*, **8** (1997) 79.
116. Aronson, B. J.; Blanford, C. F.; Stein, A., *Chem. Mater*., **9** (1997) 2842.
117. Zhao, X. S.; Lu, G. Q., *J. Phys. Chem. B*, **102** (1998) 1556.
118. Nguyen, C; Sonwane, C. G.; Bhatia, S. K.; Do, D. D., *Langmuir*, **14** (1998) 4950.
119. Long, Y.; Xu, T.; Sun, Y.; Dong, W., *Langmuir*, **14** (1998) 6173.
120. Sonwane, C. G.; Bhatia, S. K.; Calos, N., *Ind. Eng. Chem. Res.*, **37** (1998) 2271.
121. Zhao, X. S.; Ma,Q.; Lu, G. Q, *Energy Fuels*, **12** (1998) 1051.
122. Zhao, X. S.; Audsley, F.; Lu, G. Q., *J. Phys. Chem. B*, **102** (1998) 4143.
123. Sonwane, C. G.; Bhatia S. K., *Chem. Eng. Sci.*, **53** (1998) 3143.
124. Ziolek, M.; Nowak, I; Decyk, P; Kujawa, J., *Stud. Surf. Sci. Catal.*, **117** (1998) 509.
125. Tanaka, H.; Iiyama, T.; Uekawa, N.; Suzuki, T.; Matsumoto A.; Grun, M.; Unger, K. K. Klaus, K.; Kaneko, K., *Chem. Phys. Lett.*, **293** (1998) 541.
126. Rana, R. K.; Viswanathan, B., *Catal. Lett*., **52** (1998) 25.
127. Anwander, R.; Palm, C.; Stelzer, J.; Groeger, O.; Engelhardt, G., *Stud. Surf. Sci. Catal*, **117** (1998) 135
128. Sayari, A.; Kruk, M. Jaroniec, M., *Catal. Lett*., **49** (1998) 147.
129. Piwonski, I.; Zajac, J.; Deborah, J.; Roziere, J.; Partyka, S., *J. Mater. Chem.*, **8** (1998) 17.
130. Ravikovitch, P. I.; Haller, G. L.; Neimark, A. V., *Stud. Surf. Sci. Catal.*, **117** (1998) 77.
131. Liepold, A.; Ros, K.; Reschetilowski, W.; Schmidt, R.; Stocker, M.; Philippou, A.; Anderson, M. W.; Esculcas, A. P.; Rocha, J., *Stud. Surf. Sci. Catal*., **105A** (1997) 423.
132. Mulukutla, R. S.; Iwasawa, Y.; Asakura, K.; Namba, S., *Chem. Commun*., (1998) 1425.

133. Morishige, K.; Shikimi, M., *J. Chem. Phys*., **108** (1998) 7821.

134. Branton, P. J.; Hall, P. G.; Kenneth, S. W., *Spec. Publ. - R. Soc. Chem*., **213** (1997) 98.

135. Janchen, J.; Stach, H.; Busio, M.; Van Wolput, J. H. M. C., *Thermochim. Acta* **312** (1998) 33.

136. Bambrough, C. M.; Slade, R. C. T.; Williums, R. T.; Burkett, S. L.; Sims, S. D.; Mann, S., *J. Colloid Interface Sci.*, **201** (1998) 220.

137. Niessen, T. E. W.; Niederer, J. P. M. Gjervan, T.; Holderich, W. F., *Microporous and Mesoporous Mater*., **21** (1998) 67.

138. Springuel -Huet, M. A.; Fraissard, J.; Schmidt, R.; Stocker, M.; Conner, W. C., *Spec. Publ. - R. Soc. Chem.*, **213** (1997) 452.

139. Viale, S.; Garrone, E.; Di, R. F.; Chiche, B.; Fajula, F., *Stud. Surf. Sci. Catal.*, **105A** (1997) 533.

140. Bhatia, S. K.; Sonwane, C. G., *Langmuir*, **14** (1998) 1521.

141. Sayari, A.; Kruk, M.; Jaroniec, M.; Moudrakovski, I. L., *Adv. Mater*., **10** (1998) 1376.

142. Menon, V. C.; Komarneni, S., *J. Porous Mater*. **5** (1998) 43.

143. He, N-Y.; Bao S-L.; Xu, Q-H., *Stud. Surf. Sci. Catal*. **105A** (1997) 85.

144. Okumara, K.; Nishigaki, K.; Niwa, M., *Chem. Lett*., (1998) 577.

145. Neimark, A. V.; Ravikovitch, P. I.; Grun, M.; Schuth, F.; Unger K. K., *J. Colloid Interface Sci*., **207** (1998) 159.

146. Kruk, M.; Jaroniec, M.; Kim, J. M.; Ryoo, R., *Langmuir*, **15** (1999) 5279.

147. Branton, P. J.; Reynolds, P. A.; Studer, A. Sing, K. S. W.; White, J. W., *Adsorption*, **5** (1999) 91.

148. Kruk, M.; Jaroniec, M.; Sayari, A., *Langmuir*, **15** (1999) 5683.

149. Chaudhari, K.; Das, T. K.; Rajmohanan, P. R.; Lazar, K.; Sivasanker, S.; Chandwadkar, A. J., *J. Catal.* **183** (1999) 281.

150. Bellat, J. P.; Bertrand, O.; Bouvier, F.; Broyer, M.; Francois, V.; Maure, S.; Weber, G., *Stud. Surf. Sci. Catal*., **125** (1999) 737.

151. Mulukutla, R. S.; Asakura, K.; Kogure, T.; Namba, S.; Iwasawa, Y., *Phys. Chem. Chem. Phys*. **1** (1999) 2027.

152. Koh, C. A.; Montanari, T.; Nooney, R. I.; Tahir, S. F.; Westacott, R. E., *Langmuir*, **15** (1999) 6043.

153. Hartmann, M.; Racouchot, S.; Bischof, C., *Microporous and Mesoporous Mater*., **27** (1999) 309.
154. Chen, Li-W.; Chou, C-Y.; Ko, A-N., *Appl. Catal., A*, **178** (1999) L1-L6.
155. Xu, Y-M.; Wang, R-S.; Wu, F., *J. Colloid Interface Sci*., **209** (1999) 380.
156. Kosslick, H.; Lischke, G.; Parlitz, B.; Stork, W.; Fricke, R., *Appl. Catal., A*, **184** (1999) 49.
157. Nguyen, C.; Do, D. D., *Adsorpt. Sci. Technol.*, **16** (1998) 439.
158. Coluccia, S.; Marchese, L.; Martra, G., *Microporous and Mesoporous Mater*., **30** (1999) 43.
159. Denoyel, R.; Rey, E. S., *Langmuir*, **14** (1998) 7321.
160. Jaroniec, M.; Kruk, M.; Jaroniec, C. P.; Sayari, A., *Adsorption*, **5** (1999) 39.
161. Chakraborty, B.; Viswanathan, B., *Catal. Today*, **49** (1999) 253.
162. Sano, T.; Doi, K.; Hagimoto, H.; Wang, Z.; Uozumi, T.; Soga, K., *Chem. Commun*., (1999) 733.
163. Taouli, A.; Klemt, A.; Breede, M.; Reschetilowski, W., *Stud. Surf. Sci. Catal.*, **125** (1999) 307.
164. Sonwane, C.G.; Bhatia, S. K., *Langmuir*, **15** (1999) 5347.
165. Berrebi, G., *Eur. Pat. Appl.* **EP 951937** A1 27 Oct 1999, 5 pp.
166. Zhu, Z.; Chang, Z.; Kevan, L., *J. Phys. Chem. B*, **103** (1999) 2680.
167. Galarneau, A.; Desplantier, D.; Dutartre, R.; Di, R. F., *Microporous and Mesoporous Mater*., **27** (1999) 297.
168. Yiu, H. H. P.; Brown, R. R.; Barnes, P. A., *Catal. Lett*., **59** (1999) 207.
169. Cheng, M.; Kumata, F.; Saito, T.; Komatsu, T.; Yashima, T., *Appl. Catal., A*, **183** (1999) 199.
170. Anwander, R.; Nagl, I.; Widenmeyer, M.; Engelhardt, G.; Groeger, O.; Palm, C.; Roeser, T., *J. Phys. Chem. B*, **104** (2000) 3532.
171. Kruk, M.; Jaroniec, M.; Sakamoto, Y.; Terasaki, O.; Ryoo, R.; Ko, C-H., *J. Phys. Chem. B*, **104** (2000) 292.
172. Kruk, M.; Jaroniec, M.; Yang, Y.; Sayari, A., *Stud. Surf. Sci. Catal.*, **129** (2000) 577.
173. Bhoumik, A.; Tatsumi, T., *J. Catal*., **189** (2000) 31.
174. Meziani, M. J.; Zajac, J.; Partyka, S., *Langmuir*, **16** (2000) 8410.
175. Yamazaki, T.; Watanabe, M.; Saito, H., *Bull. Chem. Soc. Jpn*., **73** (2000) 1353.

176. Lin, H.-P.; Wong, S-T.; Mou, GY.; Tang, C-Y., *J. Phys. Chem. B*, **104** (2000) 8967.

177. Kawi, S.; Shen, S. C., *Stud. Surf. Sci. Catal.*, **129** (2000) 219.

178. Kruk, M.; Jaroniec, M.; *Chem. Mater.*, **12** (2000) 222.

179. Chang, Z.; Zhu, A.; Kevan, L., *J. Phys. Chem. B*, **103** (1999) 9442.

180. Piwonski, I.; Zajac, J.; Jones, D. J.; Roziere, J.; Partyka, S.; Plaza, S., *Langmuir*, **16** (2000) 9488.

181. Staszczuk, P.; Dnielkiewicz, T.; Klinowski, J., *Adsorpt. Sci. Technol.*, **18** (2000) 307.

182. Kruk, M.; Jaroniec, M.; Yang, Y.; Sayari, A., *J. Phys. Chem. B*, **104** (2000) 1581.

183. Lin, W.; Cai, Q.; Pang, W.; Yue, Y.; Zou, B., *Microporous and Mesoporous Mater.*, **33** (2000) 187.

184. Carrott, M. M. L. R.; Candeias, A. J. E.; Carrott, P. J. M.; Unger, K. K., *Langmuir*, **15** (1999) 8895.

185. Matsumoto, A.; Chen, H.; Tsutsumi, K.; Grun, M.; Unger, K. K., *Microporous and Mesoporous Mater.*, **32** (1999) 55.

186. Morris, T. -A.; Huddersman, K., *Phys. Chem. Chem. Phys.* **1** (1999) 4673.

187. Namba, S.; Aikawa, M.; Takeuchi, K.; Yomoda, D.; Inoue, Y.; Aoki, S.; Izumi, J., *Stud. Surf. Sci. Catal.* **129** (2000) 757.

188. Araujo, A. S.; Jaroniec, M., *Stud. Surf. Sci. Catal.*, **129** (2000) 187.

189. Chatterjee, M.; Iwasaki, T.; Onodera, Y.; Nagase, T.; Hayashi, H.; Ebina, T., *Chem. Matter.*, **12** (2000) 1654.

190. Chen, W-H.; Liu, H-P.; Wu, J-F.; Jong, S-J.; Mou, GY.; Liu, S-B., *Stud. Surf. Sci. Catal.* **129** (2000) 517.

191. Inoue, S.; Tanaka, H.; Hanzawa, Y.; Inagaki, S.; Fukushima, Y.; Buchel, G.; Unger, K. K.; Matsumoto, A.; Kaneko, K., *Stud. Surf. Sci. Catal.*, **128** (2000)167.

192. Zheng, S.; Gao, L.; Zhang, Q-hong; Guo, J-kun, *J. Mater. Chem.*, **10** (2000) 723.

193. Naono, H.; Hakuman, M.; Tanaka, T.; Tamura, N.; Nakai, K., *J. Colloid. Intrface Sci.*, **225** (2000) 411.

194. Kawi, S.; Shen, S. C., *Stud. Surf. Sci. Catal.*, **129** (2000) 227.

195. Kang, K. K.; Byun, C. S.; Ahn, W. S., *Stud. Surf. Sci. Catal.* **129** (2000) 335.

196. Araujo, A. S.; Jaroniec, M., *Thermochim. Acta*, **345** (2000) 173

197. Meziani, M. J.; Zajac, J.; Jones, D. J.; Partyka, S.; Roziere, J.; Auroux, A., *Langmuir*, **16** (2000) 2262.

198. Olivier, J. P., Adsorpt. Sci. Technol., *Proc. Pac. Basin Conf.*, **2nd** (2000) 472.

199. Ferreira, P.; Goncalves, I. S.; Kuhn, F. E.; Pillinger, M.; Rocha, J.; Thrusfield, A.; Xue, W-M.; Zhang, G., *J. Mater. Chem.*, **10** (2000) 1395.

200. Springuel-Huet, M.-A.; Sun, K.; Fraissard, J., *Microporous and Mesoporous Mater*., **33** (2000) 89.

201. Sonwane, C. G.; Bhatia, S. K., *J. Phys. Chem. B*, **104** (2000) 9099.

202. Olivier, J. P., *Stud. Surf. Sci. Catal*., **128** (2000) 81.

203. Anwander, R.; Gorlitzer, H. W.; Gerstberger, G.; Palm, C.; Runte, O.; Spiegler, M., *J. Chem. Soc., Dalton Trans*., (1999) 3611.

204. Lin, H.-P.; Wong, S-T.; Liu, S-B.; Mou, C-Y.; Tang, C-Y., *Stud. Surf. Sci. Catal*., **129** (2000) 15.

205. Ramirez, J.; Contreras, R.; Castillo, P.; Klimova, T.; Zarate, R.; Luna, R., *Appl. Catal*., *A*, **197** (2000) 69.

206. Neimark, A. V.; Ravicovitch, P. I.; Vishnyakov, A., *Adsorpt. Sci. Technol., Proc. Pac. Basin Conf*., **2nd**, (2000) 461.

207. Hartmann, M., *Stud. Surf. Sci. Catal*., **128** (2000) 215.

208. Padin, J.; Yang, R. T., *Chem. Eng. Sci*., **55** (2000) 2607.

209. Jeroniec, M.; Jeroniec, C. P.; Kruk, M.; Ryoo, R., *Adsorption*, **5** (1999) 313.

210. Jaroniec, M.; Kruk, M.; Sayari, A., *Stud. Surf. Sci. Catal*., **129** (2000) 587.

211. Araujo, A. S.; Jaroniec, M., *J. Colloid Interface Sci.*, **218** (1999) 462.

212. Cho, D-H.; Chang, T-S.; Ryu, S-K.; Lee, Y. K.,

213. Chevrot, V.; Llewellyn, P.L.; Rouquerol, F.; Godlewski, J.; Rouquerol, J., *Thermochim. Acta*, **360** (2000) 77.

214. Hutson, N. D.; Yang, R. T., *Ind. Eng. Chem. Res*., **39** (2000) 2252.

215. Kruk, M.; Antochshuk, V.; Jaroniec, M.; Sayari, A., *J. Phys. Chem. B*, **103** (1999) 10670.

216. Hartmann, M.; Ernst, S.; Prakash, A. M.; Kevan, L., *Stud. Surf. Sci. Catal.*, **129** (2000) 201.

217. Fudala, A.; Konya, Z.; Kiyozumi, Y.; Niwa, S. -I.; Toba, M.; Mizukami, F.; Lentz, P. B.; Nagy, J.; Kiricsi, I., *Microporous and Mesoporous Mater*., **35-36** (2000) 631.

218. Bambrough, C. M.; Slade, R. C. T.; Williams, R. T., *Stud. Surf. Sci. Catal.*, **129** (2000) 617.

219. He, N.; Li, D.; Tu, M.; Shen, J.; Bao, S.; Xu, Q., J. *Therm. Anal. Calorim.*, **58** (1999) 455.

220. Yue, Y. -H.; Gedeon, A.; Bonardet, J. -L.; D'Espinose, J. B.; Fraissard, J., *Stud. Surf. Sci. Catal*., **130C** (2000) 3035.

221. Carrot, M. M. L. R.; Candias, A. J. E.; Carrot, P. J. M.; Sing, K. S. W.; Unger, K. K., *Langmuir*, **16** (2000) 9103.

222. Chaudhari, K.; Bal, R.; Das, T. K.; Chandwadkar, A.; Srinivas, D.; Sivasanker, S., *J. Phys. Chem. B*, **104** (2000) 11066.

223. Zhao, X. S.; Lu, G. Q.; Hu, X., Adsorpt. Sci. Technol., *Proc. Pac. Basin Conf.*, **2nd**, (2000) 386.

224. Coluccia, S.; Marchese, L.; Martra, G., *Photofunct. Zeolites, Ed. Anpo, M*., (2000) 39.

225. Zhang, W. -H.; Shi, J. -L.; Wang, L. -Z.; Yan, D. -S., *Mater. Lett*., **46** (2000) 35.

226. Nguyen, C.; Do, D. D., *J. Phys. Chem. B*, **104** (2000) 11435

227. Hu, X.; Qiao, S.; Zhao, X. S.; Lu, G. Q., *Ind. Eng. Chem.*, **40** (2001) 862.

228. Zhao, X. S.; Lu, G. Q.; Hu, X., *Microporous and Mesoporous Mater*., **41** (2000) 37.

Chapter 1.2

EXPERIMENTAL

Chapter 1.2

EXPERIMENTAL

1.2.1 HYDROTHERMAL SYNTHESIS OF MCM-41

The hydrothermal synthesis of mesoporous silicate and aluminosilicate MCM-41 materials from a gel consisting of a silica source [(viz. sodiumtrisilicate (60 % SiO_2) (Fluka)], alumina source [*viz*. sodium aluminate (S. D. Fine Chemicals, India)], template [viz. dodecyltrimethylammoniumbromide (DTAB) or cetyltrimethylammoniumbromide (CTAB) (Aldrich Chemical Co.), deionised water and sulfuric acid (which is used for adjusting the pH) has been carried out in a Teflon coated stainless steel autoclave at 373 K under autogeneous pressure for 144 h. The hydrothermal synthesis of Si- or Al-Si-MCM-41 was described elsewhere[1]. The gel was prepared by following method.

1.2.1.1 Hydrothermal Synthesis of Si-MCM-41

100 g of water, 25g of Na-trisilicate and 3 ml of conc. sulfuric acid were mixed with stirring and warmed on water bath. The resulting mixture was allowed to stir for 30 min. Required amount (surfactant/silica mole ratio = 0.5) of 25% aqueous solution of DTAB (surfactant) was then added to the mixture. The resulting gel was allowed to stir for 30 min. The final gel composition was SiO_2 : 0.64 Na_2O : 0.49 $C_{12}H_{25}(CH_3)_3NBr$: 52 H_2O. The resulting gel was transferred to the Teflon lined autoclave and heated at 373 K for 144 h under autogeneous pressure. After cooling to room temperature, the resulting solid product was recovered by filtration on a Buchner funnel, washed with water, and dried in air at ambient temperature. Surfactant was removed by calcining the as-synthesized product at 813 K for 5h.

1.2.1.2 Hydrothermal Synthesis of AlSi-MCM-41

AlSi-MCM-41 was synthesised as follows: (i) 10.4 ml (25 wt%) of solution of tetramethylammonium hydroxide was combined with 14.23 g of Na-trisilicate dispersed in 50 g of water with stirring, and 29.5 g of CTAB (in 75 g of water) (surfactant/silica mole ratio = 0.5) solution were added and stirred for 30 min. (ii) 2.3 g of Na-aluminate (Si/Al = 5.0) was dispersed or dissolved in 50 g of water and then added slowly to the gel. (iii) The pH was adjusted with dilute sulfuric acid to 11.5. The resulting gel composition was SiO_2 : 0.097 Al_2O_3 : 0.298 CTAB : 0.20 TMAOH : 0.41 Na_2O: 75 H_2O. The final gel was transferred into Teflon-lined stainless steel autoclave and heated at 393 K for 120 h under autogeneous pressure. After cooling to room temperature, the resulting solid product was recovered by filtration on a Buchner funnel, washed with water, and dried in air at ambient temperature. Surfactant was removed by calcining the as-synthesized product at 813 K for 5h.

The Na^+ form of AlSi-MCM-41 was obtained by ion exchange of the as synthesized AlSi-MCM-41 with 1M $NaNO_3$ at 353 K. The NH_4^+ form of AlSi-MCM-41 was obtained by repeated (5 times) ion exchange of the Na-AlSi-MCM-41 with 1 M NH_4NO_3 at 353 K. The NH_4^+ form is then calcined at 813K for 5 h to obtain H-AlSi-MCM-41. The surface area of the Si-MCM-41, Na-AlSi-MCM-41 and H-AlSi-MCM-41 was found to be 1160, 1010 and 980 $m^2 g^{-1}$, respectively.

1.2.2 TECHNIQUES USED FOR CHARACTERIZING MESOSTRUCTURES OF MCM-41

A number of techniques are used to characterize mesoporous MCM-41. Among these, X-ray powder diffraction, transmission electron microscopy (TEM) and adsorption measurements are the essential ones to identify the structure of the

mesoporous MCM-41. Infrared spectroscopy and nuclear magnetic resonance spectroscopy have also been applied to obtain additional structural information about molecular sieves.

1.2.2.1 Powder X-Ray Diffraction (XRD)

The crystalline phase identification and phase purity of the as synthesized and calcined samples were determined by X-ray diffraction spectra which were obtained either on a Phillips diffractometer or a Siemens instrument using a monochromatic CuK_α radiation (λ = 0.15406 nm; 40 kV, 25 mA) with a 0.02 step size and a 1.2 s step time. The samples were prepared as thin layer on glass slide.

1.2.2.2 N_2 Adsorption

Surface area of the mesoporous materials was measured by N_2-adsorption at 77 K using either "Surface Area Analyzer, Quantachrome, USA" or "Omnisorb 100 CX, Coulter Corporation, USA". Surface areas and pore diameters of the samples were determined from N_2-adsorption-desorption isotherms using a commercial volumetric adsorption apparatus (Omnisorb 100 CX, Coulter Corporation, USA). Approximately 100-150 mg of the calcined sample was degassed at 673 K for 5h at 10^{-5} Torr, prior to surface area measurements. The sample was then cooled to 77K using liquid nitrogen and the sorption of N_2 was carried out at different equilibrium pressures. The weight of the degassed sample was used in the surface area calculations. To obtain the surface area, the results were fitted into the equation,

$S_{BET} = V_m \times N \times A_m$

where, Vm is the monolayer volume, N is the Avogadro number and A_m is the cross sectional area of the adsorbent.

The pore size distribution and pore diameters were calculated using the Barret-Joyner-Halenda (BJH) model.[2] The above model was chosen since it has been derived for nonintersecting cylindrical pores[3] (as in MCM-41 type materials). However, as the model uses the Kelvin equation, the validity of which is questionable for pores of diameter less than 5 nm,[2] systematic error might be present in the estimated pore diameters. However, the reported trend in the diameters for the different samples is expected to be the same.

Using Monosorb Surface Area Analyzer (Quantachroma Corp., USA) based on dynamic adsorption/desorption technique, only surface area of the mesoporous materials was measured using the single-point BET method [i.e. by measuring the adsorption of N_2 at liquid nitrogen temperature for N_2 concentration of 30 mol% (balance helium)].

Before carrying out surface area measurement experiments, the catalyst (0.05 – 0.1 g) was pretreated in situ in the sample cell at 573 K for 1h in flow of a mixture of He and N_2 to remove the traces of moisture or any other gases and the analyzer was calibrated by injecting a known amount of air.

The surface area was calculated from the observed desorption counts instead of the adsorption ones, as follows:

Surface area (m^2 g^{-1}) = (Desorption counts $\times$ 2.84) / (wt of catalyst x counts of 1 ml of air)

(2.84 m^2 area = 1 cm^3 N_2 or air, Counts are expressed in terms of surface area, m^2)

1.2.2.3 Transmission Electron Microscopy (TEM)

The samples were embedded in Epon 812 epoxy resin, which was cured. The epoxy blocks were ultramicrotomed at room temperature. The ultra thin sections

ranging in the thickness from 80 to 100 nm were prepared using a Reichert microtome. The thin sections were examined by TEM. The TEMs used for these studies were either JEOL 2000 FX or Philips CM-20 equipped with a high resolution ultrathin polepiece. Images were recorded on conventional sheet films.

1.2.2.4 Scanning Electron Microscopy (SEM)

The crystal size and morphology of the as-synthesized and calcined samples were determined by a scanning electron microscope (Model JEOL JSM 5200) equipped with energy dispersive X-ray analysis (EDAX). The samples were sputtered with gold to prevent surface charging and to protect them from thermal damage from the electron beam.

1.2.2.5 Infrared Spectroscopy

Fourier transform infrared (FTIR) spectra for the samples were recorded with a Shimadzu FTIR spectrometer (Model 8300). FTIR spectra of the mesoporous material in the framework region (450 cm^{-1} to 4000 cm^{-1}) were obtained in nujol or in the diffuse reflectance mode.

1.2.2.6 X-Ray Photo Electron Spectroscopy (XPS)

XPS measurements were carried out using V. G. Scientific ESCA–3–MK II X-ray photoelectron spectrometer with Al K_α X-ray source. The binding energy values were measured with reference to the carbon peak (B. E. for C_{1s} = 285.0 eV). The surface concentration of the elements present in the reduced and free catalysts has estimated as follows:

(Area under curve × scale)/(cross sectional area of an element × magnification).

1.2.2.7 Solid State MAS NMR Spectroscopy

The solid state magic-angle (MAS) NMR spectroscopic studies were carried out in a Bruker MSL-300 FT NMR spectrometer. For the MAS NMR studies, the finely powdered samples were placed in 7.0 mm O.D. zirconia rotors and spun at 2.5 - 3.3 kHz. For ^{27}Al signal, aluminium nitrate (1M aqueous solution) was used as the reference compound, while tetraethyl orthosilicate (δ = 82.4 ppm from tetra methyl silane) was used as the reference compound for ^{29}Si. The resonance frequencies of ^{29}Si was 59.6 MHz. For the ^{1}H-^{29}Si CP MAS experiments, the Hartmann – Hahn match condition[4] were used.

1.2.3 MEASUREMENT OF ACIDITY

The acidity of the mesoporous MCM-41 materials was measured in terms of the pyridine chemisorbed at 673 K, using the GC method.[5]

Gas chromatographic adsorption/desorption data were collected using a Perkin-Elmer Sigma 300 GC fitted with a flame ionization detector. Nitrogen, passed over mesoporous materials to remove traces of moisture, was used as the carrier gas. The flow rate was about 40 cm^3 (NTP). min^{-1} in all the experiments. The experimental set-up is shown in Fig. 1.2.1.

The catalyst column was prepared by packing about 0.5 g of the adsorbent particles (particle size: 0.3 - 0.4 mm) in a stainless steel tube (length = 5.5 cm, i.d. = 1.5 mm and o.d. = 3.0 mm). In order to minimize the dead volume, one end of the column was directly connected to the detector and the other end to the injector through a 40 cm long stainless steel capillary (about 1.5 mm o.d. and 0.7 mm i.d.), which acted as a pre-heater. The catalyst was calcined in situ by heating rate of 20 K. min^{-1} and further at 673 K for 1 h.

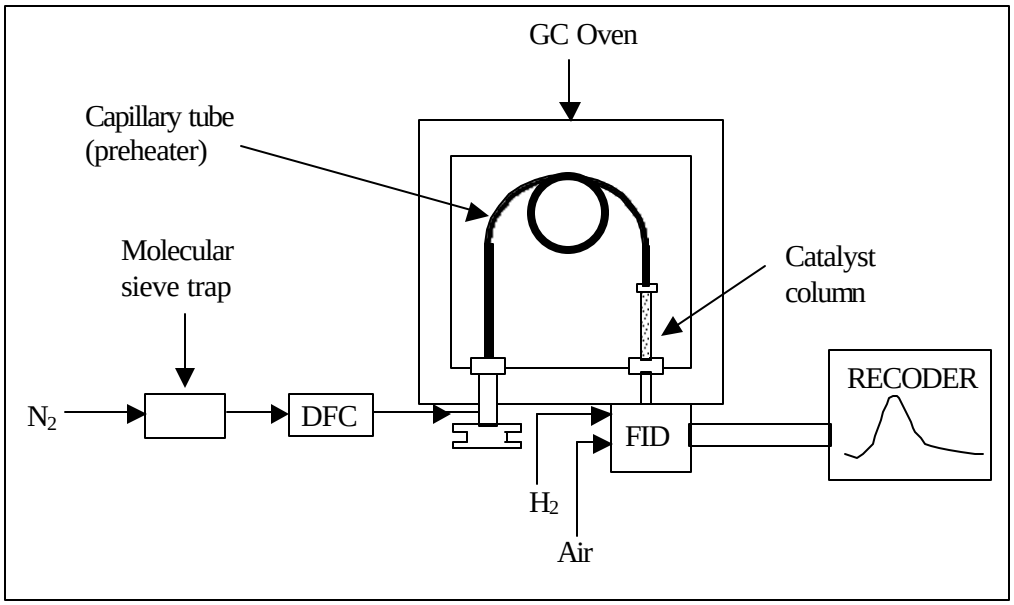

Fig. 1.2.1 Experimental arrangement for adsorption measurements using gas chromatograph

The chemisorption of pyridine in the adsorbent was measured by the GC pulse method[5] based on TPD under chromatographic conditions, as follows:

The initial temperature chosen for the TPD was 353 K. The adsorbent was pretreated in situ in a flow of N_2 (carrier gas) for 1h. After pretreatment of the adsorbent, the GC oven temperature was brought down to 353 K and a known amount of pyridine was injected into the adsorbent column. After allowing redistribution of the adsorbed species in the column, the TPD was started at a linear heating rate of 20 K min^{-1} in the flow of nitrogen. The final temperature chosen for the TPD (or the temperature at which the irreversible adsorption of the adsorbate was to be measured) was 673 K. After the final temperature was reached, the desorption of the reversibly adsorbed species was allowed to continue for a further period of 1h isothermally at

that temperature. At the end of the TPD, the adsorbent retained only the adsorbate irreversibly adsorbed at 673 K.

After recording the first TPD chromatogram, the GC oven temperature was reduced to 353 K and the procedure was repeated to obtain the second TPD chromatogram by injecting the same amount of pyridine.

The amount of pyridine chemisorbed was calculated from the expression,

$$q_i = (A^* / s)/M \qquad (1.2.1)$$

where A* is the difference between the areas of the two chromatograms obtained by the superimposition of the two chromatograms and cutting and weighing, s is the detector sensitivity (area. mol^{1}) and M is the mass of the catalyst. The irreversible adsorption (or chemisorption) in the present study is defined as the amount of adsorbate retained by the presaturated catalyst after it was swept with pure nitrogen at the temperature of chemisorption for 1h.

1.2.4 MEASUREMENT OF ADSORPTION ISOTHERMS

1.2.4.1 Experimental Procedure

Gas chromatographic adsorption / desorption and TPD data were collected using a Perkin-Elmer, Sigma 300 gas chromatograph (GC), fitted with a flame ionization detector. The experimental set-up is shown in Fig. 1.2.1. Nitrogen, passed over mesoporous materials (Si-MCM-41) to remove traces of moisture, was used as the carrier gas. The flow rate was about 40 $cm^3 min^{-1}$ in all the experiments.

The adsorbent column was prepared by packing about 1.0 g of the adsorbent particles (particle size: 0.3 - 0.4 mm) in a stainless steel tube (length = 16.5 cm, i.d. = 5.0 mm). In order to minimize the dead volume, one end of the column was directly connected to the detector and the other end to the injector through a 40 cm long

stainless steel capillary (about 1.5 mm o.d. and 0.7 mm i.d.), which acted as a pre-heater. The adsorbent was pretreated in situ by heating rate of 20 K. min^{-1} and further at 673 K for 1 h.

The adsorption isotherms of benzene, toluene, p-xylene and mesitylene on the Si-MCM-41 were measured at different temperatures (348 – 498 K) by the GC peak maxima method,[6] using nitrogen (40 cm^3 min^{-1}) as a carrier gas. After the desired temperature was attained, the carrier gas flow rate was accurately measured with soap bubble flow meter. A number of pulses of aromatic hydrocarbons of the same size were injected into the adsorbent column with a micro-liter syringe in succession in order to saturate the adsorbent with aromatic hydrocarbon adsorbed irreversibly at that temperature. The injection of the pulses was continued until elution chromatograms of the same height were obtained, which indicated that the adsorbent was completely saturated with irreversibly adsorbed adsorbate.

After checking the reproducibility of the pulse experiment, adsorbate pulses of different sizes (0.5 to 10.0 μL) were injected into the Si-MCM-41 column (i.d. = 5 mm and length = 16.5 cm) at a known temperature and the elution chromatogram of each pulse was recorded until the recorder pen reached the base line. Sufficient time was allowed between two successive pulses for the desorption of adsorbate reversibly during the passage of the previous pulse. The reproducibility of the experiment was checked from time to time by injecting pulses of the same size under identical experimental conditions and measuring the pulse retention time. The area under the desorption chromatogram was determined by the cut-and-weigh procedure. The estimation of adsorption isotherm data from the desorption chromatograms is described later in Section 1.3.1.2.2.1.

The adsorption of adsorbate on the column was found to be negligible. The pressure drop across the adsorbent bed was negligibly small (< 1 % of the outlet pressure). Before carrying out the adsorption experiment, the adsorbent was pretreated in situ in a flow of the carrier gas at 673 K for 1 h.

1.2.5 TEMPERATURE PROGRAMMED DESORPTION (TPD) OF AROMATIC HYDROCARBONS ON MESOPOROUS MCM-41 MATERIALS

1.2.5.1 Temperature Programmed Desorption (TPD) procedure

The gas chromatographic TPD data were collected using a Parkin-Elmer Sigma 300 gas chromatograph with a flame ionization detector. Nitrogen (flow rate : 40 cm^3 min^{-1}) was used as the carrier gas throughout the measurement. The catalyst column was prepared by packing 50 mg of the adsorbent particles (diameter 0.3 - 0.4 mm) in a stainless steel tube (length = 5.5 cm, i.d. = 1.9 mm and o.d. = 3.0 mm). A 40 cm long stainless steel capillary tubing (o.d. = 1.5 mm and i.d. = 0.7 mm), connected between the catalyst column and injection port, acted as the preheater; the other end of the column was directly connected to the detector.

Before the start of the TPD, the adsorbent was heated in situ at 673 K in the flow of nitrogen for 1 h. The temperature was increased to 673 K at a linear heating rate of 20 K min^{-1}.

1.2.5.2 TPD at Different Heating Rates

The initial temperature chosen for the TPD run was 323 K. Before starting the TPD run, the adsorbent was saturated with the aromatic hydrocarbon at a particular temperature [benzene at 343 K, toluene at 348 K, p-xylene at 373 K and mesitylene and naphthalene (in low boiling solvent, such as n-pentane) at 398 K] by injecting a

number of pulses of the hydrocarbon into the column and desorbing the reversibly adsorbed hydrocarbon in the stream of nitrogen for a period of 15 min. After desorbing the reversibly adsorbed hydrocarbon, the oven temperature was brought down to 323 K (the initial temperature chosen for TPD). The adsorbed hydrocarbon in the catalyst was then thermally desorbed by increasing the GC oven temperature from 323 to 673 K at a known linear heating rate. After the final temperature of TPD was reached, the desorption was continued for a further period of 1h to desorb the reversibly adsorbed hydrocarbons at 673 K. The initial adsorbate loading was calculated from the area of the TPD curve and the amount of irreversibly adsorbed hydrocarbon at 673 K was determined by the gas chromatographic pulse method[5]. The irreversible adsorption of the hydrocarbons at 673 K was negligibly small as compared to the initial adsorbate loading. The TPD curves for the benzene, toluene, p-xylene, mesitylene and naphthalene on the adsorbent were recorded at different heating rates (5, 10, 15 and 25 K min^{-1}).

1.2.5.3 TPD at Different Adsorbate Loading

Initial adsorbate loading of benzene and toluene on the MCM-41 was varied by carrying out the saturation, as described above, at different temperatures (343 - 393 K). After the saturation, the temperature was brought down to 323 K (the initial temperature chosen for TPD), and the TPD run was carried out at a linear heating rate of 15 K min^{-1} by the procedure described above. The area under the chromatograms was determined by the cut-and-weigh procedure.

The initial adsorbate loading of the aromatic hydrocarbons (viz. benzene and toluene) on a particular adsorbent referred throughout this chapter is defined as the amount of benzene or toluene retained at a particular temperature by the presaturated

adsorbent after it has been swept with pure nitrogen at that temperature for a period of 15 minutes.

TPD runs without the adsorbent under identical experimental conditions indicated that the adsorption of aromatic hydrocarbons on the column walls was negligibly small.

1.2.6 References

1. Beck, J. S.; Vertuli, J. C.; Roth, W. J.; Leonowicz, M. E.; Kresge, C. T.; Schmitt, K. D.; Chu, C. TW.; Olson, D. H.; Sheppard, E. W.; McCullen, S. B.; Higgins, J. B.; Schlenker, J. L., *J. Am. Chem. Soc.*, **114** (1992) 10834.
2. Gregg, S. J.; Sing, K. S. W., in *"Adsorption, Surface Area and Porosity"*, *Academic Press* London, (1982) Ch. 4.
3. Barrettt, E. P.; Joyner, L. G.; Halenda, P. H., *J. Am. Chem. Soc.*, **73** (1951) 373.
4. Hartmann, S. R.; Hahn, E. L.; Phys. Rev. **128** (1962) 2042.
5. Choudhary, V. R.; Nayak, V. S., *Appl. Catal.*, **4** (1982) 31.
6. Kipping, P. J.; Winter, D. G., *Nature (London)*, **205** (1965) 1002.

Chapter 1.3

RESULTS AND DISCUSSION

1.3.1 ADSORPTION OF AROMATIC HYDROCARBONS ON HIGHLY SILICEOUS MCM-41

1.3.2 TEMPERATURE PROGRAMMED DESORPTION OF BENZENE ON MESOPOROUS Si-MCM-41, Na- AlSi-MCM-41 AND H-AlSi-MCM-41

1.3.3 TEMPERATURE PROGRAMMED DESORPTION OF TOLUENE, P-XYLENE, MESITYLENE AND NAPHHALENE ON MESOPOROUS HIGH SILICA MCM-41

1.3.4 TEMPERATURE PROGRAMMED DESORPTION OF TOLUENE, P-XYLENE, MESITYLENE AND NAPHTHALENE ON Na-AlSi-MCM-41 AND H-AlSi-MCM-41

1.3.1 ADSORPTION OF AROMATIC HYDROCARBONS ON HIGHLY SILICEOUS MCM-41

1.3.1.1 Background and Brief Description of Earlier Work

MCM-41 is a member of a new family of silicate mesoporous material, designated as M41S, containing hexagonal arrays of uniform channels with 2 to 10 nm in diameter.[1,2] It can be synthesized in its high silica form (Si-MCM-41) and also in its high alumina form (Al-MCM-41).[3,4] Unlike Al-MCM-41,[5] Si-MCM-41 is stable towards thermal treatment upto 973 K, hydrothermal treatment with steam at mild conditions, mechanical grinding and also towards acid treatment at mild conditions.[6] Because of its high surface area ($\geq$ 1100 m^2 g^{-1}) and adsorption capacity,[7,8] high thermal/hydrothermal stability,[6] and mesoporous channels, Si-MCM-41 has high potential for practical use as an adsorbent both for small and bulky adsorbate molecules. Therefore, it is of great scientific and practical interest to explore the adsorption properties of Si-MCM-41 for different adsorbates. However, studies reported on the adsorption of hydrocarbons, particularly bulkier ones, are scarce.

Adsorption of N_2[1,3,9-13] and water[9,14-17] on MCM-41 has been thoroughly investigated. A few studies have also been reported on the adsorption of hydrocarbons, such as benzene[7,18,19] toluene[20] cyclopentane,[21,22] cyclohexane,[16,21-24] propane[25] and methane[26] on MCM-41. Rathousky et al.[21] and Franke et al.[22] have thoroughly studied the effect of temperature on the adsorption of cyclohexane on MCM-41. Beck et al.[7] have measured benzene adsorption isotherms at 298 K on Al-MCM-41 for studying the capillary condensation at higher benzene partial pressures. Boger et. al.[20] have reported studies on the adsorption isotherms for toluene (at 303 – 353 K), alcohols (at 333 K) and N_2 (at 77 K) on MCM-41. Very recently, Nguyen et

al.[18] have studied benzene adsorption isotherms (at 273 – 303 K) on a series of Si-MCM-41 samples, prepared by using surfactants with various carbon chain lengths, for studying the effect of temperature on capillary condensation process and hysteresis in the adsorption. Janchen et al.[19] have also studied adsorption isotherms of benzene on Al-MCM-41. However, no detailed investigation on the adsorption isotherms (above room temperature) and thermodynamics of adsorption of aromatic hydrocarbons on Si-MCM-41 is reported so far.

The present work was undertaken with the objective of measuring adsorption isotherms and studying the thermodynamics of adsorption (viz. heat of adsorption, entropy change associated with the adsorption, etc.) for different aromatic hydrocarbons (viz. benzene, toluene, p-xylene and mesitylene) on Si-MCM-41. For this purpose, the hydrocarbon adsorption isotherms at different temperatures (348 – 498 K) on Si-MCM-41 were measured using the GC peak maxima technique.[27]

1.3.1.2 Present Work

1.3.1.2.1 Characterization of Si-MCM-41

The XRD profile of calcined Si-MCM-41 is shown in Fig. 1.3.1.1. The MCM-41 structure[1,7] of the synthesized Si-MCM-41 material was confirmed by observing a typical four peak pattern[7] with a very prominent (100) reflection at low angle (2θ = 2-3^{o}) and three weaker (110), (200) and (210) reflections. The presence of four peaks indicates that the material posses a long range order in hexagonal symmetry[7].

N_2 sorption isotherm and pore size distribution of Si-MCM-41 are shown in Figs. 1.3.1.2a and 1.3.1.2b. The BET surface area, average pore diameter and pore

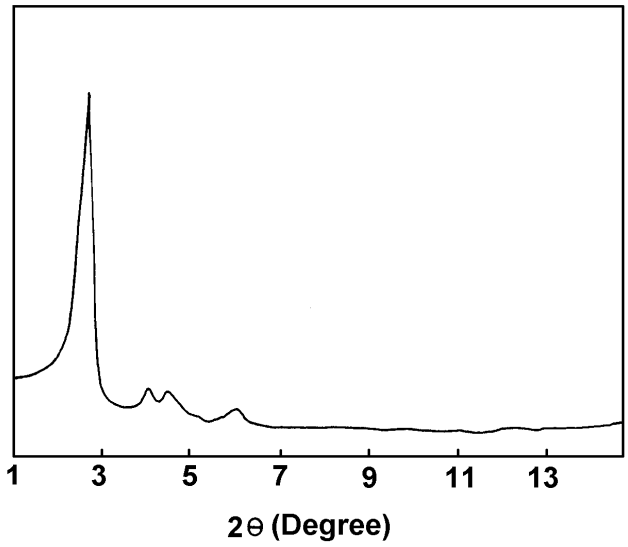

Fig. 1.3.1.1 Powder X-ray diffraction spectra of Si-MCM-41 (calcined)

volume of the material were found to be 1160 m^2 g^{-1}, 2.5 nm and 0.95 cm^3 g^{-1}, respectively. According to IUPAC classification, the isotherms of Si-MCM-41 are of type IV.[28] The isotherms exhibit three stages; the first stage is a linear part going through the origin, which is due to monolayer adsorption of N_2 on the walls of the mesopores (p/p_0 range of 0.22 – 0.38) due to capillary condensation in the mesopores. This part shows hysteresis. The p/p_0 value at which the inflection starts is related to the diameter of the mesopores. The sharpness in this step indicates the uniformity of the pore size distribution.[5] The third stage in the adsorption isotherm is an almost horizontal part after the relative pressure p/p_0 of ~0.38 and is due to multiplayer adsorption on the outer surface of the particles.[5] In addition, a hysteresis loop at relative pressure $p/p_0 > 0.8$ corresponds to capillary condensation in the interparticle pores.[28,29] A linear increase in adsorption at low pressures is observed followed by

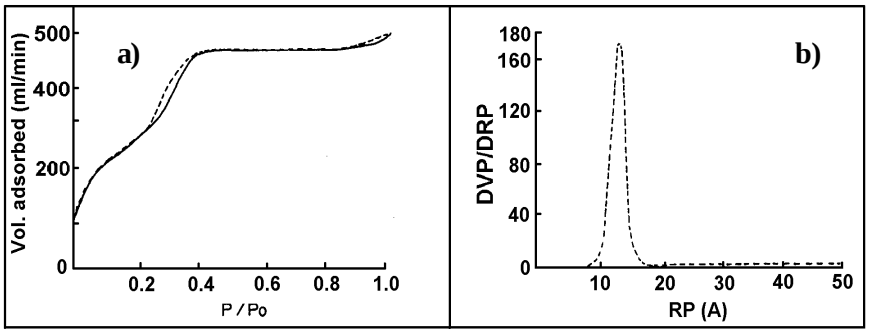

Fig. 1.3.1.2 a) N_2 adsorption-desorption isotherms and pore size distribution of Si-MCM-41

a steep increase in nitrogen uptake (at a relative pressure of p/p_0 = 0.31 – 0.41) due to capillary condensation inside the mesopores (Figs. 1.3.1.2a). This sharp step of the isotherm indicates the narrower pore size distribution.

Figures 1.3.1.3a and 1.3.1.3b present the transmission electron micrograph (TEM) and scanning electron micrograph (SEM) of Si-MCM-41, respectively. TEM micrograph shows a reasonably regular array of channels in hexagonal arrangement.

Scanning electron microscope was used to determine the particle size and morphology of the Si-MCM-41. Figure 1.3.1.3b shows the presence of nearly uniform microcrystalline particles.

^{29}Si MAS NMR spectra of the sample showed bands at −110 ppm and −102 ppm, corresponding to the Q(4Si) and Q(3Si, OH) resonance (Figs. 1.3.1.4a), respectively. ^{1}H – ^{29}Si CP MAS NMR spectra (Fig. 1.3.1.4b) showed that, as in amorphous silica, part of the silicon atoms of the Si-MCM-41 exists as silanol groups, which is consistent with that observed earlier.[30]

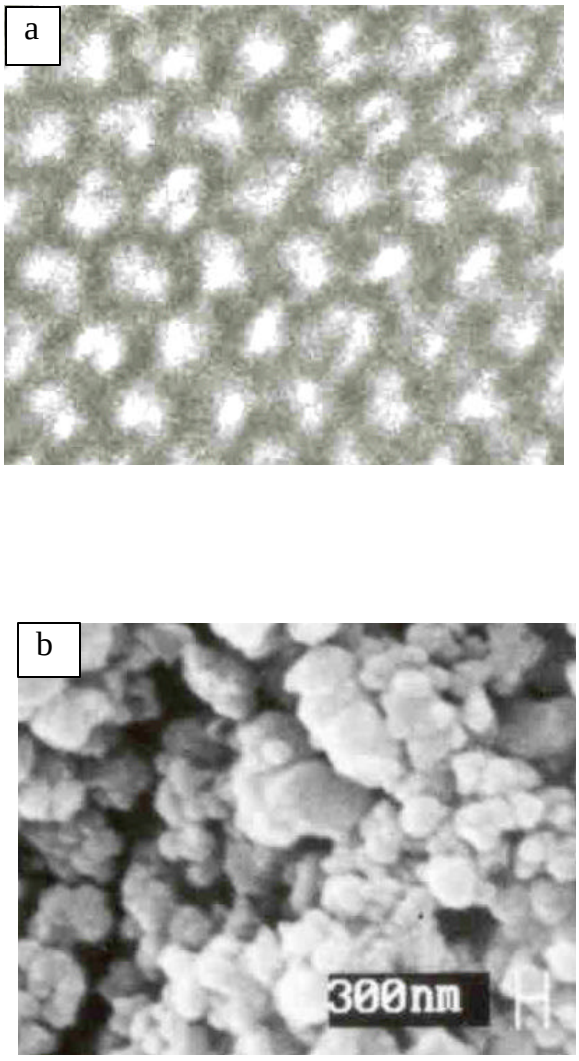

Fig. 1.3.1.3 a) Transmission electron micrographs and b) scanning electron micrographs of Si-MCM-41.

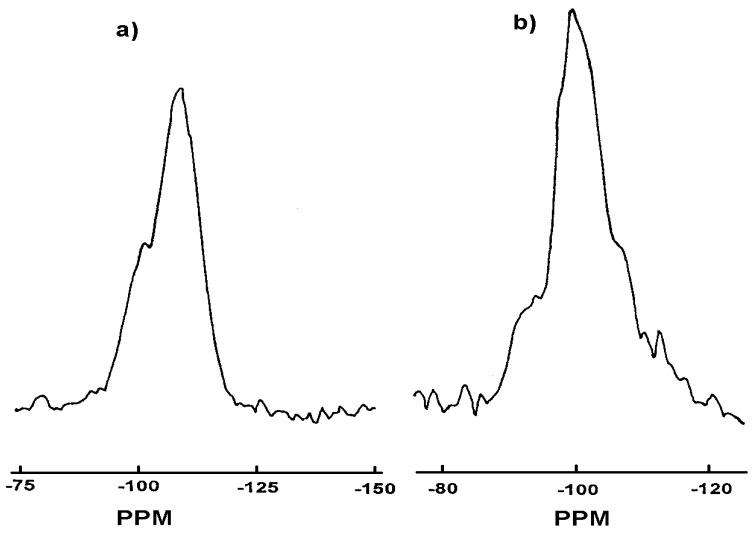

Fig. 1.3.1.4 ^{29}Si MAS NMR spectra (a) and ^{1}H – ^{29}Si CP MAS NMR spectra (b) of calcined Si-MCM-41.

1.3.1.2.2 Adsorption Isotherms of Aromatic Hydrocarbons

1.3.1.2.2.1 Estimation of adsorption data

A representative set of superimposed chromatographic elution curves for benzene on the Si-MCM-41 at 348 K is given in Fig. 1.3.1.5. It can be seen that the desorption edges of the elution peaks (obtained by injecting different amounts of benzene from 0.3 µl to 10.0 µl) show a strong dependence on the amount of adsorbate injected. This is true at all the data collected.

The peak maxima method[27] was employed for estimating the adsorption isotherm from the pulse data. In this method, the isotherm is determined from the maxima of a number of peaks of different heights (obtained by injecting varying amounts of adsorbate under the same experimental conditions), by superimposing all the chromatograms on each other and drawing a curve through the peak maxima as shown in Fig. 1.3.1.5. The curve is then used as if it were a desorption branch (or

diffused front boundary) of the elution curve and the adsorption isotherm estimated from it. By doing this it is also possible to minimize the effect of longitudinal diffusion, conventional mixing and mass transfer. This method therefore gives a more accurate estimate of the isotherm than the single injection method. The detailed procedure for the estimation of adsorption data from superimposed elution curves by the pulse maxima method has been given elsewhere.[31]

The amount of benzene adsorbed reversibly is calculated from

$$q_r = S_A/(sw) \qquad (1.3.1.1)$$

Where S_A is the shaded area (cm^2) ABDC under the curve in Fig. 1.3.1.5, s is the recorder sensitivity ($cm^2\ mmol^{-1}$) and w is the weight of the adsorbent (g).

The partial pressure, p (kPa) of benzene in the mobile phase is estimated from the relation

$$p = (hcRT)/(sF) \qquad (1.3.1.2)$$

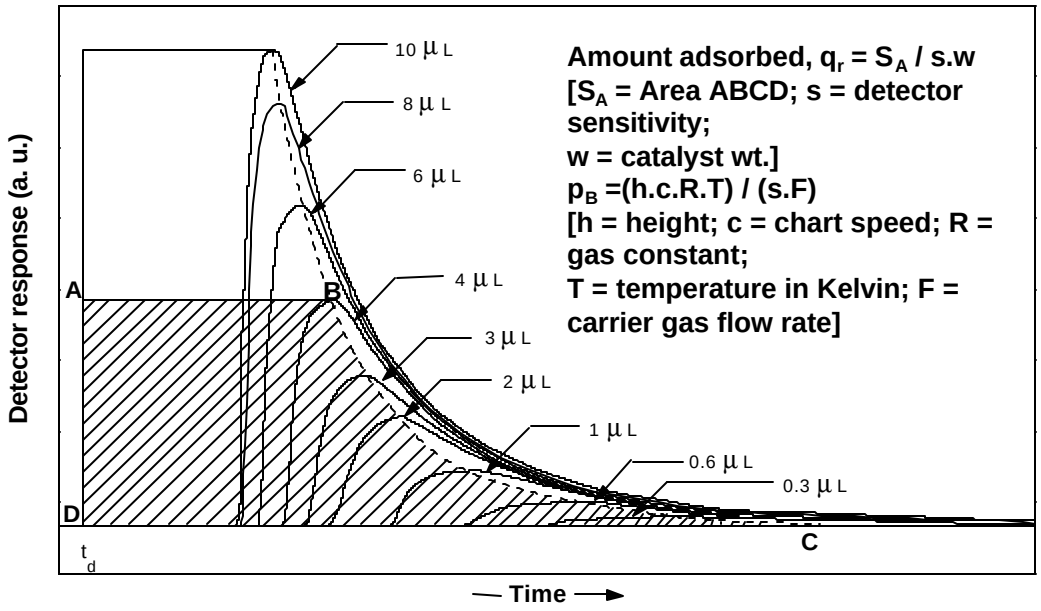

Fig. 1.3.1.5 Representative elusion peaks of benzene pulses of different sizes (superimposed on each other) on Si-MCM-41 at 348 K.

where h is height (cm), c is chart speed (cm s^{-1}), R is gas constant, T is column temperature and F is the Volumetric flow rate corrected for column conditions (cm^3 min^{-1})

Isotherms of the reversible adsorption of benzene, toluene, p-xylene and mesitylene at different temperatures are presented in Figs. 1.3.1.6 - 1.3.1.9. The pulse maxima method[27] was employed for evaluating the adsorption isotherms from the pulse data as the desorption edges of the elution curves for the adsorbates on the Si-MCM-41 at all the temperatures showed a strong dependence on the amount of adsorbate injected. The adsorption isotherm data for all the adsorption at different temperatures were obtained from the respective superimposed chromatographic elution curves by the procedure given above.

1.3.1.2.2.2 Fitting of adsorption data

Several attempts have been made to derive a standard sorption equation, which can satisfy the data on sorption in zeolites under all conditions. Although many of the equations have some degree of broad applicability, no universal adsorption equation has been arrived at.[32]

All the data for the adsorption of benzene, toluene, p-xylene and mesitylene (Figs. 1.3.1.6 – 1.3.1.9) could be fitted very well to the Freundlich adsorption equation,

$$q_r = k\, p^{1/n} \qquad \text{(where } n > 1\text{)} \qquad (1.3.1.3)$$

or $$\log q_r = \log k + (1/n) \log p \qquad (1.3.1.4)$$

(where q_r is the amount adsorbed reversibly, p is the adsorbate pressure, k is the Freundlich adsorption constant, and 1/n is the exponent to the adsorbate pressure). The linear Freundlich plots (log q_r vs. log p) for all the adsorbates are presented in

Figs. 1.3.1.10 and 1.3.1.11. Efforts were also made to fit the adsorption data to the Langmuir adsorption equation,

$$q_r = (\alpha p / (1 + \alpha p)\, q_m \qquad (1.3.1.5)$$

or $$p/q_r = [1 / \alpha q_m)] + p / q_m \qquad (1.3.1.6)$$

[where q_m is the maximum adsorption capacity (mmol g^{-1}), α is the Langmuir adsorption constant (kPa^{-1})]. However, the p/q_r vs. p plots for the adsorption of all the adsorbates, according to the Langmuir equation, are found to be non linear (Appendix 1 – 4). This shows that the adsorption of benzene, toluene, p-xylene and mesitylene on Si-MCM-41 does not follow the Langmuir type of adsorption.

The Freundlich parameters (k and n) for the adsorption of benzene, toluene, p-xylene and mesitylene are presented in Table 1.3.1.1. The temperature dependence of Freundlich adsorption constant (k) for the different adsorbates is shown in Fig. 1.3.1.12. The linear plots of log k vs. 1/T indicate a good fit of the data to the equation:

$$k = \alpha \exp (\beta/RT) \qquad (1.3.1.7)$$

The values of the parameters α and β for the adsorption of aromatic hydrocarbons are presented in Table 1.3.1.2. The Freundlich parameter, n, shows little or no temperature dependence and it is found to be more or less the same (about 1.36 ± 0.03) for all the adsorbates.

For all the adsorbates, the adsorption data could not be fitted to the Langmuir adsorption model, indicating non-homogeneity of the adsorption sites. This is consistent with the fact that the adsorption data for all the adsorbates gave an excellent fit to the Freundlich equation.

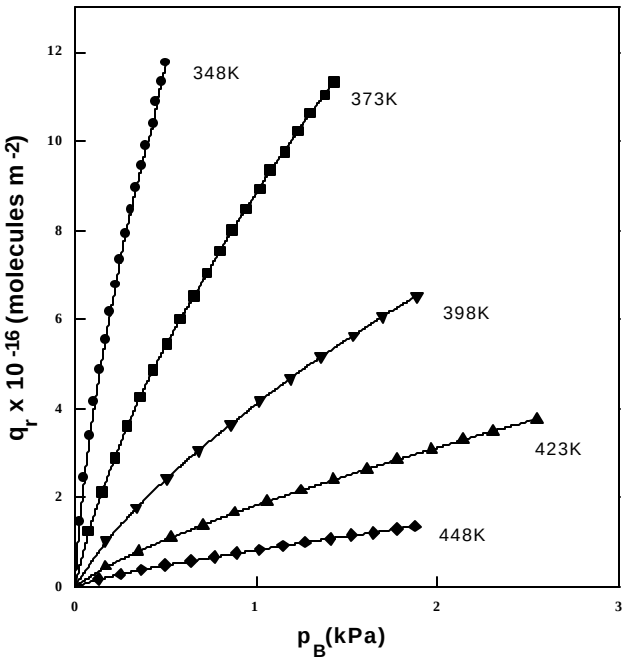

Fig. 1.3.1.6 Adsorption isotherm of benzene on Si-MCM-41 at different temperatures (p_B = partial pressure of benzene).

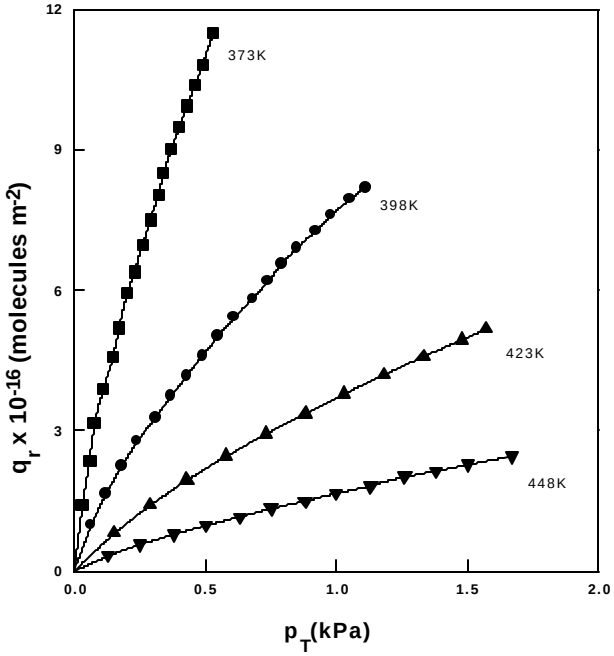

Fig. 1.3.1.7 Adsorption isotherm of toluene on Si-MCM-41 at different temperatures (p_T = partial pressure of toluene).

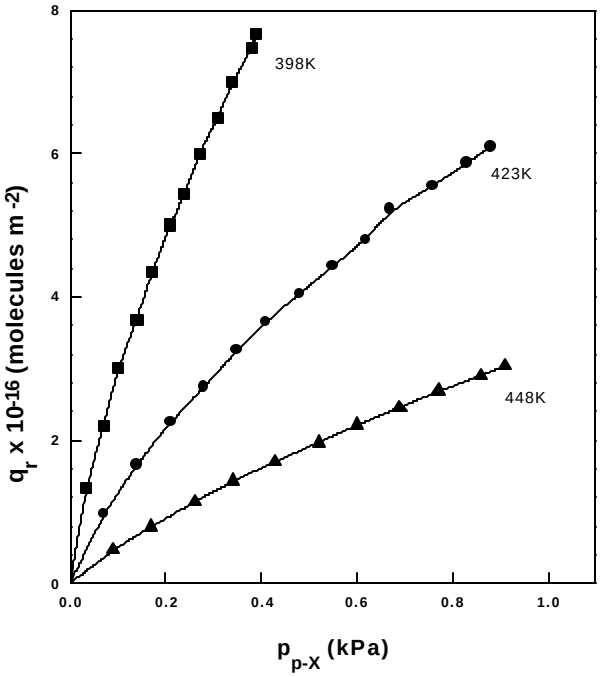

Fig. 1.3.1.8 Adsorption isotherm of p-xylene on Si-MCM-41 at different temperatures ($p_{p\text{-}X}$ = partial pressure of p-xylene).

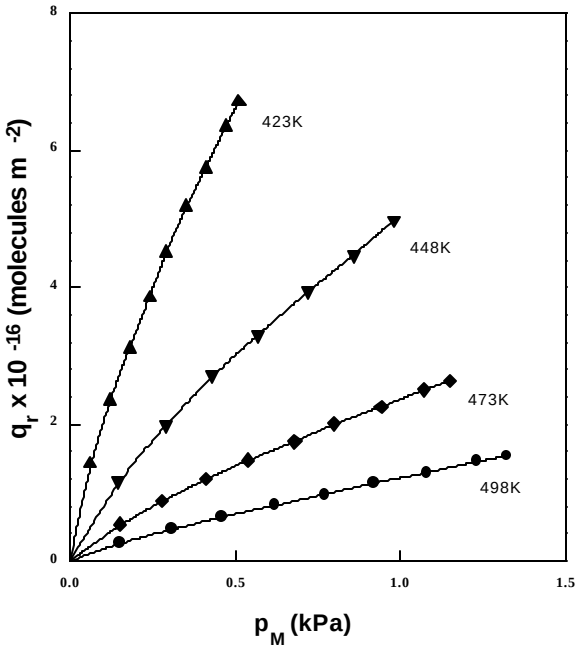

Fig. 1.3.1.9 Adsorption isotherm of mesitylene on Si-MCM-41 at different temperatures (p_M = partial pressure of mesitylene)

Although the Freundlich equation is empirical, it is quite useful for fitting adsorption data on a non-homogeneous surface with site energy distribution in a narrow range of adsorbate concentration. However, because of its empirical nature no direct information, such as heats of adsorption, can be obtained from the temperature dependence of the Freundlich adsorption parameter k.

1.3.1.2.2.3 Isosteric heat of adsorption

The isosteric heat of adsorption at different adsorbate loadings was evaluated from the adsorption isotherm data (Figs. 1.3.1.6-1.3.1.9) by means of the Clausius – Clapeyron equation[33]:

$$\log p = E - Q_a/(2.303\ RT) \qquad (1.3.1.8)$$

where p and T are the equilibrium pressure and temperature at a specific adsorbate loading, R is the gas constant and E is a constant.

Figure 1.3.1.13 shows the dependence of the isosteric heat of adsorption (Q_a) of benzene, toluene, p-xylene and mesitylene on the adsorbate loading. The isosteric heat of adsorption were obtained from the slope of the linear plots of logoff the pressure vs. the reciprocal of the absolute temperature at a constant sorbate loading by means of the above Clausius – Clapeyron equation [Eqn. 1.3.1.8]. The heat of adsorption of benzene, toluene, p-xylene and mesitylene on the Si-MCM-41 is in the following order: mesitylene > p-xylene > toluene > benzene, which is consistent with what is expected according to the ionization potential of the adsorbates. The ionization potential of adsorbates is in the following order[34]: benzene (9.3 eV) > toluene (8.8 eV) > p-xylene (8.5 eV) > mesitylene (8.4 eV). An increase in the molecular weight can also result in an increase in the heats of adsorption because of

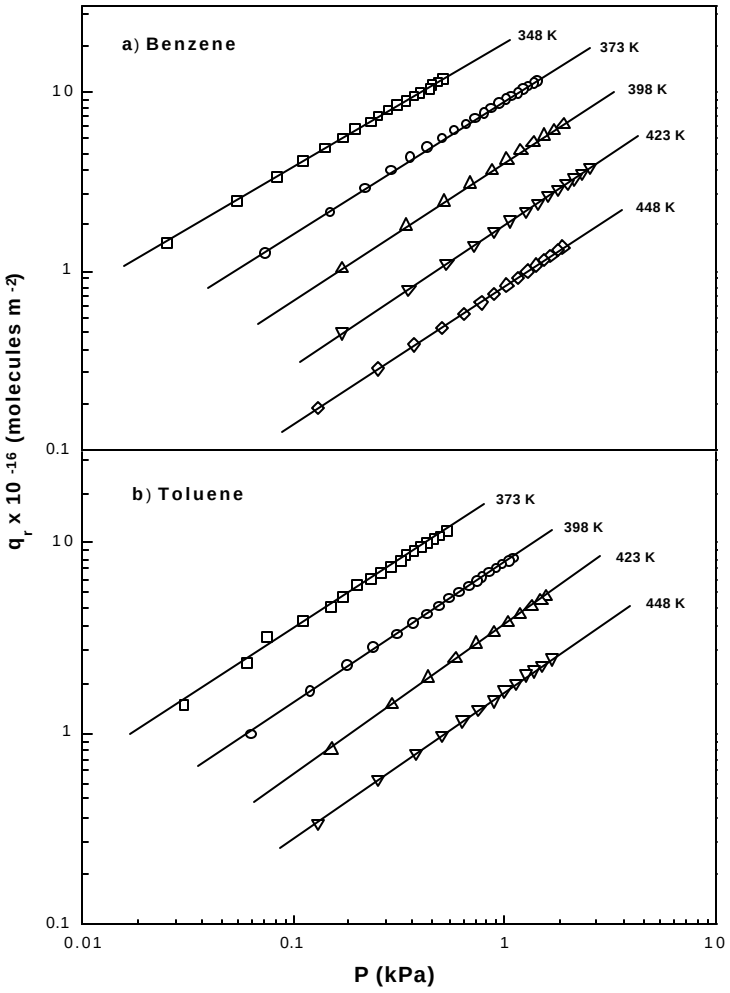

Fig. 1.3.1.10 Freundlich plots for adsorption of a) benzene and b) toluene on Si-MCM-41 at different temperatures

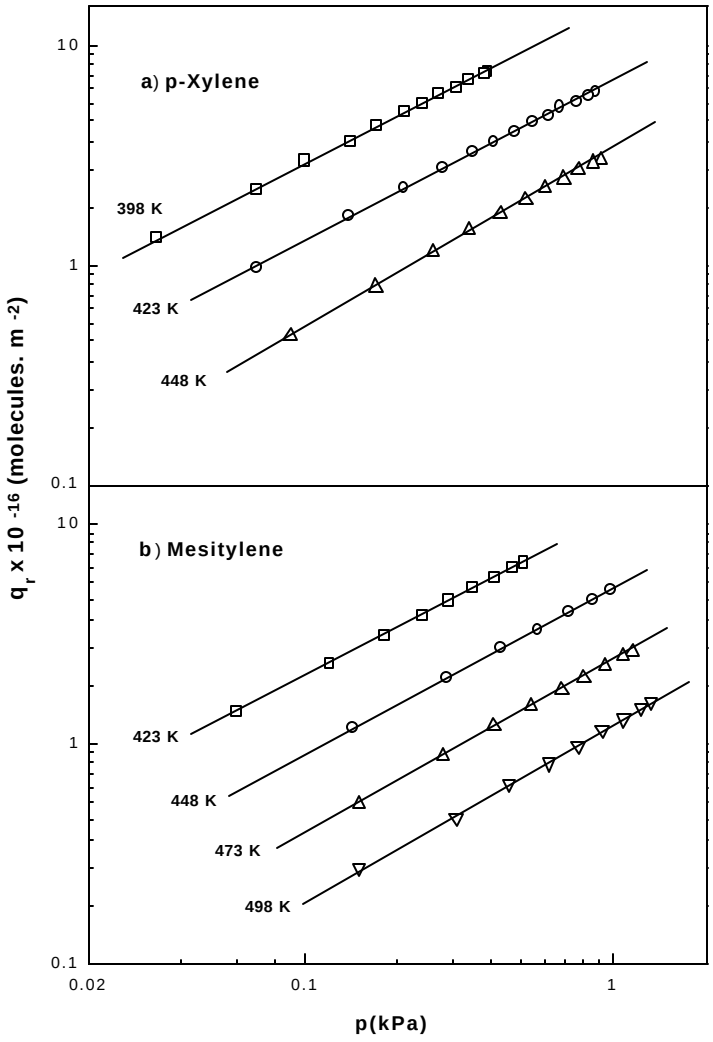

Fig. 1.3.1.11 Freundlich plots for adsorption of a) p-xylene and b) mesitylene on Si-MCM-41 at different temperatures

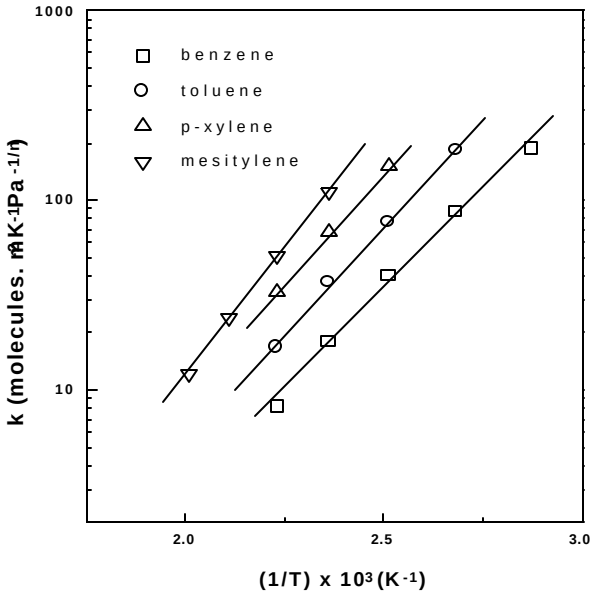

Fig. 1.3.1.12 Temperature dependence of the Freundlich constant (k) for the adsorption of benzene, toluene, p-xylene and mesitylene.

the increased dispersion forces. However, in the present case, the increase in the heats of adsorption is too large to be caused merely due to the increased dispersion forces. The presence of increased number of methyl groups attached to aromatic nucleus of the adsorbates causes an increase in the electron density in the aromatic ring, and consequently causes a decrease in the ionization potential, depending upon the number of methyl groups.

For all the adsorbates, the heat of adsorption is decreased with increasing the adsorbate loading. The initial sharp decrease in Q_a for p-xylene and mesitylene may be due to site heterogeneity. However, the continuous slow decrease in the Q_a at higher adsorbate loadings is expected due to repulsive interactions between the

Table 1.3.1.1 Freundlich parameters for adsorption of benzene, toluene, p-xylene and mesitylene on Si-MCM -41.

Adsorbate	Temperature (K)	k x 10^5 (mol $g^{-1}kPa^{-1}$)	n
Benzene	348	36.3	1.36
	373	17.0	1.35
	398	7.8	1.33
	423	3.5	1.33
	448	1.6	1.34
			(average = 1.34)
Toluene	373	35.5	1.37
	398	14.8	1.37
	423	7.1	1.35
	448	3.2	1.36
			(average = 1.36)
p-Xylene	398	28.8	1.39
	423	13.2	1.39
	448	6.3	1.38
			(average = 1.387)
Mesitylene	423	21.4	1.37
	448	9.8	1.36
	473	4.6	1.33
	498	2.3	1.34
			(average = 1.35)

Table 1.3.1.2 Arrhenius parameters (a and b) for the adsorption of aromatic hydrocarbons on Si-MCM -41

Adsorbate	α x 10^5 (mol g^{-1} $kPa^{-1/n}$)	β (kJ mol^{1})
Benzene	33.1	41.0
Toluene	28.0	44.0
p-Xylene	37.1	45.0
Mesitylene	87.1	51.7

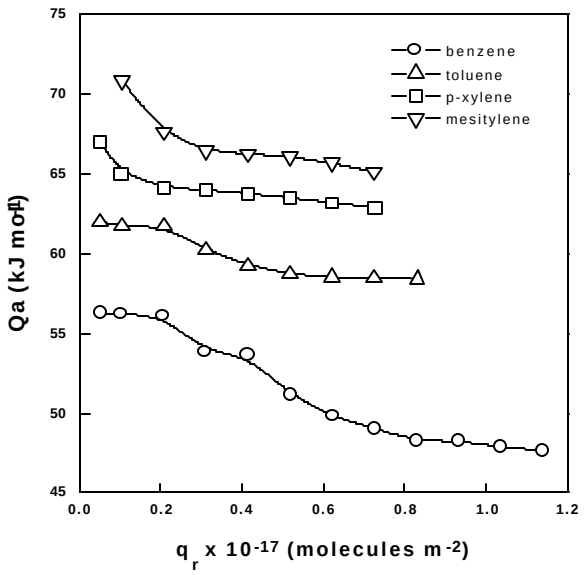

Fig. 1.3.1.13 Dependence of heat of adsorption (Q_a) on surface coverage (q_r) for the adsorption of benzene, toluene, p-xylene and mesitylene.

adsorbed aromatic hydrocarbon molecules. In case of benzene adsorption, the dependence of Q_a on the adsorbate loading is quite complex; the decrease of the Q_a is very small, large and small at lower, intermediate and higher adsorbate loadings, respectively. The large decrease in the Q_a at the intermediate adsorbate loading indicates a surface heterogeneity induced by the adsorbed benzene. Earlier, a similar observation has also been made in the case of benzene TPD over the same Si-MCM-41 material.[40] The Q_a vs. q_r curve for toluene also shows a trend somewhat similar to that for benzene. However, the decrease in the Q_a for the toluene adsorption at the intermediate adsorbate loading is smaller.

1.3.1.2.2.4 Gibb's free energy and entropy changes in adsorption

The thermodynamic data for the adsorption of benzene, toluene, p-xylene and mesitylene on the Si-MCM-41 at the different adsorbate loading are presented in

Tables 1.3.1.3 – 1.3.1.6. The thermodynamic data were evaluated from the adsorption isotherm data (Figs 1.3.1.6 – 1.3.1.9) using the following relations:

$$\Delta G = - RT \ln P/p \qquad (1.3.1.9)$$

$$\Delta G = \Delta H - T\Delta S \qquad (1.3.1.10)$$

$$S_a = S_g + \Delta S \qquad (1.3.1.11)$$

where, ΔG, ΔH (which is equal to isosteric heat of adsorption under isothermal conditions, neglecting gas imperfections) and ΔS are the standard free energy, enthalpy and entropy changes in the adsorption process, respectively; S_g is the entropy of the adsorbate vapor at the standard pressure P; S_a is the entropy of adsorbed phase; P and p are the equilibrium pressures of adsorbate phase in a standard state and the state at which the studies were conducted, respectively. The standard state pressure (P) is taken as 101.32 kPa. The values of S_g for the various adsorbates were taken from the data given elsewhere.[35]

The examination of the thermodynamic data (Tables 1.3.1.3 – 1.3.1.6) indicated that, in the adsorption of benzene, toluene, p-xylene and mesitylene, the free energy change ($-\Delta G$) decreases with increasing the adsorbate loading and the temperature. The entropy change ($-\Delta S$) also shows a variation with adsorbate loading but it is influenced to a lesser extent by the adsorbate loading and also by the adsorption temperature. For the adsorption of all the aromatic hydrocarbons, S_a, and consequently the mobility of the adsorbate phase, decreases with increasing the adsorbate loading (except for benzene), but increases with increasing the adsorption temperature. However, for the adsorption of benzene, the dependence of S_a on the adsorbate loading is complex; S_a passes through minimum and maximum with increasing the adsorbate loading (Table 1.3.1.3).

The values of the translational entropies of the three-dimensional (S_{t3D}) and two-dimensional (S_{t2D}) vapors of the adsorbates at different temperatures are given in Table 1.3.1.7. these values were obtained from the expressions[36,37]:

$$S_{t3D} = R \ln (M^{1.5}. T^{2.5}) - 9.61 \quad (1.3.1.12)$$

$$S_{t2D} = 0.667 S_{t3D} + 2.76 \ln T - 12.71 \quad (1.3.1.13)$$

where, M is the molecular weight and T is the temperature. The change of entropy in the adsorption for the mobile and localized adsorption models (with no loss of rotational degrees of freedom of adsorbed molecules) is expected to be equal to ($S_{t3D} - S_{t2D}$) and S_{t3D}, respectively. The values of the entropy change for two adsorption models are included in Table 1.3.1.7. The estimated values of the entropy change in the adsorption of benzene, toluene, p-xylene and mesitylene are 52.5 ± 0.5, 53.4 ± 0.4, 54.1 ± 0.2 and 55.5 ± 0.6, respectively, for the mobile adsorption (i. e., $S_{t3D} - S_{t2D}$) and 169 ± 3, 172 ± 2, 174 ± 2 and 177 ± 2, respectively, for the localized adsorption (i. e., S_{t3D}). It may be noted that although the S_{t3D} and S_{t2D} increase with temperature (the increase is, however, small), ($S_{t3D} - S_{t2D}$) and consequently the entropy change in the mobile adsorption is almost independent of temperature.

The observed entropy change ($-\Delta S_m$) associated with the adsorption (after correcting for the contributions for the entropy change in the vapor phase) at the different adsorbate loadings, were obtained from the observed ΔS, averaged over the adsorption temperature range, using the relation[36]:

$$\Delta S_m = \Delta S + R \ln (A^*/A) \quad (1.3.1.14)$$

where A^* is the standard molecular area (equal to 4.08 T x 10^{-16} cm^2) and A is the molecular area of the adsorbate, calculated from the density of the adsorbed liquid using the relation suggested by Emmett and Brunauer.[38]

Table 1.3.1.3 Thermodynamic data for the adsorption of benzene on Si-MCM-41.

Amount adsorbed, q_r (mmol g^{-1})	Temp. (K)	$-\Delta G$ (kJ mol^{-1})	$-\Delta S$ (J K^{-1} mol^{-1})	S_g (J K^{-1} mol^{-1})	S_a (J K^{-1} mol^{-1})
0.01(0.52×10^{16})[a]	348	24.9	90.1	284.3	194.2
	373	24.3	86.0	291.1	205.1
	398	23.2	83.9	297.8	213.9
	423	21.8	81.5	304.7	223.2
	448	19.2	82.8	311.2	228.4
0.02 (1.04×10^{16})	348	24.7	90.3	284.3	194.0
	373	23.1	88.8	291.1	202.3
	398	21.1	88.1	297.8	209.7
	423	18.6	88.9	304.7	215.8
	448	15.9	89.8	311.2	221.4
0.04 (2.07×10^{16})	348	22.8	95.6	284.3	188.7
	373	20.2	96.3	291.1	194.8
	398	18.2	95.2	297.8	202.6
	423	15.5	95.9	304.7	208.8
0.06 (3.12×10^{16})	348	20.8	94.6	284.3	189.7
	373	18.7	94.0	291.1	197.1
	398	16.4	94.0	297.8	203.8
	423	13.7	94.7	304.7	210.0
0.08 (4.15×10^{16})	348	19.8	97.1	284.3	187.2
	373	17.6	96.6	291.1	194.5
	398	15.2	96.5	297.8	201.3
	423	12.5	97.2	304.7	207.5
0.10 (5.19×10^{16})	348	18.8	92.8	284.3	191.5
	373	16.6	92.5	291.1	198.6
	398	14.2	92.7	297.8	205.1
	423	12.1	92.2	304.7	212.5
0.12 (6.23×10^{16})	348	17.9	91.5	284.3	192.8
	373	15.8	91.1	291.1	200.0
	398	13.4	91.5	297.8	206.3
0.14 (7.17×10^{16})	348	17.4	90.9	284.3	193.4
	373	15.0	91.1	291.1	200.0
0.16 (8.31×10^{16})	348	16.8	90.4	284.3	193.9
	373	14.6	90.3	291.1	200.8
0.18 (9.35×10^{16})	348	16.3	91.7	284.3	192.6
	373	14.1	91.6	291.1	199.5

[a] Values in parentheses are molecules.m^{-2}

Table 1.3.1.4 Thermodynamic data for the adsorption of toluene on Si-MCM -41.

Amount adsorbed, q_r (mmol g^{-1})	Temperature (K)	-ΔG (kJ mol^{-1})	-ΔS (J K^{-1} mol^{-1})	S_g (J K^{-1} mol^{-1})	S_a (J K^{-1} mol^{-1})
0.01	373	27.7	92.0	348.2	256.2
	398	27.0	88.1	357.0	268.9
	423	24.8	88.1	365.8	277.7
	448	22.5	88.2	374.6	286.4
0.02	373	26.5	94.6	348.2	253.6
	398	24.4	93.7	357.0	263.3
	423	21.9	94.3	365.8	271.5
	448	19.4	94.6	374.6	280.0
0.04	373	23.9	101.3	348.2	246.9
	398	21.3	101.7	357.0	255.3
	423	18.9	101.2	365.8	264.6
	448	16.2	101.7	374.6	272.9
0.06	373	22.1	102.4	348.2	245.8
	398	19.3	102.8	357.0	254.2
	423	16.9	102.4	365.8	263.4
0.08	373	20.7	103.4	348.2	244.8
	398	18.1	103.4	357.0	253.6
	423	15.6	103.1	365.8	262.7
0.10	373	19.8	104.2	348.2	244.0
	398	17.1	104.6	357.0	252.4
	423	14.6	104.4	365.8	261.4
0.12	373	19.0	105.9	348.2	242.3
	398	16.3	106.2	357.0	250.8
0.14	373	18.3	107.8	348.2	240.4
	398	15.5	107.9	357.0	249.1
0.16	373	17.7	109.1	348.2	239.1
	398	14.9	109.4	357.0	247.6

Table 1.3.1.5 Thermodynamic data for the adsorption of p-xylene on Si-MCM-41.

Amount adsorbed, q_r (mmol g^{-1})	Temp. (K)	$-\Delta G$ (kJ mol^{-1})	$-\Delta S$ (J K^{-1} mol^{-1})	S_g (J K^{-1} mol^{-1})	S_a (J K^{-1} mol^{-1})
0.01	398	29.0	95.4	403.2	307.8
	423	28.1	92.0	412.8	320.8
	448	25.7	92.2	422.1	329.9
0.02	398	26.8	95.9	403.2	307.3
	423	25.3	93.8	412.8	319.0
	448	22.6	94.6	422.1	327.5
0.04	398	24.4	99.8	403.2	303.4
	423	22.2	99.1	412.8	313.7
	448	19.4	99.9	422.1	322.2
0.06	398	22.5	104.3	403.2	298.9
	423	20.1	103.8	412.8	309.0
	448	17.4	104.0	422.1	318.1
0.08	398	21.2	106.9	403.2	296.3
	423	18.6	106.7	412.8	306.1
	448	15.8	107.1	422.1	315.0
0.10	398	20.2	108.8	403.2	294.4
	423	17.6	108.4	412.8	304.4
	448	14.7	109.0	422.1	313.1
0.12	398	19.7	109.3	403.2	293.9
	423	16.8	109.6	412.8	303.2
0.14	398	18.6	111.3	403.2	291.9
	423	15.7	111.5	412.8	301.3

Table 1.3.1.6 Thermodynamic data for the adsorption of mesitylene on Si-MCM-41.

Amount adsorbed, q_r (mmol g^{-1})	Temp. (K)	$-\Delta G$ (kJ mol^{-1})	$-\Delta S$ (J K^{-1} mol^{-1})	S_g (J K^{-1} mol^{-1})	S_a (J K^{-1} mol^{-1})
0.02	423	27.5	102.4	447.3	344.9
	448	25.0	102.3	459.9	357.6
	473	22.2	102.8	472.5	369.7
	498	19.8	103.0	483.0	380.0
0.04	423	24.1	102.7	447.3	344.6
	448	21.5	102.8	459.9	357.1
	473	18.8	103.2	472.5	369.3
	498	16.4	102.8	483.0	380.2
0.06	423	22.2	104.5	447.3	342.8
	448	19.5	104.8	459.9	355.1
	473	16.6	105.3	472.5	367.2
0.08	423	20.9	107.3	447.3	340.0
	448	18.1	107.5	459.9	352.4
	473	15.1	108.2	472.5	364.3
0.10	423	19.8	109.4	447.3	337.9
	448	16.9	109.6	459.9	350.3
0.12	423	18.9	110.5	447.3	336.8
	448	15.9	111.1	459.9	348.8
0.14	423	18.0	111.4	447.3	335.9
	448	14.9	112.0	459.9	347.9

Figure 1.3.1.14 shows a comparison between the observed entropy changes ($-\Delta S_m$) associated with the adsorption at the different adsorbate loadings and the theoretical entropy change ($S_{t3D} - S_{t2D}$) for the mobile film model[36] for the adsorption of benzene, toluene, p-xylene and mesitylene. As the adsorbate loading increases, the entropy change ($-\Delta S_m$) increases continuously for the adsorption of toluene, p-xylene and mesitylene. However, for the adsorption of benzene, the entropy change ($-\Delta S_m$) passes first through a maximum and then through a minimum with increasing the adsorbate loading.

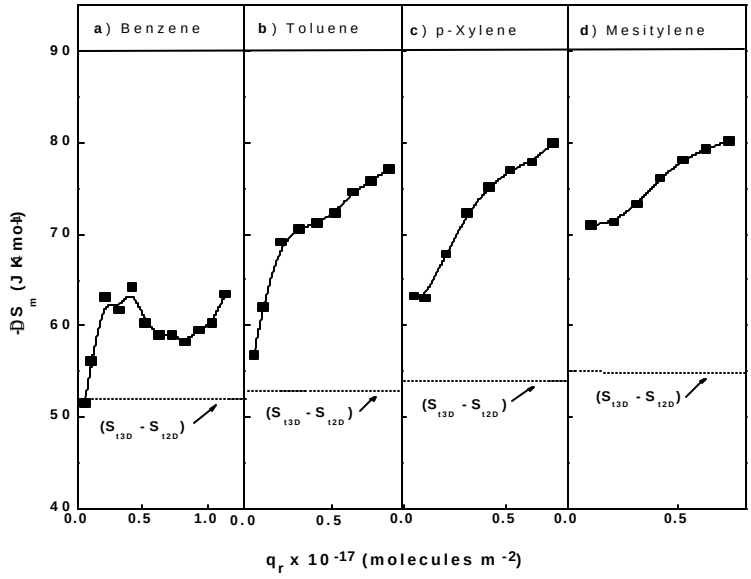

Fig. 1.3.1.14 Comparison of the observed entropy changes, $-\Delta S_m$ (solid line), at different adsorbate loading with the theoretical entropy change for mobile adsorption ($S_{t3D} - S_{t2D}$) (dotted line) in the adsorption of (a) benzene, (b) toluene, (c) p-xylene and (d) mesitylene on Si-MCM-41

Table 1.3.1.7 Theoretical entropy change in the mobile and localized adsorption of benzene, toluene, p-xylene and mesitylene.

Sorbate	Temp. (K)	S_{t3D} (J K^{-1} mol^{-1})	S_{t2D} (J K^{-1} mol^{-1})	Entropy change (J K^{-1} mol^{-1})	
				Mobile adsorption ($S_{t3D} - S_{t2D}$)	Localized adsorption (S_{t3D})
Benzene	348	166.4	114.4	52.0	166.4
	373	167.8	115.6	52.2	167.8
	398	169.2	116.6	52.6	169.2
	423	170.4	117.7	52.7	170.4
	448	171.6	118.6	53.0	171.6
Toluene	373	169.9	116.9	53.0	169.9
	398	171.2	118.0	53.2	171.2
	423	172.5	119.0	53.5	172.5
	448	173.7	120.0	53.7	173.7
p-Xylene	398	173.0	119.2	53.8	173.0
	423	174.3	120.2	54.1	174.3
	448	175.5	121.2	54.3	175.5
Mesitylene	423	175.8	121.2	54.6	175.8
	448	177.0	122.2	54.8	177.0
	473	178.1	123.1	55.0	178.1
	498	179.2	123.9	55.3	179.2

For the adsorption of all the aromatic hydrocarbons, except that for benzene at very low adsorbate loading ($q_r \leq 1.04 \times 10^{16}$ molecules m^{-2}), the observed entropy change ($-\Delta S_m$) is higher than the theoretical entropy change in the mobile adsorption ($St_{3D} - S_{t2D}$) but much lower than the theoretical entropy change in the localized adsorption (S_{t3D}). These observations clearly indicate that

- the adsorption of benzene at the very low adsorbate loading ($\leq 1.04 \times 10^{16}$ molecules m^{-2}), is completely mobile or even supermobile, but
- the adsorption of benzene at higher adsorbate loadings and that of toluene, p-xylene, and mesitylene at both the low and high adsorbate loadings are not completely mobile though not localized.

Figures 1.3.1.15 and 1.3.1.16 show the influence of temperature and adsorbate loading on the entropy of vibration (S_{vib}) of adsorbed molecules for the different adsorbates. The values of S_{vib} at the different temperatures and adsorbate loadings were estimated,[39] as follows:

$$(S_{vib})_{T,q_r} = (S_a)_{T,q_r} - (S_{t2D})_T \qquad (1.3.1.15)$$

The entropy of vibration for all the adsorbates was found to increase almost linearly with increasing the temperature at all the adsorbate loadings (Fig. 1.3.1.15). It was decreased with increasing the adsorbate loading for the adsorption of toluene, p-xylene and mesitylene. But for the adsorption of benzene, it was passed through a minimum and a maximum with increasing the adsorbate loading. The observed trends for the dependence of S_{vib} on the adsorbate loading for all the adsorbates (Fig. 1.3.1.16) were found to be opposite to that for the variation of $-\Delta S_m$ with the adsorbate loading for the respective adsorbate (Fig 1.3.1.14).

The above observations reveal that the adsorption of all the aromatic hydrocarbons is described by the mobile film model but the two dimensional translational motion parallel to the surface is itself somewhat restricted, as the observed entropy change in all the cases (except for the benzene adsorption at very low adsorbate loading) is greater than the one predicted for the model. This is consistent with the fact that the adsorption data for all the adsorbates could not be fitted in the Langmuir model, indicating the absence of ideal localized adsorption of

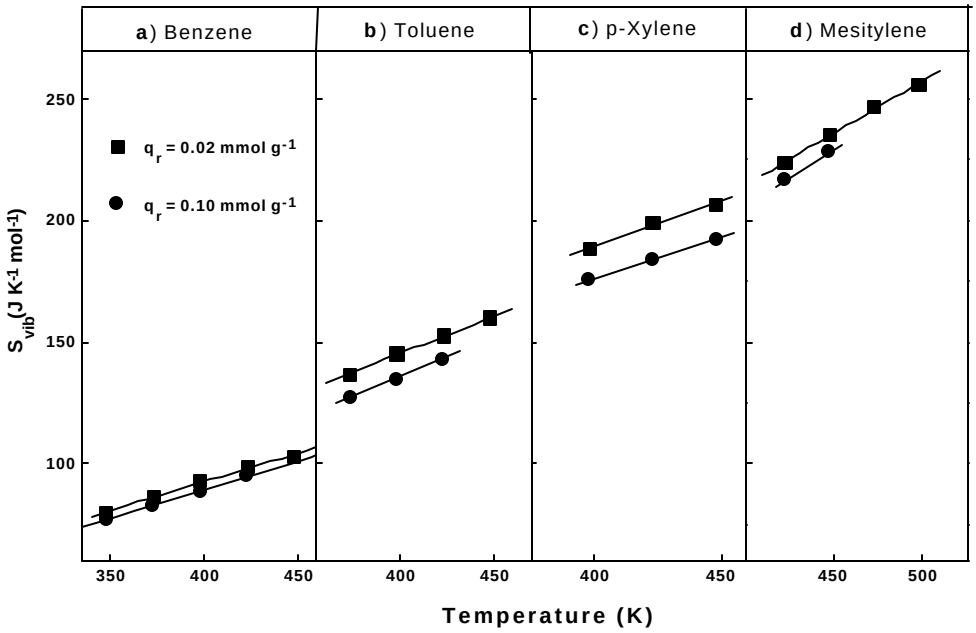

Fig. 1.3.1.15 Temperature dependence of the entropy of vibration (S_{vib}) of adsorbed (a) benzene, (b) toluene, (c) p-xylene and (d) mesitylene at two different (low and high) adsorbate loading.

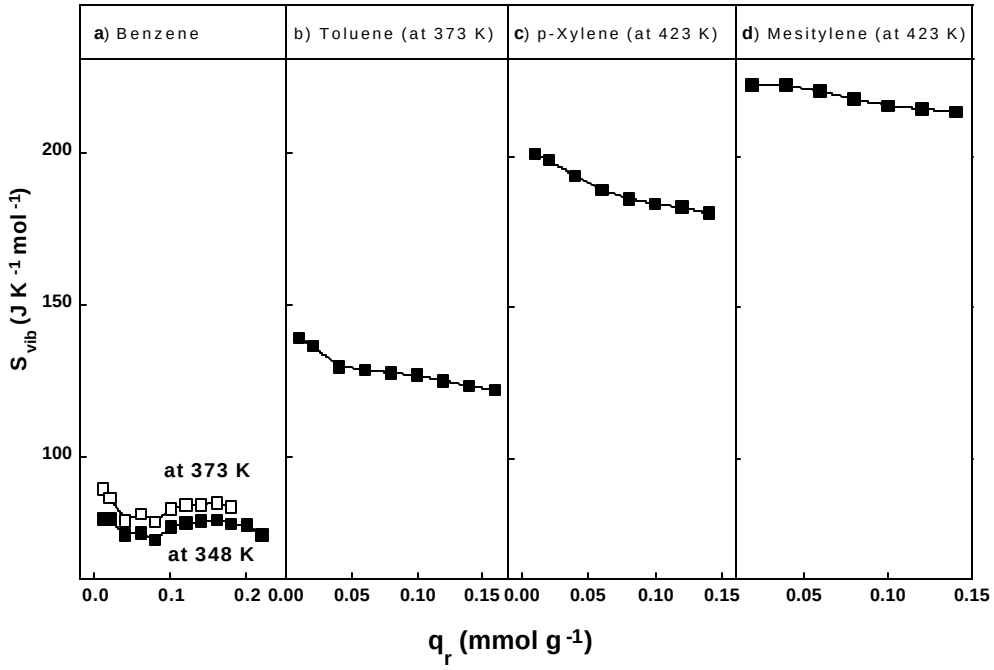

Fig. 1.3.1.16 Influence of adsorbate loading on the entropy of vibration (S_{vib}) of adsorbed (a) benzene, (b) toluene, (c) p-xylene and (d) mesitylene.

the aromatic hydrocarbons on the Si-MCM-41. The entropy change in addition to that entailed by the loss of one degree of translation suggests that some of the rotational degrees of freedom of the adsorbed molecules are lost. It is to be noted that the restriction on the rotation of adsorbed toluene, p-xylene and mesitylene molecules increases markedly, and consequently their mobility decreases, with increasing the adsorbate loading. However, in case of the benzene adsorption, the restriction on the mobility of adsorbed benzene is first increases, then decreases and again increases, and consequently the mobility of adsorbed benzene passes through a minimum and then through a maximum, with increasing the adsorbate loading.

The adsorption of aromatic hydrocarbons results from the interactions of the π-electrons of their aromatic ring with the terminal silanol groups of the Si-MCM-41. The observed unusual dependent of the mobility of adsorbed benzene on the adsorbate loading is attributed most probably to the change in nature and/or energy of the surface sites (terminal silanol groups) present in the channels of Si-MCM-41 due to the presence of adsorbed benzene at different concentrations. Our earlier studies on the TPD of benzene over the Si-MCM-41[40] also indicated the creation and/or modification of surface sites at the higher adsorbate loadings; the TPD peak multiplicity is increased (from two to four peaks) with increasing the adsorbate loading. Whereas, in the TPD of toluene, p-xylene and mesitylene over the Si-MCM-41[41], no TPD peak multiplicity is observed. The observed different behavior of the adsorption of benzene as compared to that of toluene, p-xylene and mesitylene could be explained as follows: Si-MCM-41 has a highly defect structure with at least four types of different terminal Si-OH groups (viz. isolated terminal Si-OH groups and three differently hydrogen bonded terminal Si-OH groups).[42,43] The Si-MCM-41 (used in the present studies) is also found to have a highly defect structure with

different types of terminal silanol groups.[43] At the higher adsorbate loading, the nature and/or energy of the silanol groups, both the isolated and hydrogen bonded ones, is changed, resulting in the observed benzene adsorption behavior. However, for the mono-, di- and tri-methyl benzenes, their aromatic ring is much more rich in electrons than that of benzene, because of the attached electron donating methyl group(s) and hence the alkyl benzenes in their adsorption on the Si-MCM-41 do not distinguish among the different types of terminal silanol groups and/or any small change in the nature and/or energy of the silanol groups – resulted due to the presence of adsorbed aromatic hydrocarbons. Thus the H-bonding between the silanol groups has strong influence on the benzene adsorption but not on the adsorption of the other aromatic adsorbates.

1.3.1.3 Conclusions

From the present studies on the adsorption of benzene, toluene, p-xylene and mesitylene on Si-MCM-41mesoporous adsorbent, following important conclusions can be drawn;

1. The adsorption of all the aromatic hydrocarbons follows Freundlich adsorption model.
2. The isosteric heat of adsorption of all the aromatic hydrocarbons decreases with increasing the adsorbate loading; the decrease in case of the benzene adsorption at intermediate adsorbate loadings is, however, much larger, revealing the surface heterogeneity induced by the adsorbed benzene.
3. For all of the aromatic hydrocarbons, except that of benzene at very low adsorbate loading, the observed entropy change associated with the adsorption ($-\Delta S_m$) is higher than the one predicted for the mobile film adsorption model

but much lower than the one predicted for the localized adsorption model; thus in the adsorption, the two dimensional translational motion parallel to the surface is itself somewhat restricted. The restriction in the adsorption of toluene, p-xylene and mesitylene is increased continuously but that in the adsorption of benzene is passed through a maximum and a minimum with increasing the adsorbate loading.

1.3.1.4 References

1. Kresge, C. T.; Leonowicz, M. E.; Roth, W. J.; Vartuli, J. C.; Beck, J. S. *Nature* **359** (1992) 710.
2. Kresge, C. T.; Leonowicz, M. E.; Roth, W. J.; Vartuli, J. C. *U. S. Pat.*No. **5098684**, (1992).
3. Schmidt, R.; Akporiye, D.; Stocker, M.; Ellestad, O. H. *Stud. Surf. Sci. Catal.,* **84** (1994) 61.
4. Borade, R. B.; Clearfield, A. *Catal. Lett.,* **31** (1995) 267.
5. Luan, Z.; He, H.; Zhou, W.; Cheng, C-F.; Klinovski, J. *J. Chem. Soc. Faraday Trans.* **91** (1995) 2955.
6. Choudhary, V. R.; Sansare, S. D. *Proc. Indian Acad. Sci. (Chem. Sci.),* **109** (1997) 229.
7. Beck, J. S.; Vartuli, J. C.; Roth, W. J.; Leonowicz, M. E.; Kresge, C. T.; Schmitt, K. D.; Chu, C. T.-W.; Olson, D. H.; Sheppard, E. W.; McCullan, S. B.; Higgins, J. B.; Schlenker, J. L. *J. Am. Chem. Soc*. **114** (1992) 10834.
8. Vartuli, J. C.; Kresge, C. T.; Leonowicz, M. E.; Chu, A. S.; McCullan, S. B.; Jhonson, I. D.; Sheppard, E. W. *Chem. Mater*. **6** (1994) 2070.
9. Branton, P. J.; Hall, P. G.; Sing, K. S. W.; Reichert, H.; Schüth, F.; Unger, K. K. *J. Chem. Soc. Faraday Trans.* **90** (1994) 2965.
10. Llewellyn, P. L.; Grillet, Y.; Schüth, F.; Reichert, H.; Unger, K. K. *Microporous Mater.* **3** (1994) 345.
11. Zhu, H. Y.; Zhao, X. S.; Lu, G.Q.; Do, D. D. *Langmuir,* **12** (1996) 6513.
12. Kruk, M.; Jaroniec, M.; Sayari, A. *J. Phys. Chem. B,* **101(4)** (1997) 583.
13. Ravicovitch, P. I.; Wei, D.; Chuch, W. T.; Haller, G. L.; Neimark, A. V. *J. Phys. Chem. B,* **101(19)** (1997) 3671.
14. Llewellyn, P. L.; Schüth, F.; Grillet, Y.; Rouquerol, F.; Rouquerol, J.; Unger, K. K. *Langmuir,* **11** (1995) 574.
15. Cauvel, A.; Brunel, D.; Di, Renzo, F.; Garrone, E.; Fubini, B. *Langmuir,* **13** (1997) 2773.
16. Chen, C.–Y.; Li, H. –X.; Davis, M. E. *Microporous Mater.*, **2** (1993) 17.
17. Branton, P. J.; Hall, P. G.; Sing, K. S. W.; Reichart, H.; Schuth, F.; Unger, K. K. *J. Chem. Soc. Faraday Trans.,* **90** (1994) 2965.

18. Nguyen, C.; Sonwane, C. G.; Bhatia, S. K.; Do, D. D. *Langmuir,* **14** (1998) 4950.

19. Janchen, J.; Stach, H.; Busio, M.; Van Wolput, J. H. M. C. *Thermochim. Acta*, **312** (1998) 33.

20. Boger, T.; Roesky, R.; Glaeser, R.; Ernst, S.; Eigenberger, G.; Wietkamp, J. *Microporous Mater.*, **8** (1997) 79.

21. Rathousky, J.; Zukal, A.; Franke, O.; Schulz-Ekloff, G. *J. Chem. Soc. Faraday Trans.*, **91** (1995) 937.

22. Franke, O.; Schulz-Ekloff, G.; Rathousky, J.; Starech, J.; Zukal, A. *J. Chem. Soc. Chem. Commun*., (1993) 724.

23. Chen, C. – Y.; Xiao, Si. –Q.; Davis, M. E. *Microporous Mater*., **4** (1995) 1.

24. Glaser, R.; Roesky, R.; Boger, J.; Eigerberger, G.; Ernst, S.; Weitkamp, J. *Stud. Surf. Sci. Catal.*, **105A** (1997) 695.

25. Maddox, M. W.; Sowers, S. L.; Gubbins, K. E. *Adsorption,* **2** (1996) 23.

26. Loneva, M. A.; Newman, G. K.; Harwell, J. H. *AIChE, Symp. Ser.*, **309** (1995) 40.

27. Kipping, P. J.; Winter, D. B. *Nature (London),* **205** (1965) 1002.

28. Gregg, S. J.; Sing, K. S. W., "Adsorption, Surface Area and Porosity" Academic Press, London, Ch.4 (1982).

29. Chen, X.; Huang, I.; Li, Q., *J. Phys. Chem. B*, **101** (1997) 8461.

30. Luan, Z.; Cheng, C. – F.; Zhou, W.; Klinowski, J. *J. Phys. Chem.*, **99** (1995) 1018.

31. Choudhary, V. R.; Srinivasan, K. R. *J. Catal*., **102** (1986) 289.

32. Breck, D. W., 'Zeolite Molecular Sieves', John Wiley and Sons, New York, (1974) 593.

33. Breck, D. W. *"Zeolite Molecular Sieves,"* Wiley, New York, (1974) p. 593.

34. Lide, D. R. (Ed.) *"CRC Handbook of Chemistry and Physics"*, **74th Edn.**, CRC Press, London, (1993), p10–208.

35. Stull, D. R.; Westrum, E. F.; Sinke, G, C. *"Chemical Thermodynamics of Organic Compounds."* New York, (1969).

36. Gregg, S. J. *"The Surface Chemistry of Solids*," Chapman & Hall, London, (1961) p. 74.

37. Kemball, C. *Adv. Catal.*,**2** (1950) 233.

38. Emmett, P. H.; Brunauer, S., *J. Am. Chem. Soc.*, **59** (1937) 1553.

39. de Boer, J. H. *"Dynamic Character of adsorption"*; Oxford University Press: London, (1953).

40. Choudhary, V. R.; Mantri, K., *Langmuir*, **16** (2000) 8024.

41. Choudhary, V. R.; Mantri, K. *Microporus and Mesoporous Mater*., **40** (2000) 127.

42. Jentys, A.; Pham, N. H.; Vinek, H. *J. Chem. Soc. Faraday Trans.*, **92** (1996) 3287.

43. Chen, J.; Li, Q.; Xu, R.; Xiao, F. *Angew. Chem. Int. Ed. Engl.*, **34** (1995) 2694.

1.3.2 TEMPERATURE PROGRAMMED DESORPTION OF BENZENE ON MESOPOROUS Si-MCM-41, Na-AlSi-MCM-41 AND H-AlSi-MCM-41

1.3.2.1 Background and Brief Description of Earlier Work

MCM-41[1,2] can be synthesized in its high silica form (Si-MCM-41) and also in its high alumina form (Al-MCM-41).[1-4] The later has a capacity of cation exchange similar to that of zeolites and it can be modified by exchanging its cations with other cations. Because of the presence of tetrahedral Al, H-AlSi-MCM-41 has acid sites with high strength. Its acidity can be reduced or it can be made basic by exchanging its protons with Na^+. Microporous zeolites cannot be used for the acid or base catalyzed reactions involving large molecular size or bulky reactants and/or products. However, since H-AlSi-MCM-41 is mesoporous, its different cation exchanged forms can be used for the reaction involving bulky molecules, particularly in the synthesis of fine chemicals. Recently, Corma and coworkers have reported synthesis of a number of fine chemicals using acidic and basic mesoporous MCM-41 materials[5-8].

Presence of at least four types of different terminal Si-OH groups (which are poorly acidic or non acidic in nature) in the channels of silicate and aluminosilicate MCM-41 has been detected earlier.[9,10] In addition of the terminal Si-OH groups the H^+ form of AlSi-MCM-41 contain acidic surface hydroxyl groups and the Na^+ form of AlSi-MCM-41 contains Na^+ cations in the channels. It is interesting to study the interaction of different aromatic substrates (viz. benzene, toluene, p-xylene, mesitylene and naphthalene), which are used in the synthesis of fine chemicals, with the acidic hydroxyl groups or Na^+ cations and also with the terminal Si-OH groups of these mesoporous materials. Temperature programmed desorption (TPD)[11-14] provides a great deal of information on the active sites, surface heterogeneity and adsorption on

solid catalysts/adsorbents. Studying the interactions of the aromatic hydrocarbons with MCM-41 by the TPD technique is of special interest since these materials have been gaining more and more importance because of their high potential for practical use as adsorbents, catalysts, and/or mesoporous supports for depositing active catalyst components. A few TPD studies on MCM-41 type zeolites have been performed for measurement of the acidity with ammonia[15,16] and n-butyl amine[17] as the probe molecules and for the measurement of basicity with CO_2[18] as the probe molecule. To date, however, the TPD of aromatic hydrocarbons on the MCM-41 has not been performed.

The present work was undertaken with the objective of studying the interaction of benzene molecules with the terminal silanol groups, acidic hydroxyl groups and Na present in the channels of MCM-41 by carrying out TPD of benzene over Si-MCM-41, H-AlSi-MCM-41 and Na-AlSi-MCM-41 from 323 K to 673 K at different heating rates and adsorbate loading by using gas chromatography technique.

1.3.2.2 Present Work

1.3.2.2.1 Characterization of AlSi-MCM-41

Detailed characterization of Si-MCM-41 has already been discussed in chapter 1.3.1. The MCM-41 structure[1,19] of the Na-AlSi-MCM-41 was confirmed by XRD (Fig. 1.3.2.1) by observing a typical four peak pattern[19] with a very prominent (100) reflection at low angle (2θ = 2-3^o) and three weaker (110, (200) and (210) reflections. The presence of four peaks indicates that the material posses a long range order in hexagonal symmetry[19].

N_2 sorption isotherm and pore size distribution of Si-MCM-41 are shown in Figs. 1.3.2.2a and 1.3.2.2b. The BET surface area, average pore diameter and pore

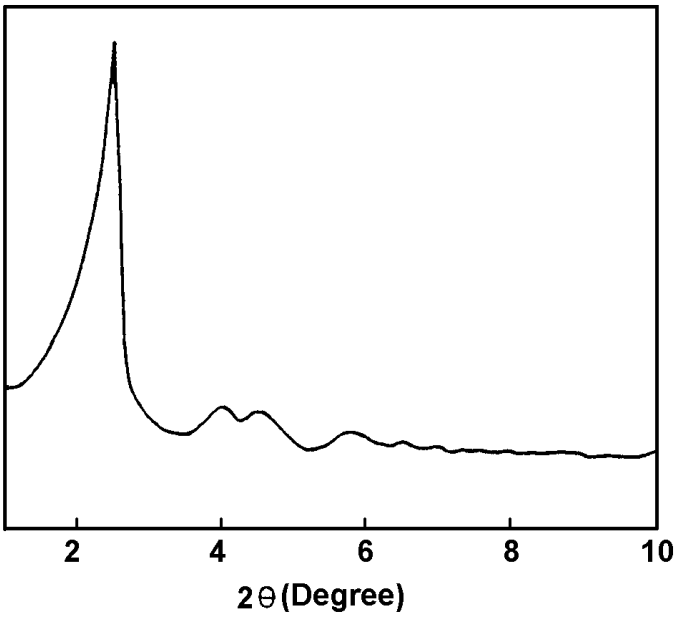

Fig. 1.3.2.1 Powder X-ray diffraction spectrum of AlSi-MCM-41 (calcined)

volume of the material were found to be 1010 m^2 g^{-1}, 3.0 nm and 1.12 cm^3 g^{-1}, respectively. According to IUPAC classification, the isotherms of MCM-41 are of type IV.[20] The isotherms exhibit three stages; the first stage is a linear part going through the origin, which is due to monolayer adsorption of N_2 on the walls of the mesopores (p/p_0 range of 0.15 – 0.35) due to capillary condensation in the mesopores. This part shows hysteresis. The p/p_0 value at which the inflection starts is related to the diameter of the mesopores. The sharpness in this step indicates the uniformity of the pore size distribution.[21] The third stage in the adsorption isotherm is an almost horizontal part after the relative pressure p/p_0 of ~0.35 and is due to multiplayer adsorption on the outer surface of the particles.[21] In addition, a hysteresis loop at relative pressure $p/p_0 > 0.8$ corresponds to capillary condensation in the interparticle pores.[20,22] A linear increase in adsorption at low pressures is observed followed by a steep increase in nitrogen uptake (at a relative pressure of $p/p_0 = 0.31 – 0.41$) due to

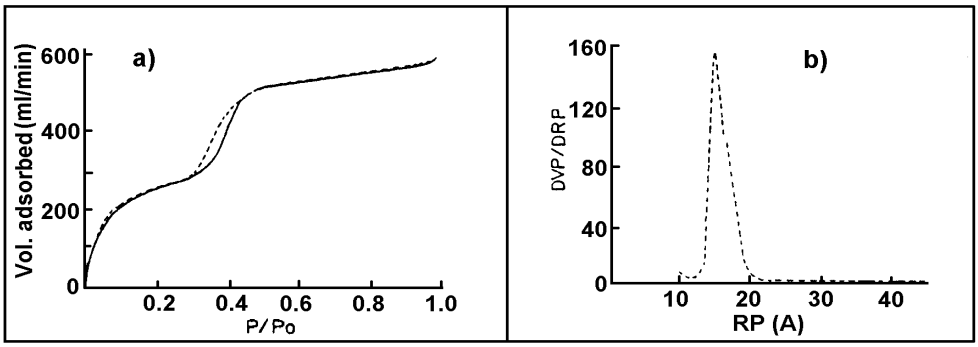

Fig. 1.3.2.2 N_2 adsorption-desorption isotherms (a) and pore size distribution (b) of AlSi-MCM-41

capillary condensation inside the mesopores (Figs. 1.3.2.2a). This sharp step of the isotherm indicates the narrower pore size distribution.

Figures 1.3.2.3a and 1.3.2.3b present the transmission electron micrograph (TEM) and scanning electron micrograph (SEM) of Si-MCM-41, respectively. TEM micrograph shows a reasonably regular array of channels in hexagonal arrangement.

Scanning electron microscope was used to determine the particle size and morphology of the Si-MCM-41. Figure 1.3.2.3b shows the presence of uniform microcrystalline particles.

The bands at -110 and -102 ppm in ^{29}Si MAS NMR (Fig 1.3.2.4a) correspond to the Q (4Si) resonance and (3Si, OH) resonance, respectively. The ^{1}H – ^{29}Si CP MAS NMR spectra (Fig. 1.3.2.4b) show that, like in amorphous silica, part of the silicon atoms in the Si-MCM-41 exists as silanol groups.[23] Similarly, Figs. 1.3.2.4c and 1.3.2.4e show that like in amorphous silica, part of the silicon atoms in the H-AlSi-MCM-41 exists as silanol groups. ^{27}Al MAS NMR (Fig. 1.3.2.4d) shows a peak

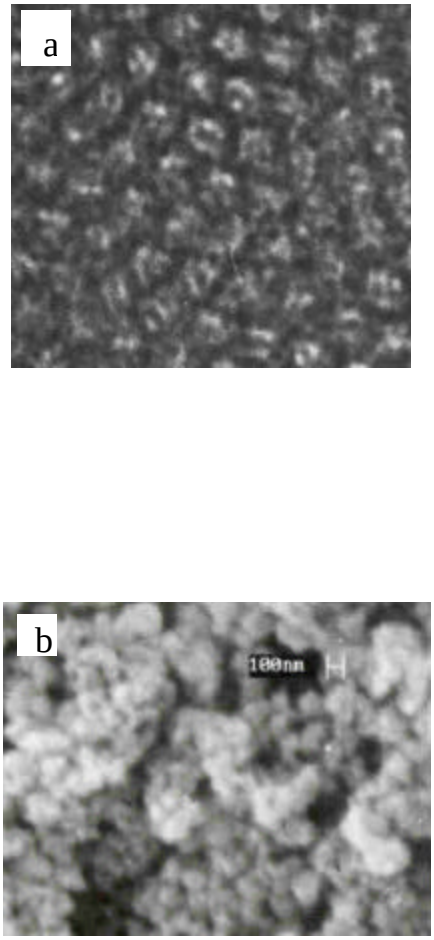

Fig. 1.3.2.3 a) Transmission electron micrograph and b) scanning electron micrograph of AlSi-MCM-41

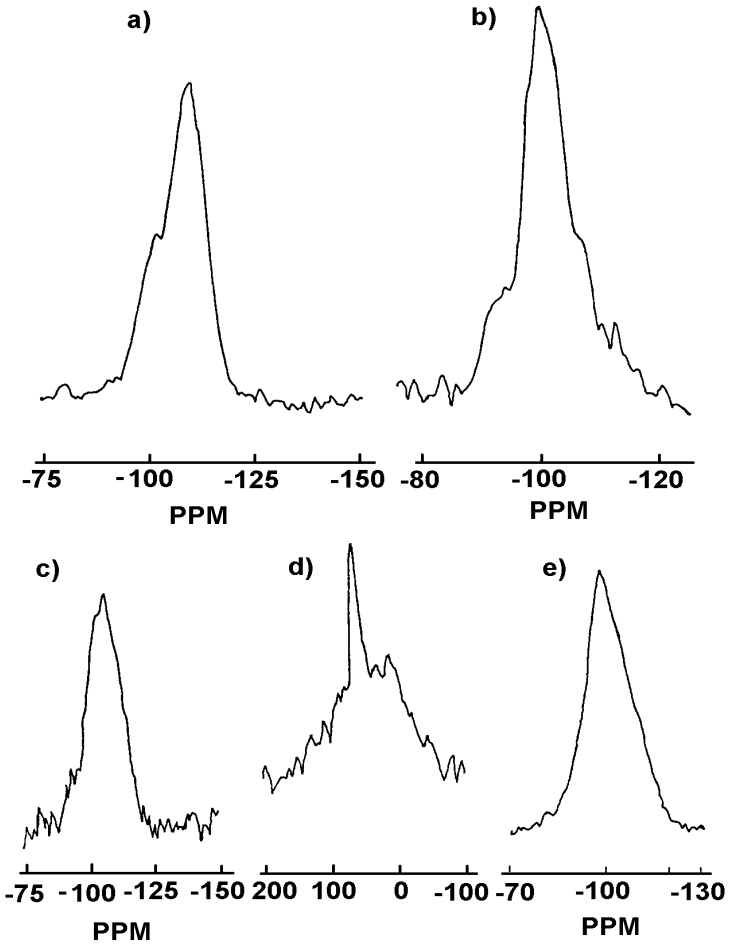

Fig. 1.3.2.4 ^{29}Si MAS NMR of Si-MCM-41 (a), ^{1}H-^{29}Si CP MAS NMR of Si-MCM-41 (b), ^{29}Si MAS NMR of H-AlSi-MCM-41 (c), ^{27}Al MAS NMR of H-AlSi-MCM-41 (d) and ^{1}H-^{29}Si CP MAS NMR of H-AlSi-MCM-41 (e).

at 55.4 ppm (corresponding to 4-coordinated Al) and a peak at 7.6 ppm (corresponding to 6-coordinated Al), indicating presence of both framework and extra-framework Al, respectively, in the H-AlSi-MCM-41. The intensity of the peak at 7.6 ppm is, however, low, indicating that the concentration of non-framework Al is small.

Acidity (measured in terms of the pyridine adsorbed irreversibly at 673 K) of the Si-MCM-41, Na-AlSi-MCM-41 and H-AlSi-MCM-41 was found to be 0.0, 0.005 and 0.082 mmol g^{-1}, respectively.

1.3.2.2.2 TPD of benzene from Si-MCM-41

TPD chromatograms for benzene on the Si-MCM-41 (adsorbate loading = 10.7 ± 0.2 μmol g^{-1}) at different heating rates (5 – 25 K min^{-1}) are shown in Fig. 1.3.2.5. All the TPD chromatograms have four distinct peaks. The TPD chromatograms at lower heating rate (5 K min^{-1}), however, showed better resolution of the peaks.

In the present TPD studies, there is a possibility of readsorption of benzene during the TPD runs, as the adsorbent bed is not shallow. Hence, the heat of adsorption of benzene was estimated from the TPD peak maximum temperatures (corresponding to the different peaks) at different heating rates, using the following expression:

$$-\log \beta = \alpha + (\Delta H/2.21R)\,(1/T_m) \qquad (1.3.2.1)$$

where β is the linear heating rate; α, the constant; ΔH, the heat of adsorption; R, the gas constant; and T_m, the temperature corresponding to peak maximum. This expression was developed for the case of readsorption occurs freely.[11-14] In case of the diffusion controlled desorption, the term "$\Delta H/2.21$ R" in Eq. (1.3.2.1) is changed to "$\Delta H/2.19$ R", which would make a small change in the estimated value of the heat of adsorption. In the present case, the adsorbent is mesoporous and its particle size is also quite small (particle diameter 0.3 - 0.4 mm) and hence, the desorption is not diffusion controlled. A change in the particle size of the adsorbent from 0.35 mm

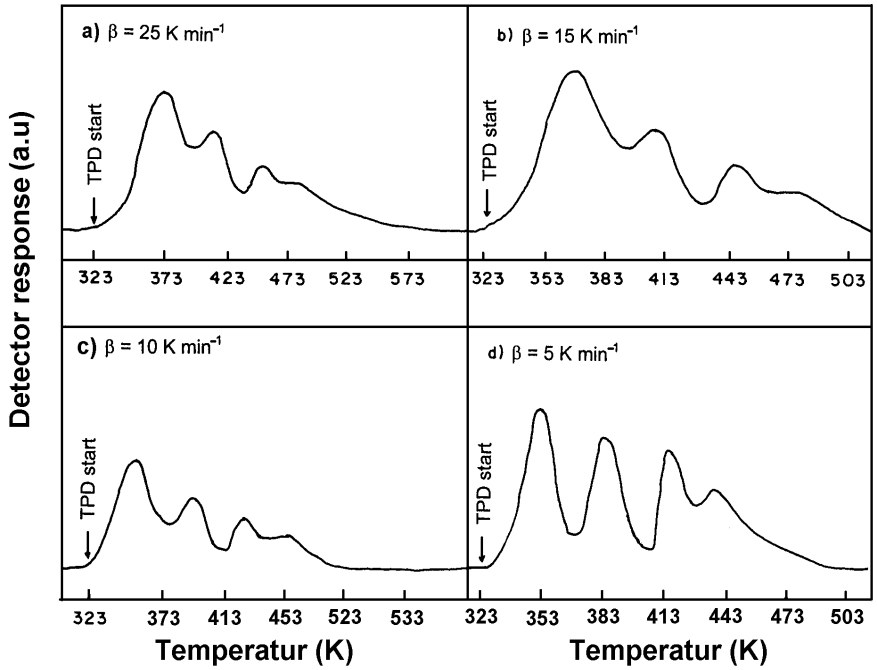

Fig. 1.3.2.5 TPD chromatograms of benzene on Si-MCM-41 at different heating rates (initial adsorbate loading of benzene = 10.7 ± 0.2 μmol. g^{-1}).

(average) to 0.2 mm (average) has caused no significant change in the TPD at a linear heating rate of 25 K min^{-1}.

The plots of log β vs. $1/T_m$, [according to Equation (1.3.2.1)] for the TPD of benzene are presented in Fig. 1.3.2.6. The heat of adsorption of benzene, corresponding to the different TPD peaks, obtained from the slopes of these linear plots are included in Table 1.3.2.1.

The TPD chromatograms from the Si-MCM-41 at different initial adsorbate loading (at a linear heating rate of 15 K min^{-1}) are presented in Fig. 1.3.2.7. In this case, it is interesting to note that the TPD chromatogram at higher initial adsorbate loading (10.7 μmol g^{-1}) shows four peaks but those at lower initial adsorbate loading (≤ 2.0 μmol g^{-1}) show only two broad peaks with or without a small shoulder at the

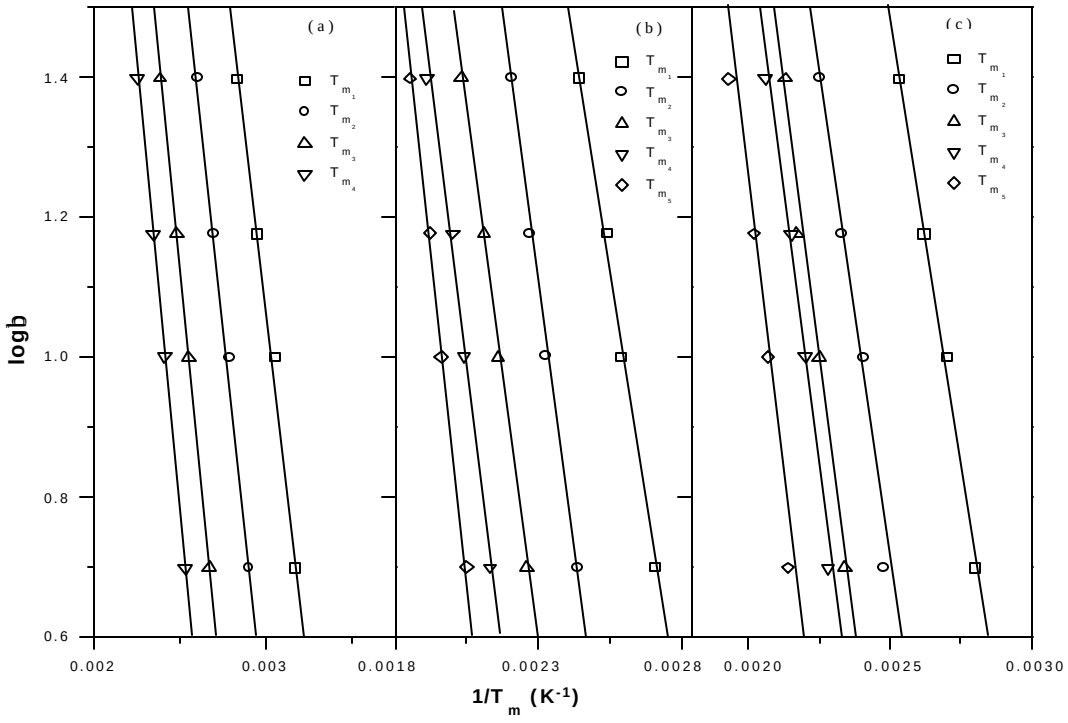

Fig. 1.3.2.6 Plots of log β vs. $1/T_m$ [according to Eq. (1.3.2.1)] for the TPD of benzene from (a) Si-MCM-41, (b) Na-AlSi-MCM-41 and (c) H-AlSi-MCM-41.

second peak. A variation of TPD peak maximum temperature for the two peaks (T_{m1} and T_{m2}) with the adsorbate loading is shown in Fig. 1.3.2.8; the T_{m1} and T_{m2} are decreased with increasing the adsorbate loading.

1.3.2.2.3 TPD of benzene on Na-AlSi-MCM-41 and H-AlSi-MCM-41

The TPD chromatograms of benzene from the Na-AlSi-MCM-41 and H-AlSi-MCM-41 at different linear heating rates (5, 10, 15, 25 K min^{-1}) are presented in Figs. 1.3.2.9 and 1.2.7.10, respectively. All the TPD chromatograms for both the MCM-41 samples show distinct five peaks.

The values of heat of adsorption of benzene on MCM-41, obtained from the linear log β vs. $1/T_m$ plots [according to the Equation (1.3.2.1)] are included in Table

1.3.2.1. The values of heat of adsorption obtained from the first peak (in the lower temperature region) are much lower than that obtained from the other peaks at the higher temperature region.

It is interesting to know from the data in Table 1.3.2.1 that benzene is adsorbed more strongly on the Na-AlSi-MCM-41 than on the H-AlSi-MCM-41. However, the heat of adsorption of benzene on the H-AlSi-MCM-41is very significantly higher than that on the Si-MCM-41. These results reveal that the interaction of benzene with Na^+, acidic – OH group and non-acidic (or weakly acidic) – OH groups of MCM-41 is in the following order: Na^+ > acidic – OH (or H^+) > non-acidic (or weakly acidic) – OH. This is consistent with that observed earlier for the adsorption of benzene on NaY, CeNaY, Silicalite (ZSM-5 type), H-ZSM-5 and H. Na-ZSM-5 zeolites.[24,25]

Table 1.3.2.1: Estimated heat of adsorption (-DH) corresponding to different peaks in the TPD of benzene on Si-MCM-41, Na-AlSi-MCM-41 and H-AlSi-MCM-41.

Adsorbent	Heat of adsorption (–ΔH), kJ. mol^{-1}				
	1st peak	2nd peak	3rd peak	4th peak	5th peak
Si-MCM-41	37.5	42.1	44.5	45.6	–
Na-Al-Si-MCM-41	47.7	54.3	56.0	58.6	64.0
H-Al-Si-MCM-41	46.6	54.0	55.5	57.9	60.2

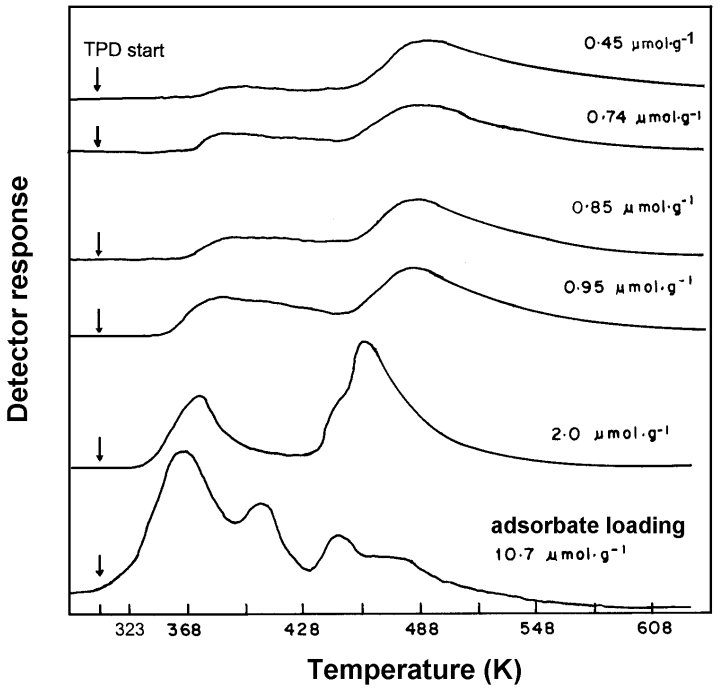

Fig. 1.3.2.7 TPD chromatograms for benzene on Si-MCM-41 at different initial adsorbate loading (linear heating rate = 15K. min^{-1})

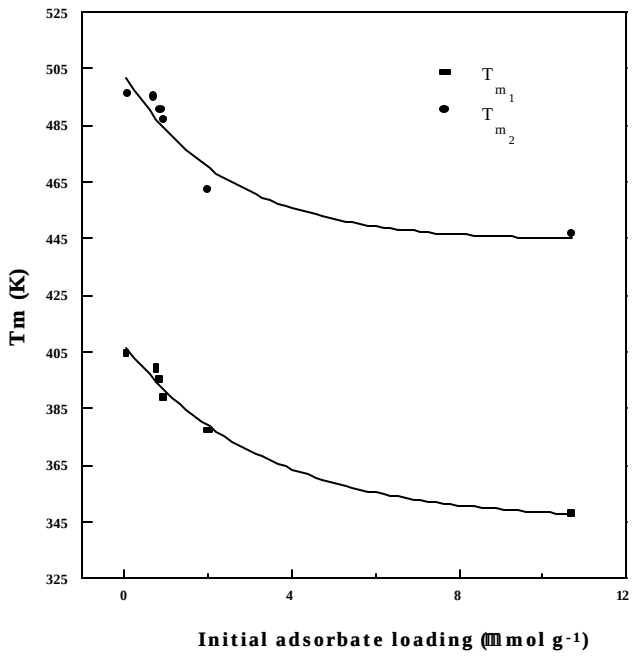

Fig. 1.3.2.8 Variation of peak maximum temperature (T_{m1} and T_{m2}) with initial adsorbate loading in the TPD of benzene on Si-MCM-41.

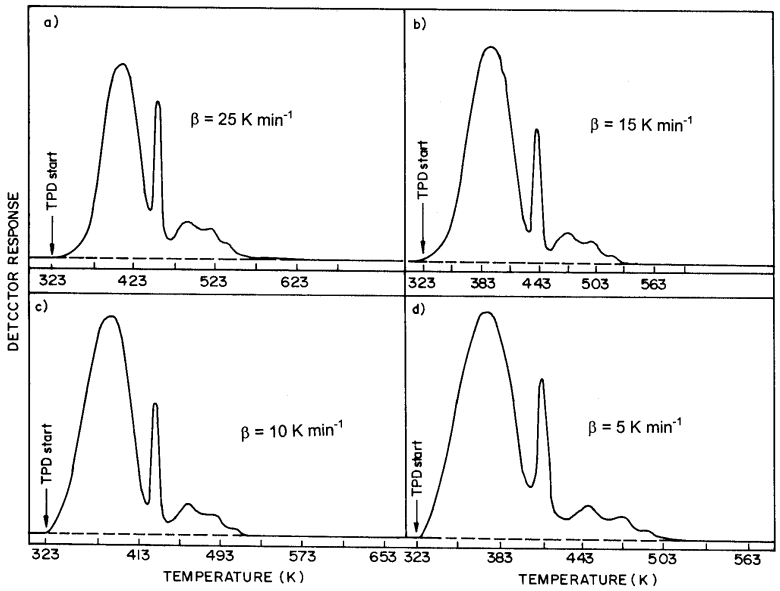

Fig. 1.3.2.9 TPD chromatograms of benzene on Na-AlSi-MCM-41 at different heating rates (initial adsorbate loading of benzene = 34.4 ± 0.5 μmol. g^{-1}.

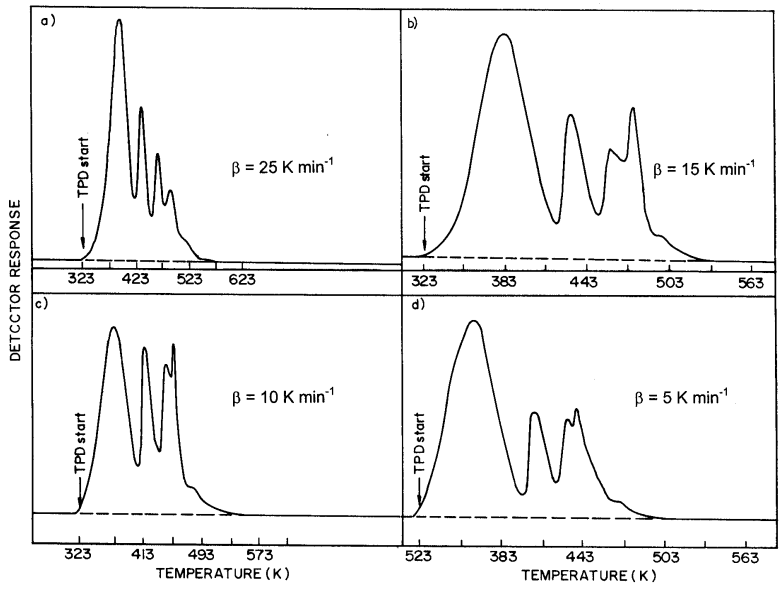

Fig. 1.3.2.10 TPD chromatograms of benzene on H-AlSi-MCM-41 at different heating rates (initial adsorbate loading of benzene = 50.1 ± 0.8 μmol. g^{-1}.

1.3.2.2.4 General Discussion

The broad ^{29}Si MAS NMR spectra of calcined Si-MCM-41 (Fig. 1.3.2.4a) are identical to those for amorphous silica, indicating an irregular local arrangement of Si-O-Si bonds and pore walls and a wide range of bond angles.[23] ^{1}H – ^{29}Si CP MAS NMR spectra (Fig. 1.3.2.4b) show that the material has a large number of defects and, as in amorphous silica; an appreciable part of the silicon atoms exists in the form of terminal silanol (Si-OH) groups.

The ^{27}Al MAS NMR spectrum of H-AlSi-MCM-41 (Fig. 1.3.2.4d) shows two peaks. The peak at 55.4 ppm corresponds to 4-coordinated (or tetrahedral) Al and a low intensity peak at 7.6 ppm corresponds to 6-coordinated (non-framework) Al. The presence of octahedral Al in the H-AlSi-MCM-41 is expected due to the dealumination (conversion of tetrahedral Al to octahedral Al) of the material during its calcination (813 K). Similarly, a non-framework Al as Al_2O_3 is also expected in the Na-AlSi-MCM-41.

The ^{29}Si MAS NMR spectra of H-AlSi-MCM-41 (Fig. 1.3.2.4c) have three peaks showing following main features. The peak at −110 ppm results from Si (4Si) (Q_4) structural units and it is also found in the spectra of purely siliceous MCM-41 (Si-MCM-41). The peak at −106 ppm results from Si (3Si, 1Al) sites and confirms that the aluminum has been incorporated into the framework. The shoulder at −102 ppm is due to Q_3 silicons on $Si(OSi)_3OH$ sites. The ^{1}H – ^{29}Si CP MAS NMR (Fig. 1.3.2.4e) of this material also shows that, as in amorphous silica, part of the silica atoms exists as terminal silanol groups.

In the IR spectra of Si-MCM-41, the sharp peak at 3745 cm^{-1} is assigned to isolated silanol groups,[9,10] e.g. at sites terminating the particles. The other three bands (in the range of 3700 – 3440 cm^{-1}), which are shifted to lower wave numbers

compared to isolated hydroxyl groups, can be assigned to the different types of hydrogen bonded silanol groups.[9] These hydroxyl groups are formed on defect sites resulting from structural imperfections, which is consistent with the observations made from the $^{1}H - {}^{29}Si$ CP MAS NMR of Si-MCM-41.

In the TPD chromatograms (Fig. 1.3.2.5) of benzene on Si-MCM-41, four distinct peaks are observed. Also, the heat of adsorption (Table 1.3.2.1) for the corresponding TPD peaks is found to be higher for the peaks at higher temperatures. It is interesting to note that, the heat of adsorption corresponding to the TPD peak [37.5 kJ mol^{-1} (Table 1.3.2.1)] is closed to the heat of adsorption of benzene (37.8 kJ mol^{-1}) in high silica ZSM-5 (Silicalite-I), observed earlier in the TPD of benzene on ZSM-5.[25] The adsorption of benzene is expected to result from weak interaction of the π-electrons of benzene ring with the silanol groups present in the Si-MCM-41. The observed four distinct peaks in the TPD of benzene indicate the presence of four distinct different types of benzene adsorption sites. The isolated Si-OH and the differently H-bonded Si-OH groups are responsible for the observed TPD peak multiplicity. The H-bonding between the Si-OH group may be affected in the presence of adsorbed benzene, depending upon the adsorbate concentration.

In the TPD of benzene from the Na-AlSi-MCM-41 and H-AlSi-MCM-41 materials, five distinct peaks are observed (Figs. 1.3.2.9 and 1.3.2.10). For these materials, one extra TPD peak in comparison to that for the Si-MCM-41, is observed. The observed 5^{th} extra peak is expected due to the interaction of benzene with Na^{+} from the Na-AlSi-MCM-41 or H^{+} from the H-AlSi-MCM-41. Other four peaks in both the cases are mostly due to the interaction of π-electrons of benzene with different type of terminal Si-OH groups present in the adsorbents and/or with sites. In this case also, the heat of adsorption corresponding to the different peaks is higher for

the peaks at higher temperatures. Multiple peaks (two peaks) were observed earlier in the TPD of benzene on H.Na-ZSM-5 zeolite;[25] the second peak (at higher temperature) was due to the strong interaction of benzene with Na-cations in the zeolite.

It is interesting to note from Table 1.3.2.1 that, not only the heat of adsorption corresponding to 5th peak (which is expected mostly due to the interaction of benzene with Na^+ or H^+) in the TPD for H-AlSi-MCM-41 and Na-AlSi-MCM-41 is higher, but also the heat of adsorption corresponding to all the other four peaks is higher than that observed for the Si-MCM-41. This indicates that the energy of interaction of benzene with the different types of silanol groups in H (or Na)-AlSi-MCM-41 is increased because of the presence of H^+ (or Na^+) and/or non-framework Al_2O_3.

The decrease in the number of TPD peaks for the Si-MCM-41 from four to two with decreasing the adsorbate loading from 10.7 to 0.95 μmol g^{-1} (Fig. 1.3.2.7) is unusual and hence very interesting. At the low adsorbate loading, the adsorbate interacts with two distinct types of adsorption sites, probably isolated silanol groups and hydrogen bonded silanol groups. It seems that, at the low adsorbate loading, the adsorbate does not distinguish between the differently hydrogen bonded silanol groups. The observed decrease in the peak maximum temperature of these two peaks (T_{m1} and T_{m2}) with increasing the adsorbate loading (Fig. 1.3.2.8) shows a site energy distribution among the two groups of sites, represented by the two TPD peaks. When benzene interacts with silanol groups, particularly those bonded by hydrogen bonds, the interaction of π-electrons of benzene ring with the hydrogen from the silanol groups is expected to affect the hydrogen bonding between the silanol groups, changing their site energy distribution and thereby inducing more surface heterogeneity. The presence of O–H---π (electrons) hydrogen bonds has already been

observed in the crystals of organic compounds.[26,27] At the high adsorbate loading, the observed four TPD peaks (Fig. 1.3.2.7) are expected most probably because of the modification of hydrogen bonding between the silanol groups, making them energetically more distinct. This is, however, only a speculation and further detailed studies are essential for understanding the observed surface heterogeneity induced due to the presence of the adsorbate at high loading.

1.3.2.3 Conclusions

From the TPD of benzene over Si-MCM-41 and H (or Na)-AlSi-MCM-41 mesoporous adsorbents at different heating rates and adsorbate loading, following important conclusions have been drawn:

1. Both the high silica (Si-MCM-41) and high alumina (AlSi-MCM-41) MCM-41 materials have surface heterogeneity because of the presence of different types of terminal silanol groups and H^+ or Na^+, as indicated by the TPD peak multiplicity (four and five TPD peaks, respectively).
2. The heat of adsorption of benzene on the H (or Na)-AlSi-MCM-41 is, in general, higher than that on the Si-MCM-41, due to the stronger interaction of benzene with H^+ or Na^+ and also because of the modification of the strength of different sites (terminal silanol groups) by the presence of H^+, Na^+ or non-framework Al_2O_3; the interaction of benzene with Na^+ is stronger than that with H^+.
3. Surface heterogeneity (or creation of more distinct sites) is induced in the Si-MCM-41 due to the presence of adsorbed benzene at high concentration.

4. There is a site energy distribution among the two different groups of sites, involved in the adsorption of benzene (at low adsorbate loading) on the Si-MCM-41.

1.3.2.4 References

1. Kresge, C. T.; Leonowicz, M. E.; Roth, W. J.; Vartuli, J. C.; Beck, J. S., *Nature*, **359** (1992) 710.
2. Kresge, C. T.; Leonowicz, M. E.; Roth, W. J.; Vartuli, J. C., *U. S. Pat.* No., 5098684, (1992).
3. Schmidt, R.; Akporiye, D.; Stocker, M.; Ellestad, O. H., *Stud. Surf. Sci. Catal.*, **84** (1994) 61.
4. Borade, R. B.; Clearfield, A., *Catal. Lett.*, **31** (1995) 267.
5. Climent, M. J.; Corma, A.; Iborra, S.; Navarro, M. C.; Primo, ., *J. Catal.* **161** (1996) 783.
6. Corma, A.; Iborra, S.; Miquel, S.; Primo, J., *J. Catal.*, **173** (1998) 315.
7. Climent, M. J.; Corma, A.; Guil-Lopez, R.; Iborra, S.; Primo, J., *J. Catal.*, **175** (1998) 70.
8. Rodriguez, I.; Iborra, S.; Rey, F.; Corma, A., *Appl. Catal. A*, **194-195** (2000) 241.
9. Jentys, A.; Pham, N. H.; Vinek, H., *J. Chem. Soc. Faraday Trans.*, **92** (1996) 3287.
10. Chen, J.; Li, Q.; Xu, R.; Xiao, F., *Angew. Chem. Int. Ed. Engl.*, **34** (1995) 2694.
11. Cvetnovic, R. J.; Amenomiya, Y.,*Adv. Catal.*, **17** (1967) 103.
12. Smutek, M.; Cerny, S.; Buzek, F., *Adv. Catal.*, **24** (1975) 343.
13. Cvetnovic, R. J.; Amenomiya, Y., *Catal. Rev.*, **6** (1972) 21.
14. Amenomiya, Y., *Chemtech.* (1976) 129.
15. Kim, J. –H. ; Tanabe, M. ; Niwa, M. , *Microporous Mater.*, **10** (1997) 85.
16. Okumara, K.; Nishigaki, K.; Niwa, M., *Chem. Lett.*, (1998) 577.
17. Reddy, K. M.; Song, C., *Mater. Res. Soc. Symp. Proc.*, **454** (1997) 125.
18. Kloeststra, K. R.; Van, L. M.; Van, B. H., *J. Chem. Soc. Faraday Trans.*, **93** (1997) 1211.
19. Beck, J. S.; Vartuli, J. C.; Roth, W. J.; Leonowicz, M. E.; Kresge, C. T.; Schmitt, K. D.; Chu, C. T.-W.; Olson, D. H.; Sheppard, E. W.; McCullan, S. B.; Higgins, J. B.; Schlenker, J. L. *J. Am. Chem. Soc*. **114** (1992) 10834.
20. Gregg, S. J.; Sing, K. S. W., *"Adsorption, Surface Area and Porosity"* Academic Press, London, Ch.4 (1982).

21. Luan, Z.; He, H.; Zhou, W.; Cheng, C-F.; Klinovski, J. *J. Chem. Soc. Faraday Trans*. **91** (1995) 2955.

22. Chen, X.; Huang, I.; Li, Q., *J. Phys. Chem. B*, **101** (1997) 8461.

23. Luan, Z.; Cheng, C. – F.; Zhou, W.; Klinowski, J. *J. Phys. Chem.* **99** (1995) 1018.

24. Choudhary, V. R.; Srinivasan, K. R.; Akolekar, D. B., *Zeolites*, **9** (1989) 115.

25. Choudhary, V. R.; Srinivasan, K. R.; Singh, A. P., *Zeolites* **10** (1990) 16.

26. Desiraju, G. R. *Acc. Chem. Res*.**29** (1996) 441.

27. Allen, F. H.; Howard, J. A. K.; Hoy, V. J.; Desiraju, G. R.; Reddy, D. S.; Wilson, C. C. *J. Am. Chem. Soc.*, **118** (1996) 4081.

1.3.3 TEMPERATURE PROGRAMMED DESORPTION OF TOLUENE, P-XYLENE, MESITYLENE AND NAPHTHALENE ON MESOPOROUS HIGH SILICA MCM-41

1.3.3.1 Background and Brief Description of Earlier Work

As described in Section 1.3.2.1, only a few TPD studies on MCM-41 type zeolites have been performed for measurement of the acidity with ammonia[1,2] and n-butyl amine[3] as the probe molecules and for the measurement of basicity with CO_2[4] as the probe molecule. The TPD of benzene on Si-MCM-41 has been described in the earlier Section (Section 1.3.2). This study showed that it is also interesting to investigate the interaction of other aromatic hydrocarbons with the terminal Si-OH groups of Si-MCM-41.

The present investigation was undertaken with the objective of studying the interaction of aromatic hydrocarbons (viz. toluene, p-xylene, mesitylene and naphthalene) with the adsorption sites in purely siliceous MCM-41 zeolite. For this purpose, TPD of toluene, p-xylene, mesitylene and naphthalene at different heating rates (5 – 25 K min^{-1}) and TPD of toluene at different initial adsorbate loading (0.51 – 16.3 μmol g^{-1}) was performed using gas chromatographic technique.

1.3.3.2 Present Work

Representative TPD curves for toluene, p-xylene, mesitylene and naphthalene (at the heating rate of 15 K min^{-1}) on the siliceous MCM-41 is shown in Fig. 1.3.3.1. All the TPD curves for toluene, p-xylene, mesitylene and naphthalene on Si-MCM-41 exhibit a single asymmetric peak, with a small hump at high temperature indicating slow desorption, particularly for naphthalene. The asymmetric shape of the TPD curves suggests that the desorption is of first order.[5-8] The data of peak maximum

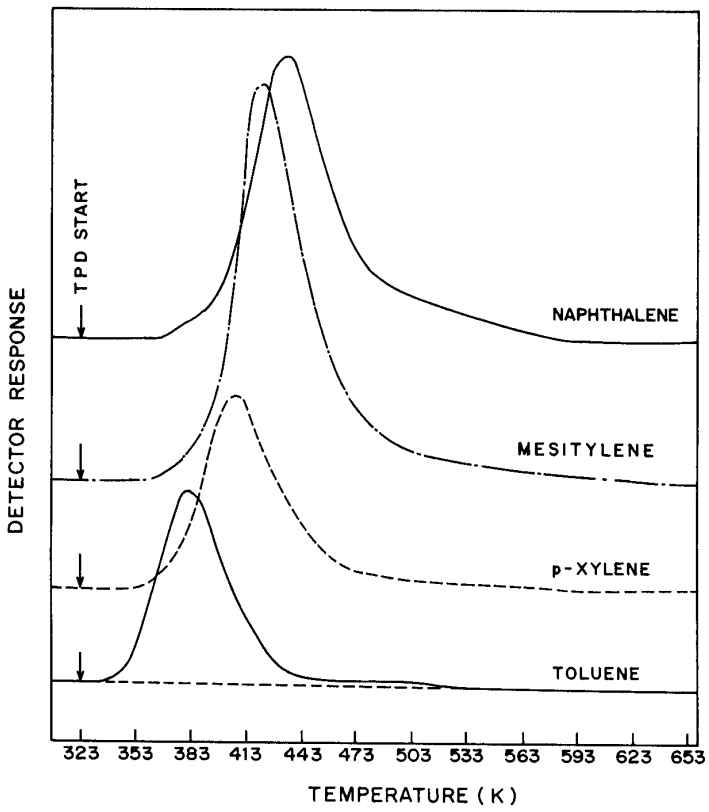

Fig. 1.3.3.1 TPD curves of aromatic hydrocarbons on Si-MCM-41 (heating rate: 15 K min^{-1}).

temperatures at the different heating rates for the aromatic hydrocarbons are given in Table 1.3.3.1.

A comparison of the TPD data (Fig. 1.3.3.1 and Table 1.3.3.1) shows that both the desorption start temperature (i. e., the temperature at which the adsorbed aromatic hydrocarbons start desorbing) and the TPD peak maximum temperature (T_m) increase with increasing molecular weight of the adsorbate (aromatic hydrocarbons).

The plots of log β vs. $1/T_m$, according to the expression,

$$- \log \beta = \alpha + (\Delta H / 2.21R) (1/T_m) \qquad (1.3.3.1)$$

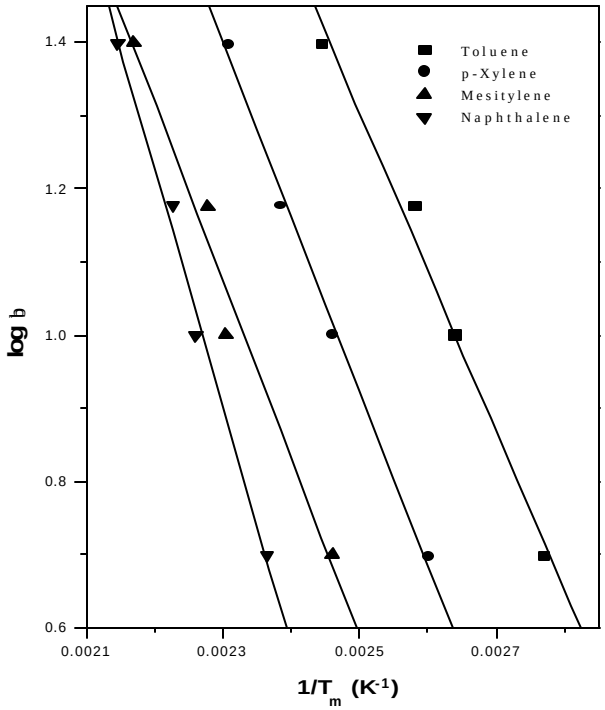

Fig. 1.3.3.2 Plots of log*b* vs. $1/T_m$ (according to Eq. 1.3.3.1) for the TPD of aromatic hydrocarbons from Si-MCM-41.

(where β is the linear heating rate; ΔH, the heat of adsorption; R, the gas constant; T_m, the temperature corresponding to peak maximum of the TPD curve; and α, the constant which includes the diffusion and entropy terms), derived for the case of readsorption occurring freely,[5-8] are shown in Fig. 1.3.3.2. The values of heats of adsorption for the aromatic hydrocarbons, obtained from the slope of the linear plots (Fig. 1.3.3.2), are included in Table 1.3.3.1.

Figure 1.3.3.3 shows that the heats of adsorption of aromatic hydrocarbons decreases exponentially with the increase in the ionization potential of the aromatic hydrocarbons. The values of ionization potential of the aromatic hydrocarbons are taken from Reference 9.

Table 1.3.3.1: Peak maximum temperature (at the different heating rates) data for TPD of aromatic hydrocarbons from the Si-MCM-41 and their heats of adsorption.

Aromatic hydrocarbon	Peak maximum temperature, T_m (K)				Heats of adsorption kJ mol^{-1}
	25 K. min^{-1}	15 K. min^{-1}	10 K. min^{-1}	5 K. min^{-1}	
Benzene [a]	-	-	-	-	37.5
Toluene	408	388	379	361	40.0
P-xylene	433	418	407	385	43.6
Mesitylene	461	439	435	407	45.0
Naphthalene	465	448	442	424	59.8

[a] Data from ref. 10 (Section 1.3.2).

In the earlier studies for the adsorption of aromatic hydrocarbons on H-ZSM-5[11] and H-(or Na-)Al-Si-MCM-41[12] (Section 1.3.4), a similar dependence of adsorption heats on ionization potential of the adsorbate was observed. The heats of adsorption of toluene, p-xylene and mesitylene on H-ZSM-5 was 65.7, 70.7 and 81.0 kJ mol^{-1},[11] respectively, and that on H-Al-Si-MCM-41 was 48.0, 51.5 and 53.9 kJ mol^{-1},[12] respectively. The higher heats of adsorption for the H-ZSM-5 and H-Al-Si-MCM-41 zeolites are expected mostly because of stronger interaction of the aromatic hydrocarbons with their protonic acid sites. The heats of adsorption of benzene on H-ZSM-5,[11] silicalite-I[11] and Si-MCM-41[10] was 51.3, 37.8 and 37.5 kJ mol^{-1}, respectively. The heats of adsorption of benzene on the high silica MCM-41 (Si-MCM-41) is almost same as that on the high silica ZSM-5 (silicalite-I).

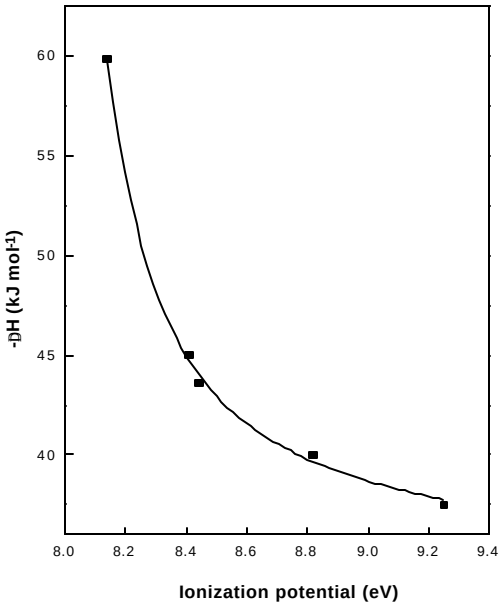

Fig. 1.3.3.3 Dependence of the heats of adsorption of aromatic hydrocarbons on their ionization potential.

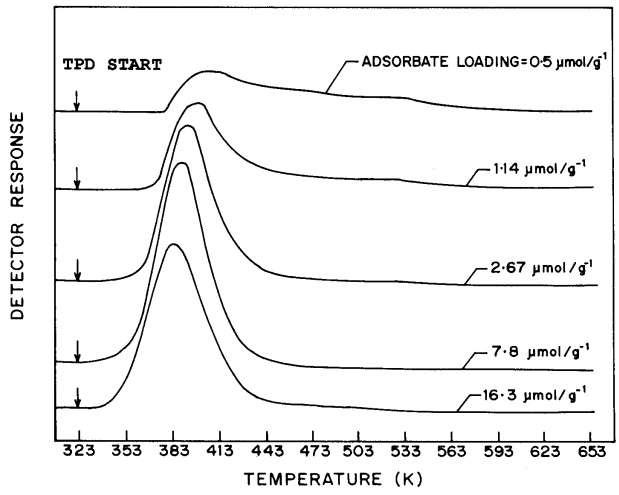

Fig. 1.3.3.4 TPD curves for toluene on Si-MCM-41 at different initial adsorbate loadings

The TPD curves from Si-MCM-41 at different initial adsorbate loading of toluene at the linear heating rate of 15 K min^{-1} are presented in Fig. 1.3.3.4. The TPD curves were recorded at different detector attenuation. The variation of T_m with the initial adsorbate loading of toluene is shown in Fig. 1.3.3.5. The T_m decreases almost exponentially with the increase in the adsorbate loading. This "clearly" indicates a presence of site-energy distribution on the Si-MCM-41 zeolite for the adsorption of toluene.[5-7]

There is a strong possibility of readsorption of the aromatic hydrocarbons on the siliceous MCM-41 as the adsorbent bed length to diameter ratio is high (>>1) and also the adsorbate molecules can freely diffuse in the mesopores of the adsorbents. Hence, it is more appropriate to use the expression for TPD with readsorption of aromatic hydrocarbon [Equation (1.3.3.1)] for analyzing the TPD data.

The heats of adsorption of aromatic hydrocarbons increases with the decrease in their ionization potential (Fig. 1.3.3.3). This is consistent with that observed earlier in the adsorption of aromatic hydrocarbons on H-ZSM-5[11] and H-(or Na-)Al-Si-MCM-41.[12]

The adsorption of aromatic hydrocarbons in the Si-MCM-41 is expected to result from weak interaction of the π-electrons of the aromatic ring(s) with the terminal silanol (Si–OH) groups, which are poorly acidic or non acidic in nature, present in the siliceous MCM-41 materials.[13,14] The electron donating alkyl groups increase the electron density of the aromatic ring, making it more susceptible for interacting with the adsorption sites (terminal silanol groups). The heats of adsorption of naphthalene is significantly higher than that for the other hydrocarbons. This is not just because of the higher molecular weight but is also due to stronger interaction between the two condensed benzene aromatic nuclei of naphthalene and the silanol groups. The

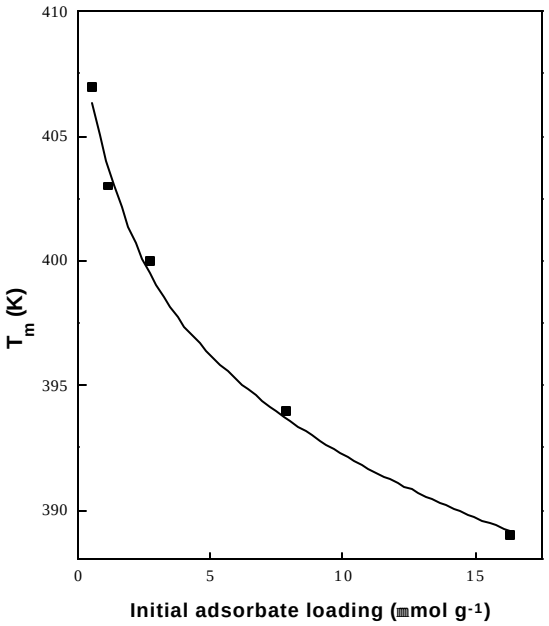

Fig. 1.3.3.5 Variation of T_m with initial adsorbate loading for the TPD of toluene.

dependence of the heat of adsorption on the ionization potential of the aromatic hydrocarbons (Fig. 1.3.3.3) is consistent with the above.

The site energy distribution, indicated by the increase in T_m with decreasing the adsorbate loading in the TPD of toluene (Fig. 1.3.3.5) is expected due to the interaction of toluene π-electrons with the different silanol groups[13,14] present in the high silica MCM-41. At least four types of terminal silanol groups (isolated Si–OH and three other types of Si–OH groups involving hydrogen bonds) have been observed in MCM-41.[14] The different types of terminal silanol groups are expected to impart surface heterogeneity or site energy distribution on the high silica MCM-41.

1.3.3.3 Conclusions

From the TPD of toluene, p-xylene, mesitylene and naphthalene over mesoporous high silica MCM-41, the following important conclusions can be made:

1. The desorption of the hydrocarbons is of first order, as indicated by the asymmetric TPD peak.
2. The heat of adsorption increases with decreasing ionization potential of the aromatic hydrocarbons. It indicates weak interaction between the π-electrons of aromatic ring(s) and the terminal silanol groups of the high silica MCM-41.
3. The adsorbent has a site energy distribution, indicated by the increase in the TPD peak maximum temperature with decreasing the adsorbate loading in the case of toluene TPD.

1.3.3.4 References

1. Kim, J. –H. ; Tanabe, M. ; Niwa, M. , *Microporous Mater.*, **10** (1997) 85.
2. Okumara, K.; Nishigaki, K.; Niwa, M., *Chem. Lett.*, (1998) 577.
3. Reddy, K. M.; Song, C., *Mater. Res. Soc. Symp. Proc.*, **454** (1997) 125.
4. Kloeststra, K. R.; Van, L. M.; Van, B. H., *J. Chem. Soc. Faraday Trans.*, **93** (1997) 1211.
5. Cvetnovic, R. J.; Amenomiya, Y., *Adv. Catal.*, **17** (1967) 103.
6. Smutek, M.; Cerny, S.; Buzek, F., Adv. *Catal.*, **24** (1975) 343.
7. Cvetnovic, R. J.; Amenomiya, Y., *Catal. Rev.*, **6** (1972) 21.
8. Amenomiya, Y., *Chemtech.* (1976) 129.
9. Lide, D. R. (Ed.) *"CRC Handbook of Chemistry and Physics"*, **7th Edn.**, CRC Press, London, (1993) p10 – 208.
10. Choudhary, V. R.; Mantri, K., *Langmuir*, **16** (2000) 8024.
11. Choudhary, V. R.; Srinivasan, K. R.; Singh, A. P., *Zeolites*, **9** (1990) 16.
12. Choudhary, V. R., Mantri, K., *Microporous and Mesoporous Mater.*, **46** (2001) 47.
13. Jentys, A.; Pham, N. H.; Vinek, H., *J. Chem. Soc., Faraday Trans.*, **92** (1996) 3287.
14. Chen, J.; Li, Q.; Xu, R. ; Xiao, F., *Angew. Chem. Int. Ed. Engl.*, **34** (1995) 2694.

1.3.4 TEMPERATURE PROGRAMMED DESORPTION OF TOLUENE, p-XYLENE, MESITYLENE AND NAPHTHALENE ON Na-AlSi-MCM-41 AND H-AlSi-MCM-41

1.3.4.1 Background and Brief Description of Earlier Work

The AlSi-MCM-41 has a capacity of cation exchange similar to that of zeolites and it can be modified by exchanging its cations with other cations.[1-3] Because of the presence of tetrahedral Al, H-AlSi-MCM-41 has acid sites with high strength. Its acidity can be reduced or it can be made basic by exchanging its protons with Na^+. Microporous zeolites can not be used for the acid or base catalyzed reactions involving large molecular size or bulky reactants and/or products. However, since H-AlSi-MCM-41 is mesoporous, its different cation exchanged forms can be used for the reaction involving bulky molecules, particularly in the synthesis of fine chemicals. Recently, Corma and coworkers have reported synthesis of a number of fine chemicals using acidic and basic mesoporous MCM-41 materials.[4-7]

Presence of at least four types of different terminal Si-OH groups (which are poorly acidic or non acidic in nature) in the channels of MCM-41 has been detected earlier.[8,9] In addition of the terminal Si-OH groups the H^+ form of AlSi-MCM-41 contain acidic surface hydroxyl groups and the Na^+ form AlSi-MCM-41 contains Na^+ cations in the channels. It is interesting to study the interaction of different aromatic substrates, which are used in the synthesis of fine chemicals, with the acidic hydroxyl groups or Na^+ cations and also with the terminal Si-OH groups of these mesoporous materials. Temperature programmed desorption (TPD) technique[10-13] could very well be used for this purpose. In the earlier Section (Section 1.3.3), studies on the TPD of aromatic compounds over high silica MCM-41 having no acidity[4] have been described. The earlier studies[14] on the TPD of benzene over high silica MCM-41 and

high alumina MCM-41 in its H^+ and Na^+ forms (Section 1.3.2) have indicated the presence of different types of benzene adsorption sites, four sites on Si-MCM-41 and five sites on Na or H-AlSi-MCM-41. It is also interesting to study the interaction of other aromatic hydrocarbons, including bulkier ones with the different terminal Si-OH groups and acidic hydroxyl groups or Na^+ cations present in the channels of H-AlSi-MCM-41 and Na-AlSi-MCM-41.

The present work was undertaken with the objective of studying the interaction of different aromatic hydrocarbons (viz. toluene, p-xylene, mesitylene and naphthalene) with the adsorption sites present in the mesoporous channels of H-AlSi-MCM-41 and Na-AlSi-MCM-41 using the TPD technique.

1.3.4.2 Present Work

A detailed characterization of AlSi-MCM-41[1] has been discussed in Chapter 1.3.2. TPD curves for toluene, p-xylene, mesitylene and naphthalene at different heating rates on the H-AlSi-MCM-41 are shown in Figs 1.3.4.1 and 1.3.4.2. At all the heating rates, TPD curves for toluene on H-AlSi-MCM-41 exhibit three distinct peaks, but the TPD curves for p-xylene, mesitylene and naphthalene on the H-AlSi-MCM-41 show a single asymmetric peak with hump(s) at lower and/or higher temperatures. TPD curves of the aromatic hydrocarbons on the Na-AlSi-MCM-41 are presented in Figs. 1.3.4.3 and 1.3.4.4. In this case the TPD curves for all the hydrocarbons show single asymmetric peak with humps.

The asymmetric shape of the TPD curves (Figs 1.3.4.1 - 1.3.4.4) suggests that the desorption of the hydrocarbons from both the adsorbents is of first order.[10-12] Data of the TPD peak maximum temperatures at the different heating rates for the aromatic hydrocarbons are given in Table 1.3.4.1.

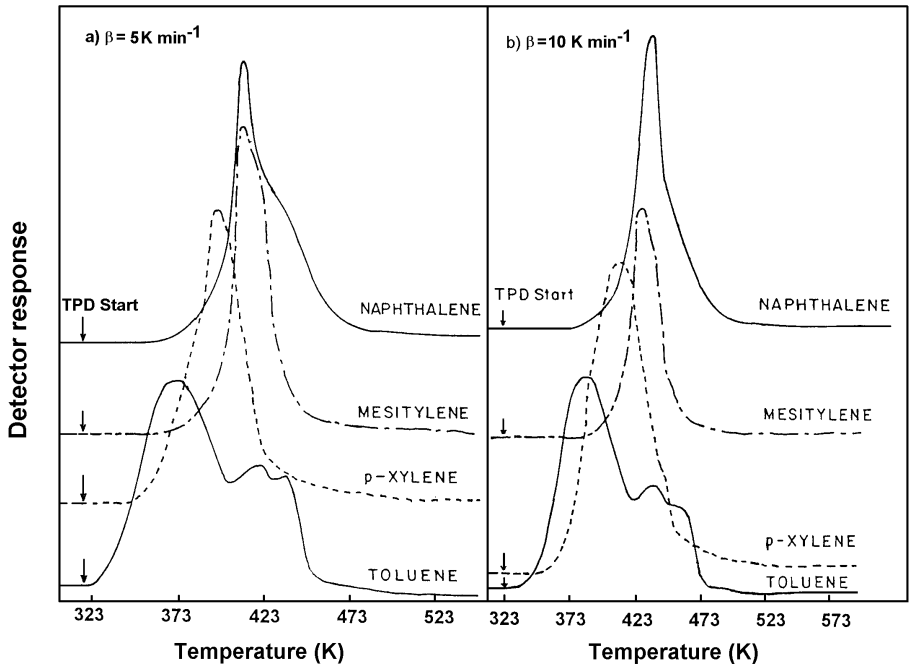

Fig. 1.3.4.1 TPD curves of aromatic hydrocarbons over the H-AlSi-MCM-41 at the linear heating rate of 5 K min^{-1} and 10 K min^{-1}.

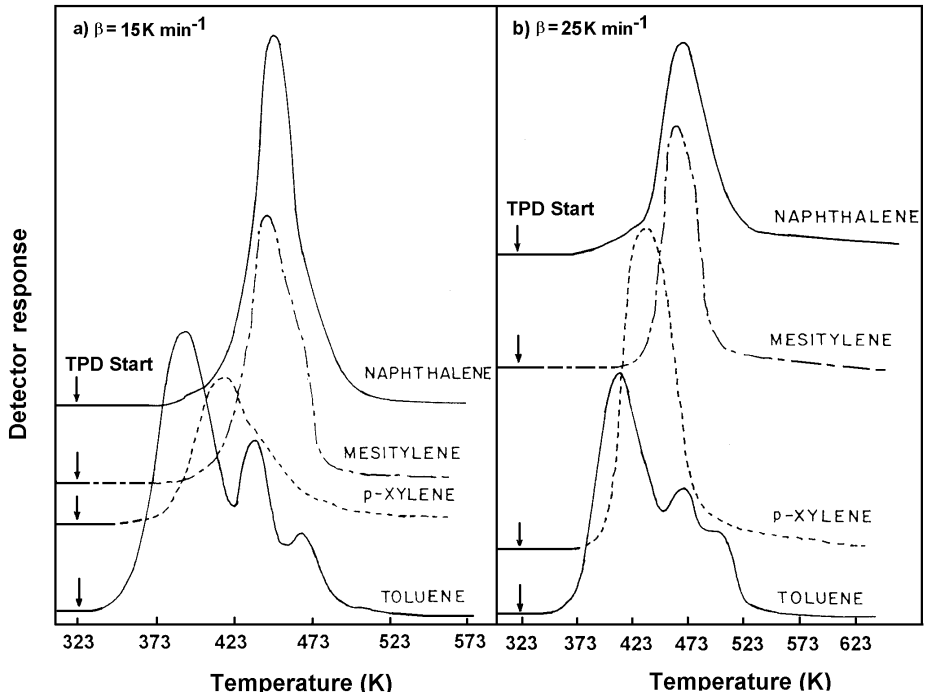

Fig. 1.3.4.2 TPD curves of aromatic hydrocarbons over the H-AlSi-MCM-41 at the linear heating rate of 15 K min^{-1} and 25 K min^{-1}.

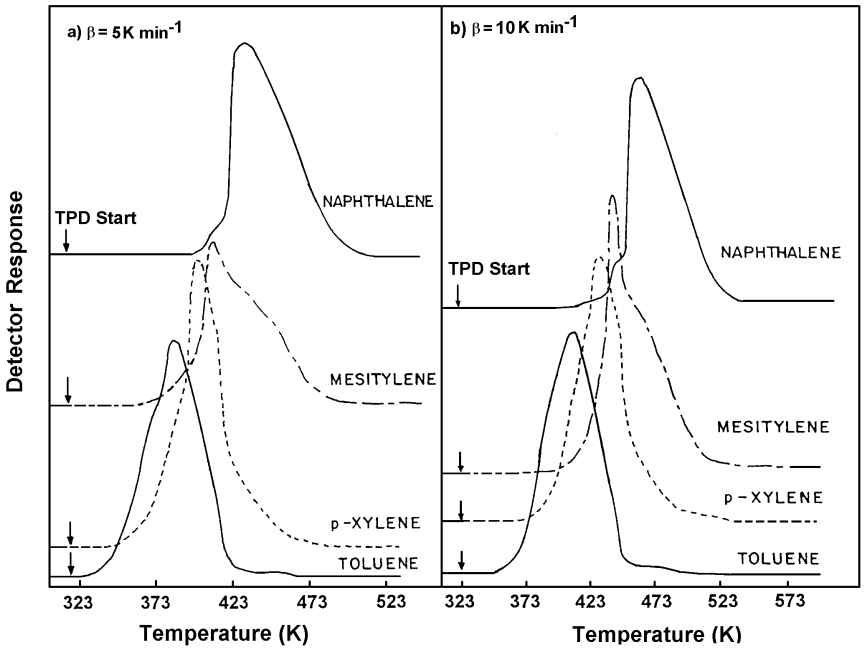

Fig. 1.3.4.3 TPD curves of aromatic hydrocarbons over the Na-AlSi-MCM-41 at the linear heating rate of 5K min^{-1} and 10K min^{-1}.

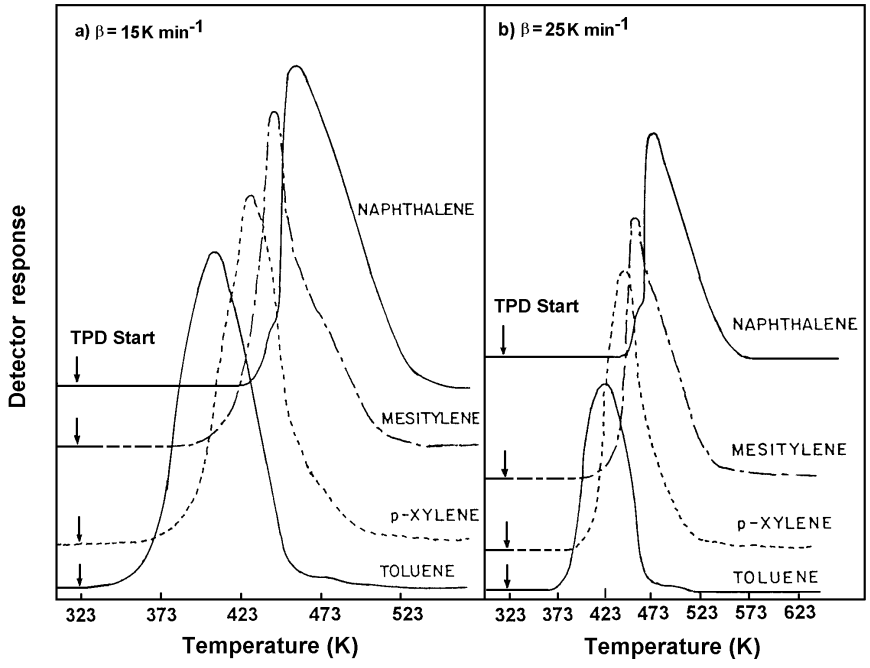

Fig. 1.3.4.4 TPD curves of aromatic hydrocarbons over the Na-AlSi-MCM-41 at the linear heating rate of 15K min^{-1} and 25K min^{-1}.

A comparison of the TPD data (Figs 1.3.4.1 - 1.3.4.4 and Table 1.3.4.1) shows that both the desorption start temperature (i. e., the temperature at which the adsorbed aromatic hydrocarbons start desorbing) and the TPD peak maximum temperature (T_m) increase with increasing the number of methyl groups or aromatic rings in the aromatic hydrocarbons. In the present TPD studies, there is a possibility of readsorption of aromatic hydrocarbons during the TPD runs, as the adsorbent bed is not shallow. Hence, the heat of adsorption of the adsorbate were estimated from the TPD peak maximum temperatures at different heating rates, using the following expression:

$$- \log \beta = \alpha + (\Delta H / 2.21R) (1/T_m) \qquad (1.3.4.1)$$

(where β is the linear heating rate; ΔH, the heat of adsorption; R, the gas constant; T_m, the temperature corresponding to peak maximum of the TPD curve; and α, the constant which includes the diffusion and entropy terms), derived for the case of readsorption occurring freely.[10-12] Linear plots of log β vs. $1/T_m$ (according to Eq. (1.3.4.1)) for the TPD of aromatic hydrocarbons over the H-AlSi-MCM-41 and Na-AlSi-MCM-41 are shown in Figs 1.3.4.5 and 1.3.4.6, respectively. In case of the diffusion controlled desorption, the term "$\Delta H/2.21$ R" in Eq. 1.3.4.1 is changed to "$\Delta H/2.19$ R", which would make a small change in the estimated value of the heat of adsorption.

In our earlier TPD studies, the heat of adsorption of toluene, p-xylene and mesitylene on H-ZSM-5 zeolite[15] was found to be 65.7, 70.7 and 81.0 kJ mol^{-1}, respectively, and that on Si-MCM-41[16] was found to be 40.0, 43.6 and 45.0 kJ mol^{-1}, respectively. For both the H-AlSi-MCM-41 and Na-AlSi-MCM-41 adsorbents, the

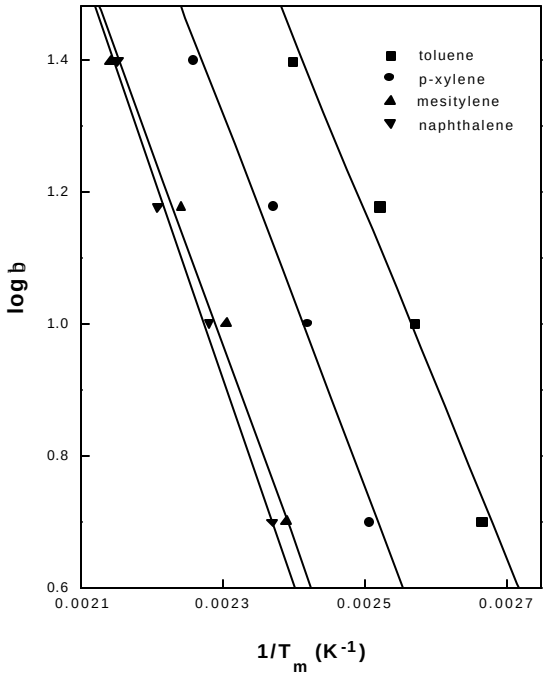

Fig. 1.3.4.5 log β vs. $1/T_m$ plots (according to Eq. (1.3.4.1)) for the TPD of aromatic hydrocarbons over the H-AlSi-MCM-41.

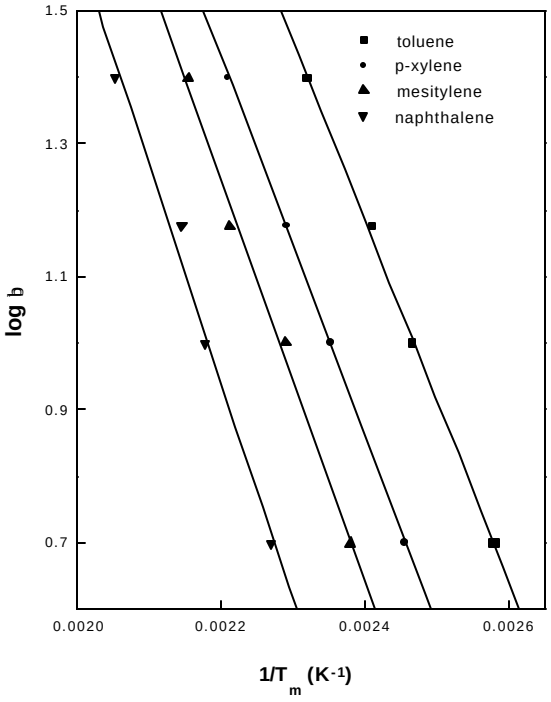

Fig. 1.3.4.6 log β vs. $1/T_m$ plots (according to Eq. (1.3.4.1)) for the TPD of aromatic hydrocarbons over the Na-AlSi-MCM-41.

Table 1.3.4.1 Peak maximum temperature(s) (at different heating rates) and heat of adsorption (-ÄH) data for the TPD of aromatic hydrocarbons from H-AlSi-MCM-41 and Na-AlSi-MCM-41.

Aromatic hydrocarbon	Peak number	Peak maximum temperature, T_m (K)				Heat of adsorption (-ÄH), kJ mole^{-1}
		25 K min^{-1}	15 K min^{-1}	10 K min^{-1}	5 K min^{-1}	
Adsorbent: H-AlSi-MCM-41						
Toluene	1st	417	397	389	375	48.0
	2nd	470	442	443	422	56.2
	3rd	494	469	463	440	59.3
p-Xylene	1st	443	422	413	402	51.5
Mesitylene	1st	467	447	434	418	52.8
Naphthalene	1st	471	453	439	419	58.2
Benzene[a]	1st	-	-	-	-	46.6
Adsorbent: Na-AlSi-MCM-41						
Toluene	1st	431	415	404	390	49.8
p-Xylene	1st	453	436	425	406	52.4
Mesitylene	1st	464	452	434	417	54.3
Naphthalene	1st	487	466	459	438	60.1
Benzene[a]	1st	-	-	-	-	47.7

[a] Data from the TPD of benzene from Section 1.3.2 (Ref. 14).

heat of adsorption of the respective aromatic hydrocarbon are lower than that for H-ZSM-5 but higher than that for Si-MCM-41 (Table 1.3.4.1). This is mostly because of the much higher acidity of H-ZSM-5 and the absence of acid sites in Si-MCM-41. The lower heat of adsorption when compared to H-ZSM-5 is also attributed to the much larger (mesoporous) channel size of the Al-MCM-41 than that of the adsorbed molecules. In case of H-ZSM-5 zeolites, the contribution to the heat of adsorption by the dispersion forces responsible for physical adsorption, even at high temperature, is

very significant. The observed higher heat of adsorption when compared to that for the Si-MCM-41 is due to stronger interaction of the adsorbate with protons and Na^+ cations in the H-AlSi-MCM-41 and Na-AlSi-MCM-41 respectively.

It is interesting to note from Table 1.3.4.1 that the heat of adsorption of aromatic hydrocarbons corresponding to the main peak in the TPD for Na-AlSi-MCM-41 is higher than that observed for the H-AlSi-MCM-41. Also the TPD peak maximum for each of the aromatic hydrocarbons is at higher temperature side for the Na-AlSi-MCM-41. These observations indicate that the interaction of the aromatic hydrocarbons (their π-electrons) with the Na^+ cations are stronger than that with the zeolitic protons. This is consistent with that observed for the TPD of benzene over H- or Na-AlSi-MCM-41[14] and NaY, CeNaY and CeNaX[17] and of aromatic hydrocarbons over H- or Na-ZSM-5.[15]

The adsorption of aromatic hydrocarbons on the H- or Na-AlSi-MCM-41 is expected to result from the interaction of the π-electrons of a single (for toluene, p-xylene and mesitylene) or a fused double (for naphthalene) aromatic rings with the protons or Na^+ cations and also with the silanol groups present in the AlSi-MCM-41. The π-electron density on the aromatic ring(s) is increased with increasing the number of methyl groups (which are electron donating groups) or with increasing the number of condensed aromatic rings. The observed heat of adsorption of the aromatic hydrocarbons is consistent with this; the heat of adsorption on both the Na- and H-AlSi-MCM-41 is increased with increasing the number of methyl groups attached to the benzene ring or with increasing the number of condensed aromatic rings (Table 1.3.4.1). Figure 1.3.4.7 shows the variation of the heat of adsorption with the ionization potential [which is decreased with increasing the π-electron density of the aromatic ring(s)] of the aromatic hydrocarbons. The heat of adsorption is decreased

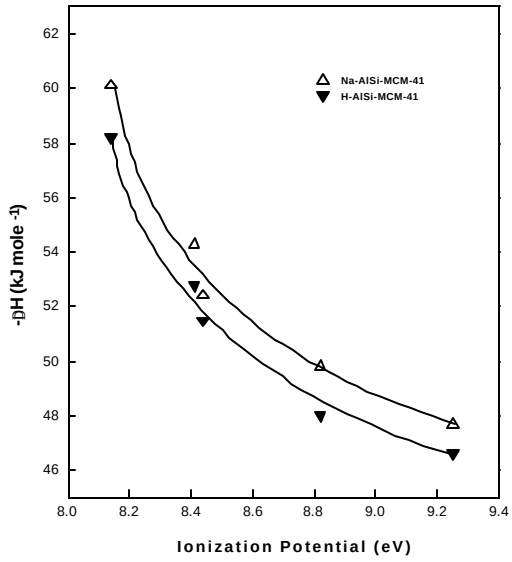

Fig. 1.3.4.7 Dependence of the heat of adsorption of aromatic hydrocarbons on their ionization potential.

exponentially with the increase in the ionization potential of the aromatic hydrocarbons (the values of ionization potential of the aromatic hydrocarbons are taken from Ref. 18). This is quite consistent with what expected from the above discussion and also with the earlier studies for the adsorption of aromatic hydrocarbons on H-ZSM-5[15] and Si-MCM-41.[16]

In the TPD of toluene on the H-AlSi-MCM-41 (Figs 1.3.4.2 and 1.3.4.3), three distinct peaks are observed and also the heat of adsorption (Table 1.3.4.1) for the corresponding TPD peaks is found to be higher for the peaks at higher temperatures. The observed three distinct peaks in the TPD of toluene indicate the presence of at least three energetically different types of toluene adsorption sites. In case of the benzene TPD on Si-MCM-41 and H- or Na-AlSi-MCM-41[14] four and five, respectively, distinct peaks were observed earlier. At least four types of terminal silanol groups, isolated Si-OH and three other types of Si-OH groups involving H-

bonds, have been observed in MCM-41.[8,9] The protons, isolated Si-OH and differently H-bonded Si-OH groups and their interactions with π-electrons of toluene seem to be responsible for the observed peak multiplicity in the toluene TPD.

A TPD peak multiplicity is observed only for the TPD of toluene over the H-AlSi-MCM-41 but not for the TPD of other aromatic hydrocarbons over both the adsorbents and even not for the TPD of toluene over the Na-AlSi-MCM-41. Similarly, a peak multiplicity was observed for the TPD of benzene over Si-MCM-41 and H- or Na-AlSi-MCM-41[14] but not for the TPD of higher aromatic hydrocarbons over Si-MCM-41.[16] This complex observation can be explained as follows. H- or Na-AlSi-MCM-41 contains at least five different sites – H^+ or Na^+ ions, isolated terminal Si-OH and three differently H-bonded terminal Si-OH, the terminal Si-OH groups being poorly acidic or non-acidic ones. The nature and/or energy of the terminal Si-OH sites is not expected to change drastically due to the presence of adsorbed benzene or toluene which has a low π-electron density. However, when an aromatic compound having high π-electron density is adsorbed, it may drastically change the nature and energy of the sites, particularly the differently H-bonded terminal Si-OH, making them indistinctive and/or ineffective for the adsorption, when compared to the stronger adsorption sites (H^+ or Na^+). Hence, the presence of these weaker adsorption sites is seen mostly as a hump at lower temperature side of some of the TPD peaks (Figs. 1.3.4.2 -1.3.4.5). The hump at the higher temperature side is, however, due to the energetically stronger sites and not because of cracked hydrocarbon products. The maximum temperature of the TPD was not high enough to crack the aromatic hydrocarbons.

1.3.4.3 Conclusions

From the studies on TPD of toluene, p-xylene, mesitylene and naphthalene on mesoporous Na-or H-AlSi-MCM-41 materials, following important conclusions have been drawn:

1. TPD of toluene over H-AlSi-MCM-41 shows peak multiplicity (three distinct peaks) but that of toluene over Na-AlSi-MCM-41 and other aromatic hydrocarbons over the H- or Na-AlSi-MCM-41 show only a single asymmetric peak with small humps or shoulders.
2. The heat of adsorption of the aromatic hydrocarbons over both the AlSi-MCM-41 adsorbents are in the following order: toluene < p-xylene < mesitylene < naphthalene. It is increased with decreasing the ionization potential of the hydrocarbons, indicating that the adsorption involves interactions of the π-electrons of the aromatic hydrocarbons with the adsorption sites on the AlSi-MCM-41 materials.
3. The heat of adsorption and hence, the interaction of the aromatic hydrocarbons with the Na^+ cations are stronger than that with the protons present in the AlSi-MCM-41 materials.

1.3.4.4 References

1. Kresge, C. T.; Leonowicz, M. E.; Roth, W. J.; Vartuli, J. C.; Beck, J. S., *Nature*, **359** (1992) 710.
2. Schmidt, R.; Akporiye, D.; Stocker, M.; Ellestad, O. H., *Stud. Surf. Sci. Catal.*, **84** (1994) 61.
3. Borade, R. B.; Clearfield, A., *Catal. Lett.*, **31** (1995) 267.
4. Climent, M. J.; Corma, A.; Iborra, S.; Navarro, M. C.; Primo, J., *J. Catal.*, **161** (1996) 783.
5. Corma, A.; Iborra, S.; Miquel, S. ; Primo, J., *J. Catal.* **173** (1998) 315.
6. Climent, M. J.; Corma, A. ; Guil-Lopez, R. ; Iborra, S. ; Primo, J., *J. Catal.*, **175** (1998) 70.
7. Rodriguez, I.; Iborra, S.; Rey, F. ; Corma, A. , *Appl. Catal. A*, **194 – 195** (2000) 241.
8. Jentys, A.; Pham, N. H.; Vinek, H., *J. Chem. Soc., Faraday Trans.*, **92** (1996) 3287.
9. Chen, J.; Li, Q.; Xu, R. ; Xiao, F., *Angew. Chem. Int. Ed. Engl.*, **34** (1995) 2694.
10. Cvetnovic, R. J.; Amenomiya, Y., *Adv. Catal.*, **17** (1967) 103.
11. Smutek, M.; Cerny, S.; Buzek, F., Adv. *Catal.*, **24** (1975) 343.
12. Cvetnovic, R. J.; Amenomiya, Y., *Catal. Rev.*, **6** (1972) 21.
13. Amenomiya, Y., *Chemtech.* (1976) 129.
14. Choudhary, V. R.; Mantri, K., *Langmuir*, **16** (2000) 8024.
15. Choudharay, V. R.; Srinivasan, K. R.; Singh, A. P., *Zeolites*, **10** (1990) 16.
16. Choudhary, V. R.; Mantri, K., *Microporous Mesoporous Mater.*, **40** (2000) 127.
17. Choudharay, V. R.; Srinivasan, K. R.; Akolekar, D. B., *Zeolites*, **9** (1989) 115.
18. Lide, D. R.; (Ed.) *"CRC Handbook, of Chemistry and Physics"*, **74th Edn.**, CRC Press, London, (1993) p. 10 – 208.

Chapter 2.2

EXPERIMENTAL

Chapter 2.2

EXPERIMENTAL

2.2.1 MODIFICATION OF Si-MCM-41

2.2.1.1 Impregnation of $InCl_3$, $GaCl_3$, $FeCl_3$ and $ZnCl_2$ on Si-MCM-41

Si-MCM-41 supported $InCl_3$, $GaCl_3$, $FeCl_3$ and $ZnCl_2$ catalysts with the metal chloride loading of 1.1 mmol g^{-1} were prepared by impregnating the respective metal chloride from its acetonitrile solution on Si-MCM-41 (surface area = 1160 m^2 g^{-1}), using an incipient wetness technique, followed by evaporating the solvent under moisture-free N_2 at 120°C for 8h. Si-MCM-41 supported $InCl_3$ at different loading (0.45 and 2.2 mmol g^{-1}) were also prepared using same process. All the catalysts were stored in a decicator.

2.2.1.2 Grafting of $AlCl_3$ on Mesoporous Si-MCM-41

A 10 g of the Si-MCM-41 was dried at 300°C for 6h. It was then allowed to cool to room temperature in a decicator. The dried Si-MCM-41 was then transferred to a 500 ml conical flask (fitted with a water reflux condenser) containing 250 ml of dry carbon tetrachloride. The Si-MCM-41 – CCl_4 mixture was refluxed with vigorous stirring for 1.5h while bubbling moisture-free N_2 (30 ml min^{-1}) through it to remove traces of moisture from the mixture. Thereafter, 4.6 g (34.5 mmol) or 1.33 g (10 mmol) anhydrous $AlCl_3$ (Aldrich) was added to the mixture and the resulting mixture was refluxed under the N_2 flow for 3 h. The HCl gas evolved in the grafting reaction,

$$n(\rightarrow Si{-}OH) + AlCl_3 \longrightarrow (\gg Si{-}O)_n + AlCl_{3-n} + nHCl \qquad (2.2.1)$$

was measured quantitatively by an acid-base titration (by absorbing the HCl gas in an aqueous NaOH solution) as a function of time. After the reaction, the $AlCl_3$-grafted Si-MCM-41 was filtered and washed with hot CCl_4 under dry N_2 and the filtrate was analyzed for its $AlCl_3$ content. The catalyst was dried under vacuum at 30°C and then stored in decicator. It was characterized for its specific surface area, bulk and surface Al/Si and Cl/Al ratios (by EDAX and XPS, respectively). It was also characterized by IR and ^{27}Al MAS NMR. The $AlCl_x$-grafted Si-MCM-41 was thermally treated at different temperatures under N_2 and flowing or static air for 1 h.

The resulting solid material was characterized for its surface area (using a Surface Area Analyzer, Quantachrome, USA), bulk and surface Al/Si and Cl/Al ratios (by EDAX and XPS, respectively) and $Al_{(tetrahedral)}$ / $Al_{(octahedral)}$ ratio from ^{27}Al MAS NMR. The strong acid sites on the thermally treated material was measured in terms of the pyridine chemisorbed at 400^{o}C, using the GC pulse technique. The IR spectra of the $AlCl_x$ grafted Si-MCM-41 was obtained by Nujol technique. The techniques used for characterizing the samples are described in Part-I (Chapter 1.2).

2.2.2 CATALYTIC REACTIONS

2.2.2.1 Esterification and Dehydration Reactions

Esterification of *tert*-butanol by acetic anhydride or dehydration of *tert*-butanol over the different Si-MCM-41 supported metal chloride catalysts was carried out in a magnetically stirred glass reactor (capacity 25 cm^3) fitted with a reflux condenser and a thermometer for measuring the reaction temperature. The outlet of the reflux condenser was connected to a constant pressure gas collector. The volume of the reaction mixture in the reactor was 10 cm^3. The reactor was kept in a constant temperature water bath. The iso-butylene formed in the reaction was measured quantitatively by collecting it in the gas collector at the atmospheric pressure. The products of the esterification were analyzed by a gas chromatograph (with flame ionization detector and SE - 30 column), using n-hexane as an internal standard.

2.2.2.2 Benzylation and Acylation Reactions

The experimental set up used for the benzylation or acylation reactions is shown in Fig. 2.2.1. The benzylation and benzoylation reactions over the catalysts were carried out in a magnetically stirred glass reactor (capacity 25 cm^3) fitted with a reflux condenser, having a low dead volume, mercury thermometer and arrangement for continuously bubbling moisture-free N_2 (30 cm^3 min^{-1}) through the liquid reaction mixture. The reaction was started by injecting benzyl chloride or benzoyl chloride in the benzylation or benzoylation reaction mixture, containing benzene and the catalyst, under benzene reflux (at 80^{o}C). The course of the reaction was followed by measuring quantitatively the HCl evolved in the reaction by acid-base titration (by absorbing the HCl carried by N_2 in a 0.1 M NaOH solution containing phenolphthalein indicator) as a function of time and also by analyzing the reaction mixture for unconverted benzyl chloride or benzoyl chloride and benzylation product or benzoylation products

at the end of the experiment by gas chromatography. There was a good agreement between the benzyl or benzoyl chloride conversion obtained from the acid-base titration and that from the GC analysis. The conversion data were corrected for a small time lag (1.1 min) between the evolution of HCl in the reaction and the analysis of the evolved HCl by the titration. In all the cases, the product formed was mainly mono-benzylated or acylated, and there was no formation of poly-benzyl chloride or poly-acyl chloride. The amount of benzylated or acylated product formed was equivalent (within 2-4 % error) to the amount of benzylating or acylating agent consumed in the reaction.

2.3.1 HIGHLY SELECTIVE Si-MCM-41 SUPPORTED $InCl_3$,

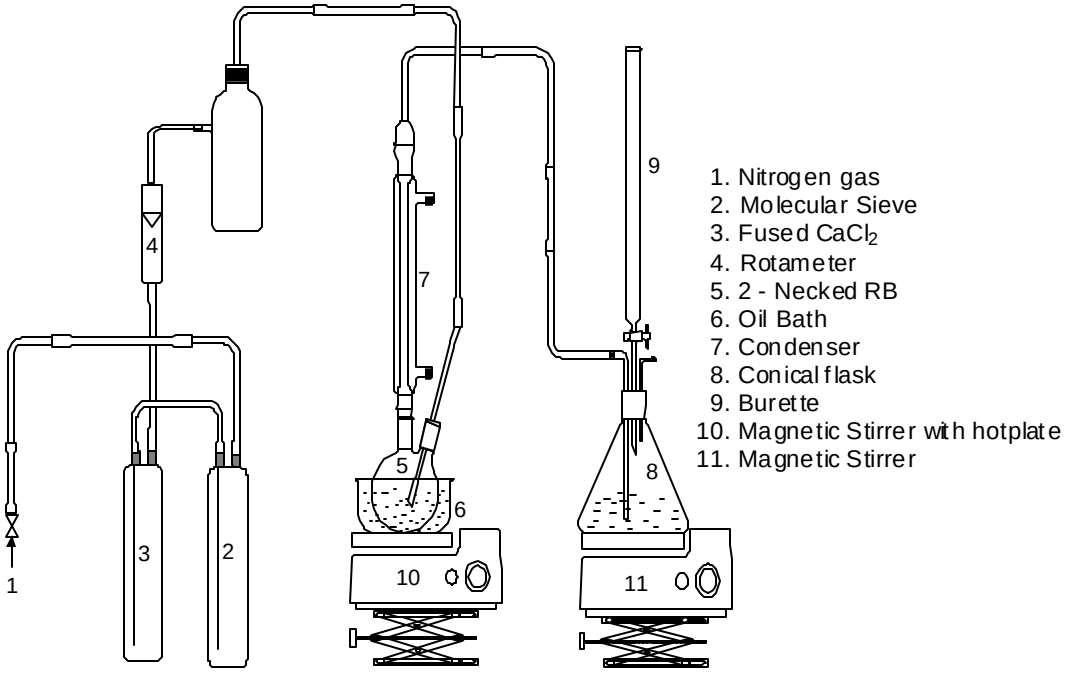

Fig. 2.2.1 Typical liquid phase reaction setup for benzylation or acylation of aromatic compounds

Chapter 2.3
RESULTS AND DISCUSSION

2.3.1 HIGHLY SELECTIVE SI-MCM-41 SUPPORTED $InCl_3$, $GaCl_3$, $FeCl_3$ AND $ZnCl_2$ CATALYSTS FOR LOW TEMPERATURE ESTERIFICATION OF *TERT* – BUTANOL BY ACETIC ANHYDRIDE

2.3.2 $AlCl_x$-GRAFTED Si-MCM-41 PREPARED BY REACTING ANHYDROUS $AlCl_3$ WITH TERMINAL Si-OH GROUPS: AN ACTIVE SOLID CATALYST FOR BENZYLATION AND ACYLATION REACTIONS

2.3.3 $AlCl_3$–GRAFTED Si-MCM-41 : INFLUENCE OF THERMAL TREATMENT CONDITIONS ON SURFACE PROPERTIES AND INCORPORATION OF Al IN THE STRUCTURE OF MCM-41

2.3.1 HIGHLY SELECTIVE Si-MCM-41 SUPPORTED $InCl_3$ $GaCl_3$, $FeCl_3$ AND $ZnCl_2$ CATALYSTS FOR LOW TEMPERATURE ESTERIFICATION OF *TERT*-BUTANOL BY ACETIC ANHYDRIDE

2.3.1.1 Background and Brief Description of Previous Work

Esterification of normal alcohols by carboxylic acids using homogeneous acid catalysts (viz. mineral acids) is well known.[1] However, the preparation of *tert*-butyl ester by the esterification of *tert*-butanol using an acid catalyst is very difficult because of the very high reactivity of *tert*-butanol. In the presence of acid catalyst, *tert*-butanol undergoes dehydration to iso-butylene, even at the room temperature. Earlier methods used for the esterification of *tert*-butanol are either highly cumbersome or involve use of highly toxic reagents[2-4]. Recently Nagasawa et. al.[6,7] used activated basic alumina at mild conditions (at room temperature under argon) for the esterification of *tert*-butanol by acid chlorides or acid bromides. Although they got a good yield of *tert*-butyl ester, the amount of catalyst relative to the reactants used by them was very large (catalyst/reactants wt. ratio = 2.1 ± 0.4). It is not of practical interest to use such a large amount of catalyst, and moreover the removal of high molecular weight adsorbed products from the catalyst is quite difficult and also expensive too. Other important drawback of their butyl ester synthesis method is the use of an acid halide as esterification agent, because of which a highly toxic gaseous hydrogen halide by-product is formed, in stoichiometric quantities. Hence, there is a need to develop an environmentally benign method for the esterification of *tert*-butanol using more active, selective and reusable solid catalyst, having almost no activity for the dehydration of *tert*-butanol. The work was undertaken for this purpose.

In this work, the use of mesoporous Si-MCM-41 supported $InCl_3$, $GaCl_3$, $FeCl_3$ and $ZnCl_2$, as the highly selective catalysts for the esterification of *tert*-butanol by an acetic anhydride, producing acetic acid as a harmless by-product, at a temperature close to room temperature has been reported. Dehydration of *tert*-butanol over these catalysts at different temperatures (26 – 80°C) has also been investigated.

2.3.1.2 Present Work

Results of the esterification of *tert*-butanol by acetic anhydride and also of the dehydration of *tert*-butanol to iso-butylene over Si-MCM-41 supported metal chloride catalysts are presented in Tables 2.3.1.1 and 2.3.1.2, respectively. TOF (turn over frequency) of the catalysts is defined as the number of molecules of *tert*-butanol converted per molecule of metal chloride present in the catalyst per second.

A comparison of the activity (TOF) of each catalyst for the esterification and dehydration reactions at 26°C (Tables 2.3.1.1 and 2.3.1.2) shows that all the Si-MCM-41 supported metal chloride catalysts have much lower activity for the dehydration of *tert*-butanol to iso-butylene. The dehydration activity of all the catalysts is very low at the room temperature (26°C). It is, however, increased exponentially with increasing the temperature.

For their performance in the esterification at 26°C, the catalysts are compared in Table 2.3.1.1. Following important observations can be made from the comparison:

- All the Si-MCM-41 supported metal chloride catalysts show high selectivity (>99%) but they differ significantly in their esterification activity. Among the catalysts, the $InCl_3$/ Si-MCM-41 shows the best performance, giving 99.95%

Table 2.3.1.1 Results of the esterification of *tert*-butanol by acetic anhydride over Si-MCM-41 supported $InCl_3$, $GaCl_3$, $FeCl_3$ and $ZnCl_2$ catalysts at 26°C [reaction mixture = *tert*-butanol (t-B) + acetic anhydride (AA) + catalyst; volume of reaction mixture = 10 cm^3; t-B/AA molar ratio = 1.1; reaction time = 2h; catalyst/(t-B + AA) wt. ratio = 0.057; t-B = *tert*-butanol; AA = acetic anhydride, t-BA = *tert*-butyl acetate; and i-B = iso-butylene].

Catalyst	Conversion (%)		Selectivity (%)		TOF × 10^3 (s^{-1})
	t-B	AA	t-BA	i-B	
$InCl_3$/Si-MCM-41	55.5	61.0	99.9	0.1	7.4
$InCl_3$/Si-MCM-41[a]	51.2	56.3	98.6	1.4	6.8
$GaCl_3$/Si-MCM-41	46.5	52.1	99.9	0.1	6.2
$FeCl_3$/Si-MCM-41	33.7	37.5	99.9	0.1	4.5
$ZnCl_2$/Si-MCM-41	40.0	42.9	99.9	0.1	5.3
Si-MCM-41	2.04	2.3	100	0.0	-

[a] 3rd reuse of the catalyst.

- selectivity for *tert*-butyl acetate at 61.0% and 55.5% conversion of acetic anhydride and *tert*-butanol, respectively. The support itself shows only a very little activity for the esterification.
- Even in the 3rd reuse, the $InCl_3$/ Si-MCM-41 catalyst shows only a slightly lower activity and selectivity indicating the reusability of the catalyst for the esterification.
- The Si-MCM-41 supported metal chloride catalysts have the esterification activity in the following order: $InCl_3 > GaCl_3 > ZnCl_2 > FeCl_3$.

Table 2.3.1.2 Activity of Si-MCM-41 supported metal chloride catalysts (loading of metal chloride = 1.1 mmol g^{-1}) for dehydration of *tert*-butanol at different temperatures (reaction mixture = 10 ml *tert*-butanol + 0.2 g catalyst; reaction time = 0.5 h).

Catalyst	TOF × 10^3 (s^{-1})		
	26°C	50°C	80°C
$InCl_3$/Si-MCM-41	0.23 (0.086)[a]	1.78 (0.67)	6.54 (2.46)
$GaCl_3$/Si-MCM-41	0.17 (0.064)	1.02 (0.38)	6.31 (2.37)
$FeCl_3$/Si-MCM-41	0.23 (0.086)	1.80 (0.68)	5.97 (2.25)
$ZnCl_2$/Si-MCM-41	0.17 (0.064)	1.69 (0.64)	6.20 (2.33)

[a]Conversion (%) of *tert*-butanol is given in the round brackets.

Dependence of both the conversion and selectivity on the reaction time in the esterification over the $InCl_3$/ Si-MCM-41 catalyst at different loading of $InCl_3$ (0.45, 1.1 and 2.2 mmol g^{-1}) is shown in Fig 2.3.1.1. The esterification reaction is very slow at the lower catalyst loading, but at the higher loading, it is quite fast. By increasing the loading from 0.5 to 2.2 mmol g^{-1}, the time required for the half reaction is reduced from 29 to 5 h. The change or decrease in the selectivity for *tert*-butyl acetate with increasing the reaction time even for the higher catalyst loading is negligibly small.

In the overall esterification process following reactions are involved.

Main Reaction:

$$(CH_3)_3COH + (CH_3CO)_2O \rightarrow CH_3COOC(CH_3)_3 + CH_3COOH \qquad (2.3.1.1)$$

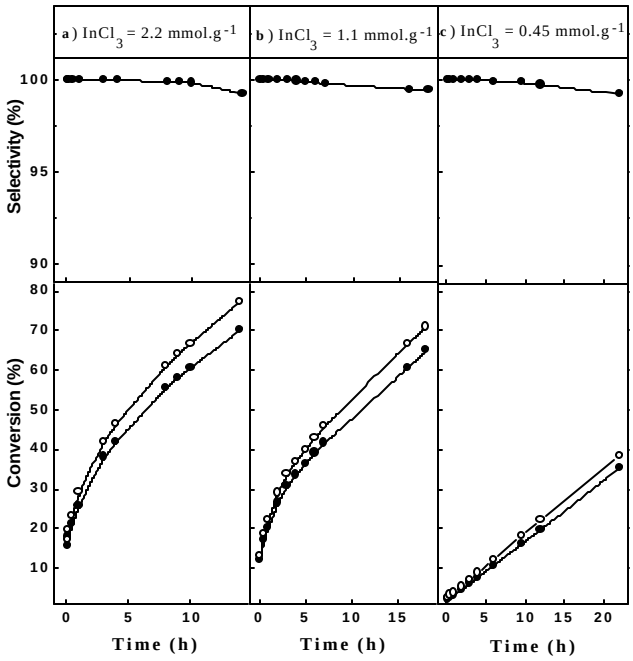

Fig. 2.3.1.1 Dependence of the conversion of *tert*-butanol (–•–) and acetic anhydride (–○–) and selectivity for *tert*-butyl acetate in the esterification over the $InCl_3$/Si-MCM-41 catalyst with different $InCl_3$ loading at 26°C (t-B/AA = 1.1 and catalyst/(t-B + AA) wt. ratio = 0.028)

Side Reactions:

$$(CH_3)_3COH \rightarrow (CH_3)_2C=CH_2 + H_2O \qquad (2.3.1.2)$$

$$(CH_3CO)_2O + H_2O \rightarrow 2CH_3COOH \qquad (2.3.1.3)$$

In the process, acetic acid in stoichiometric amounts is formed as a by-product. However, it has a commercial value and moreover it can be converted back to acetic anhydride and recycled in the process. Thus, this process is free from any serious problem of handling and/or treating highly corrosive and toxic by-product, such as hydrogen halide produced in the process based on the use of an acid halide as an esterification agent.[6,7] Also, the amount of catalyst used relative to the reactant is much smaller. Other important feature of the present catalysts is that they are

mesoporous and hence can be used even with very bulky substrates and/or products, generally involved in the organic synthesis.

The Si-MCM-41 supported metal chloride catalysts are acidic (Lewis acid) in nature. However, the strength of their Lewis acid sites is expected to be much lower than that of $AlCl_3$ which is a strong Lewis acid [order of cation size: In^{+3} (8.1 nm) > Zn^{+2} (7.4 nm) > Fe^{+3} (6.4 nm) > Ga^{+3} (6.2 nm) > Al^{+3} (5.1 nm), higher the cation size lower is the strength of lewis acid]. A following probable mechanism is proposed for the esterification of *tert*-butanol by acetic anhydride over the soft (or weak) Lewis acid sites (G).

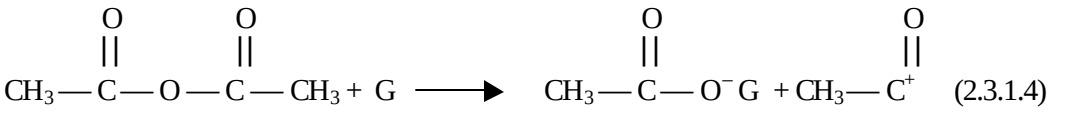

(2.3.1.4)

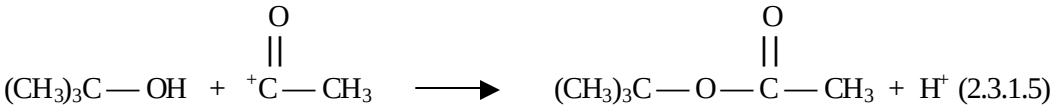

(2.3.1.5)

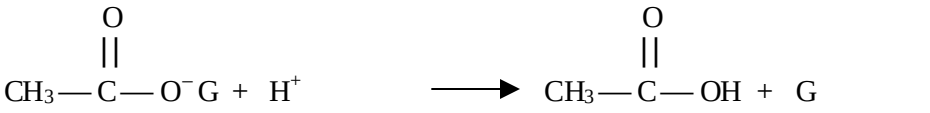

(2.3.1.6)

The dehydration of *tert*-butanol over the catalysts (Table 2.3.1.2), is expected to occur by the following mechanism.

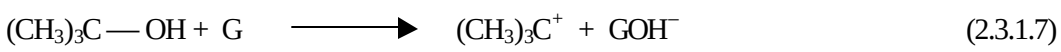

(2.3.1.7)

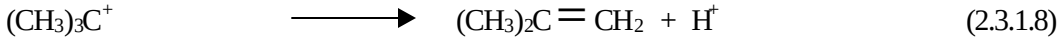

(2.3.1.8)

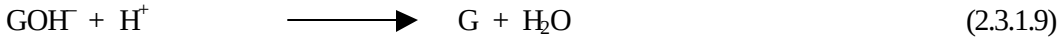

(2.3.1.9)

Since the Lewis acid sites of the catalysts are of low strength, there is a little or no dehydration of *tert*-butanol in the estetrification (Table 2.3.1.1).

In summary, the Si-MCM-41 supported metal chloride catalysts, particularly the $InCl_3$/Si-MCM-41 and $GaCl_3$/Si-MCM-41 catalysts show high promises for their use in the selective esterification of *tert*-butanol by an acid anhydride.

2.3.1.3 References

1. Patai, S. (Ed) *"The Chemistry of Carboxylic Acid and Esters"*, John Wiley and Sons Ltd., New York, (1969).
2. Anderson, G. W.; Callahan, F. M., *J. Am. Chem. Soc*. **82** (1960) 3359.
3. Kaiser E. M.; Woodruff, R. A., *J. Org. Chem.* **35** (1970) 1198.
4. Takimoto, S.; Inanaga, J.; Katsuki, J.; Yamaguchi, M., *Bull. Chem. Soc. Jpn.*, **49** (1976) 2335.
5. Armstrong, A.; Brackenridge, I.; Jackson. R.F.W.; Kirk, J. M., *Tetrahedron Lett*. **29** (1988) 2483.
6. Nagasawa, K.; Yoshitake, S.; Amiya, T.; Ito, K.., *Synth. Commun.* **20** (1990) 2033.
7. Nagasawa, K.; Ohhashi, K.; Yamashita, A.; Ito, K., *Chem. Lett.*, (1994) 209.

2.3.2 $AlCl_x$-GRAFTED Si-MCM-41 PREPARED BY REACTING ANHYDROUS $AlCl_3$ WITH TERMINAL Si-OH GROUPS: AN ACTIVE SOLID CATALYST FOR BENZYLATION AND ACYLATION REACTIONS

2.3.2.1 Background and Brief Description of Earlier Work

Anhydrous $AlCl_3$ is a well known homogeneous acidic (Lewis acid) catalyst for the liquid phase Friedel-Crafts reactions.[1] However, its use as a homogeneous catalyst in the Friedel-Crafts reactions is limited because of the following problems: use of stoichiometric amount or even more, difficult separation from the reaction product causing a large volume liquid waste, corrosive nature, high toxicity and no reuse in the subsequent batches. For its effective use in the Friedel-Crafts reactions, $AlCl_3$ is to be anchored on solid supports without affecting its catalytic activity. In order to develop new solid acid catalysts, efforts have been made to anchor $AlCl_3$ on silica gel, alumina, mesoporous silica or silica alumina and other inorganic metal oxides by treating them with $AlCl_3$ by vapor deposition[2] or in anhydrous liquid medium.[3,4] Immobilized aluminum chloride catalysts have been reported for Friedel-Crafts alkylation of aromatic hydrocarbons by alkenes,[4-7] chloroalkanes[4] and benzyl alcohol.[8]

In this work, it is found that $AlCl_x$ (bulk Cl/Al ratio = 1.43) grafted mesoporous high silica MCM-41 (Si-MCM-41), prepared by reacting anhydrous $AlCl_3$ with the terminal Si-OH groups of Si-MCM-41 in dry CCl_4, shows high catalytic activity in the liquid phase Friedel-Crafts type benzylation and acylation reactions.

2.3.2.2 Present Work

The benzylation and benzoylation reactions over the catalyst were carried out in a magnetically stirred glass reactor. The reactor and procedures for carrying out the

reactions are described in the experimental section (Chapter 2.2). Results of these Friedel-Crafts reactions are presented in Fig. 2.3.2.2.

The results (Fig. 2.3.2.2) show that the $AlCl_x$-grafted Si-MCM-41 has high benzylation and benzoylation activity, even for the benzylation and benzoylation of benzene. As expected, the catalytic activity for the toluene benzylation or benzoylation is higher because of the presence of electron donating methyl group.[1] The catalyst can be reused in the subsequent experiments but with somewhat reduced activity. This is most probably due to its momentary exposure to atmosphere during its reuse. When the catalyst was exposed to atmosphere for a longer period (above 2-3 min), its benzylation activity was totally killed and also its color changed from brown to white due to the adsorption of moisture from the atmosphere.

Figure 2.3.2.1 shows the ^{27}Al MAS NMR spectrum. The $Al_{(tetrahedral)}$ / $Al_{(octahedral)}$ ratio was obtained by comparing the area under the curve of respective Al sites. The surface concentration of the elements (viz. Al, Si, Cl) present in the $AlCl_3$-grafted Si-MCM-41 was obtained from the XPS spectra (Fig. 2.3.2.3). From comparison of the catalyst characterization data (Table 2.3.2.1), following important observations can be made:

- After the $AlCl_3$ grafting, the structure of Si-MCM-41 is retained with a small decrease in its surface area and the IR peak at 3730 cm^{-1} (which corresponds to terminal Si-OH groups[9]) is disappeared, indicating the consumption of hydroxyl groups in the reaction (reaction 2.2.1).

Table 2.3.2.1 Data on characterization of Si-MCM-41 and $AlCl_x$ grafted Si-MCM-41

	Si-MCM-41	$AlCl_x$ grafted Si-MCM-41
Color	White	Brown
Surface area (m^2g^{-1})	1170	930
Crystal structure	MCM-41	MCM-41
Bulk Al/Si ratio (by EDAX)	0.0	0.17
Surface Al/Si ratio (by XPS)	0.0	0.43
Bulk Cl/Al ratio (by EDAX)	0.0	1.43 [a]
Surface Cl/Al ratio (by XPS)	0.0	0.85
$Al_{(tetrahedral)}$ / $Al_{(octahedral)}$ ratio	-	0.84
IR peaks in the region of 2500 to 4000 cm^{-1}	Sharp peak at 3730 cm^{-1} and broad peak at 3402 cm^{-1}	Broad peak at 3400 cm^{-1}

[a] This value is very close to that (1.45) obtained from the amount of $AlCl_3$ consumed and HCl evolved in the grafting reaction.

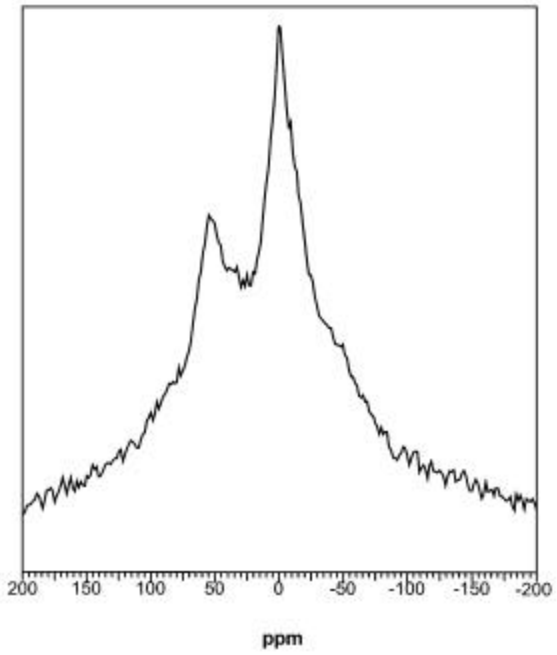

Fig. 2.3.2.1 ^{27}Al MAS NMR of $AlCl_x$-grafted Si-MCM-41

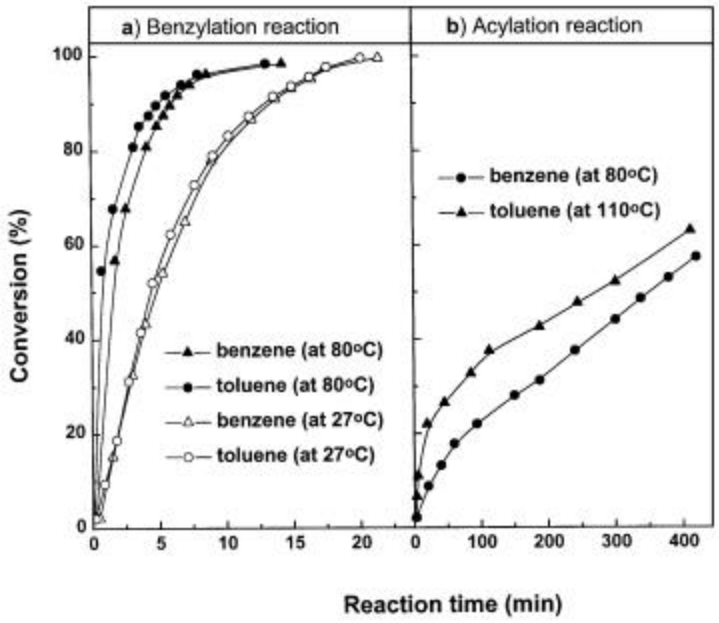

Fig. 2.3.2.2 Conversion vs. time curves for a) benzylation of benzene and toluene by benzyl chloride and b) benzoylation of benzene and toluene by benzoyl chloride [reaction mixture: 13 ml of benzene (or toluene) + 1.0 ml of benzyl chloride (or benzoyl chloride) + 0.1 g (for benzylation) or 0.4 g (for benzoylation) catalyst].

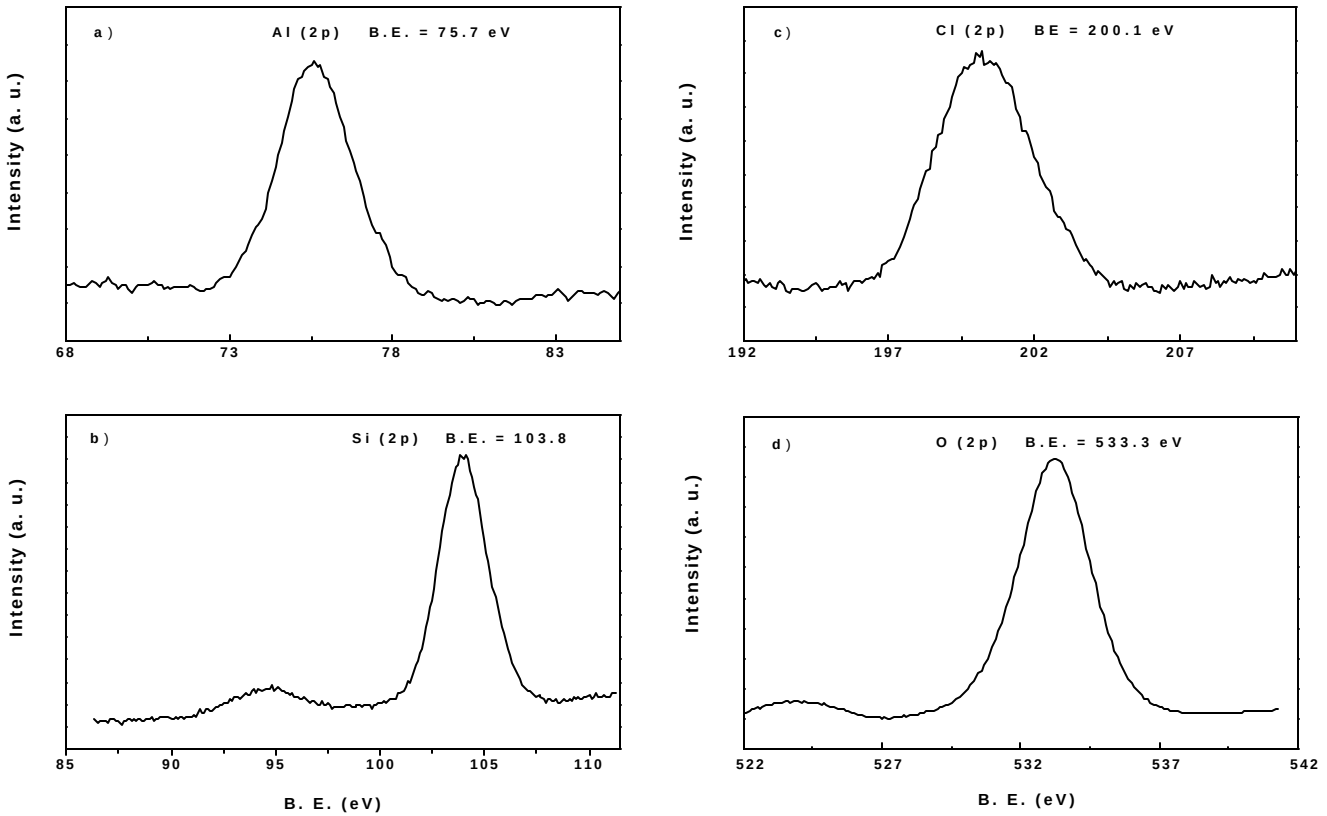

Fig. 2.3.2.3 X-ray photoelectron spectroscopy for the elements, a) Al (2p), b) Si (2p), c) Cl (2p) and d) O (2p) present in the $AlCl_x$-grafted Si-MCM-41.

- The surface Al/Si ratio is higher than the bulk Al/Si ratio and also the surface Cl/Al ratio is lower than the bulk Cl/Al ratio. This indicates that the reaction of $AlCl_3$ at the external surface occurs to a larger extent, and also consumes more Si-OH groups according to reaction 2.3.1 than that in the mesoporous channels.

The two ^{27}Al MAS NMR peaks (Fig. 2.3.2.1), one at 54.25 ppm and second at –1.78 ppm, indicate the presence of Al in the $AlCl_x$-grafted-Si-MCM-41 in both the tetrahedral and octahedral forms. The grafting reaction is expected to proceed according to reaction 2.3.1, forming $(\rightarrow Si-O)_n AlCl_{3-n}$ species in the catalyst. Based on the surface and bulk Cl/Al ratios (Table 2.3.2.1), the Al-containing species in the catalyst are as follows:

At the external surface: $(\rightarrow Si-O)_2AlCl$ and $(\rightarrow Si-O)_3 Al$

In the mesoporous channels: $(\rightarrow Si-O)AlCl_2$ and $(\rightarrow Si-O)_2AlCl$.

In summary, the $AlCl_x$-grafted Si-MCM-41 is a highly active and also a reusable (if not exposed to atmosphere) mesoporous solid catalyst for the Friedel-Crafts type benzylation and acylation reactions. However, like anhydrous $AlCl_3$, it is highly moisture sensitive and loses its activity on exposure to moist atmosphere. The active species on the catalyst are $(\rightarrow Si-O)_nAlCl_{3-n}$ (n = 1 - 3).

2.3.2.3 References

1. Olah, G. A.; *"Friedel-Crafts and Related Reactions"*, Wiley-Interscience, New York, (1963) p. 1.
2. Olah, G. A.; Suryaprakash, G. K.; Sommar, J., *"Superacids"*, Wiley, New York, (1985) p. 53.
3. Getty, E. E.; Draga, R. S., *Inorg. Chem.*, **29** (1990) 1186.

4. Clark, J. H.; Martin, K.; Teasdale, A. J.; Barlow, S. J., *J. Chem. Soc., Chem. Commun.*, (1995) 2037.

5. Clark, J. H.; Price, P. M. ; Martin, K.; Macquarrie, D. J.; Bastock, T. W., *J. Chem. Research (S)*, (1997) 430.

6. Price, P. M.; Clark, J. H.; Martin, K.; Macquarrie, D. J.; Bastock, T. W.; *Organic Process Research & Development*, **2** (1998) 221.

7. Jun, S.; Ryoo, R., *J. Catal*., **195** (2000) 237.

8. Hu, X.; Foo, M. L.; Chuah, G. K.; Jaenicke, S., *J. Catal*. **195** (2000) 412.

9. Chen, J.; Li, Q.; Xu, R.; Xiao, F., *Angew. Chem. Int. Ed. Engl.*, **34** (1995) 2694.

2.3.3 $AlCl_3$-GRAFTED Si-MCM-41: INFLUENCE OF THERMAL TREATMENT CONDITIONS ON SURFACE PROPERTIES AND INCORPORATION OF Al IN THE STRUCTURE OF MCM-41

2.3.3.1 Background and Brief Description of Earlier Work

Aluminium chloride (an important Lewis acid catalyst) could be immobilized by its grafting on the surface of inorganic solids.[1-6] The $AlCl_3$ grafting could be accomplished by reacting an anhydrous $AlCl_3$ from non-aqueous solvent with inorganic solids with the evolution of HCl, which is a side product of the reaction. Recently, the grafting of $AlCl_3$ on Si-MCM-41 has been reported for producing a highly active Lewis acid catalyst for the Friedel-Crafts alkylation reactions.[7,8] Earlier studies[3] showed that the $AlCl_3$ grafting by refluxing anhydrous $AlCl_3$ in CCl_4 solution with SiO_2 results in both 4 and 6 coordinated Al species on the silica surface. Very recently, Jun and Ryoo[7] have observed the incorporation of Al in its tetrahedral and octahedral symmetry for the $AlCl_3$ grafted KIT-1 (a mesoporous aluminosilicate molecular sieve with disordered three dimensional channel network).

Si-MCM-41 (a mesoporous silica) has a highly defect structure with different types of terminal Si-OH groups.[9,10] It is therefore, interesting to study the reaction of anhydrous $AlCl_3$ with the terminal Si-OH groups of Si-MCM-41 for incorporating Al in the structure of MCM-41. The present work was undertaken for this purpose and also for studying the influence of thermal treatment temperature and gas atmosphere on the incorporation of Al in its tetrahedral and octahedral symmetry and surface properties of the $AlCl_x$-grafted Si-MCM-41.

2.3.3.2 Present Work

2.3.3.2.1 Grafting of $AlCl_3$ on Si-MCM-41

Data on the HCl evolved in the reaction between the terminal Si-OH groups of Si-MCM-41 and anhydrous $AlCl_3$ as a function of the reaction period are presented in Fig. 2.3.3.1. The reaction was stopped when there was no more evolution of HCl (i.e., after 3 h) in the reaction.

For the $AlCl_3$ concentrations of 1.0 and 3.45 mmol $g^{-1}_{(Si\text{-}MCM\text{-}41)}$, the Al grafting on the Si-MCM-41 was 1.0 and 3.2 mmol $g^{-1}_{(Si\text{-}MCM\text{-}41)}$, respectively, and the Cl/Al ratio of the grafted $AlCl_x$-species was 0.83 and 1.43, respectively (Table 2.3.3.1). The change in the Cl/Al ratio from three to observed ones indicates that, in the grafting of $AlCl_3$, more than one terminal hydroxyl groups are involved. The reactions involved in the grafting process are as follows:

$$(-OH) + AlCl_3 \longrightarrow (-O-)AlCl_2 + HCl \qquad (2.3.3.1)$$

$$2(-OH) + AlCl_3 \longrightarrow (-O-)_2 AlCl + 2\,HCl \qquad (2.3.3.2)$$

$$3(-OH) + AlCl_3 \longrightarrow (-O-)_3 Al + 3\,HCl \qquad (2.3.3.3)$$

Figure 2.3.3.2 shows that the IR band at about 3730 cm^{-1}, which corresponds to –OH groups of the Si-MCM-41, is decreased or vanished after the grafting. This is consistent with the fact that the – OH groups are consumed in the above reactions. The XPS analysis showed that the Cl/Al ratio at the external surface of the $AlCl_3$-grafted Si-MCM-41 is lower than the bulk Cl/Al ratio (Table 2.3.3.1). The surface

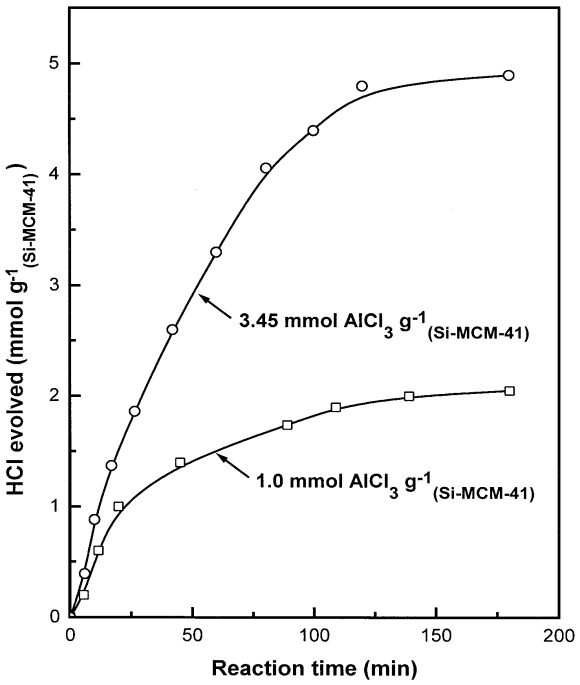

Fig. 2.3.3.1 HCl evolved in the grafting of $AlCl_3$ on Si-MCM-41 at different concentrations of $AlCl_3$ in the reaction mixture.

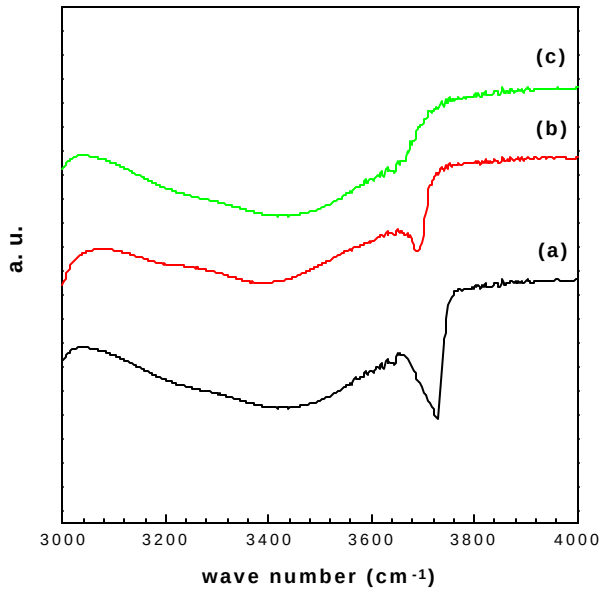

Fig. 2.3.3.2 IR spectra of Si-MCM-41 (a) and $AlCl_3$-grafted Si-MCM-41 obtained using $AlCl_3$ concentrations of 1.0 mmol $g^{-1}_{(Si\text{-}MCM\text{-}41)}$ (b) and 3.45 mmol $g^{-1}_{(Si\text{-}MCM\text{-}41)}$ in the grafting.

Table 2.3.3.1 Effect of thermal treatment conditions on bulk and surface properties of $AlCl_x$-grafted Si-MCM-41 prepared using two different concentration of $AlCl_3$ in the grafting.

Concentration of $AlCl_3$ (mmol g^{-1})	Thermal treatment conditions			Al/Si ratio		$Al_{(tetrahedral)}$ / $Al_{(octahedral)}$	Cl/Al Ratio		Acidity (mmol. g^{-1})
	Gas atmosphere	Temperature (^oC)	Time (h)	Bulk	At external surface		Bulk	At external surface	
1.0	Vacuum	80	12	0.06	0.31	1.53	0.83	0.20	--
	Air	500	1	-	-	4.5	0.02	0.01	0.06
	N_2	400	1	-	-	6.4	0.13	0.05	0.08
3.45	Vacuum	80	12	0.17	0.43	0.84	1.43	0.85	--
	Air	500	1	0.17	0.20	4.6	0.04	0.02	0.13
	N_2	400	1	-	-	8.2	0.20	0.08	0.27
	N_2	800	1	0.17	0.006	≈0.0	0.087	≈0.0	≈0.0

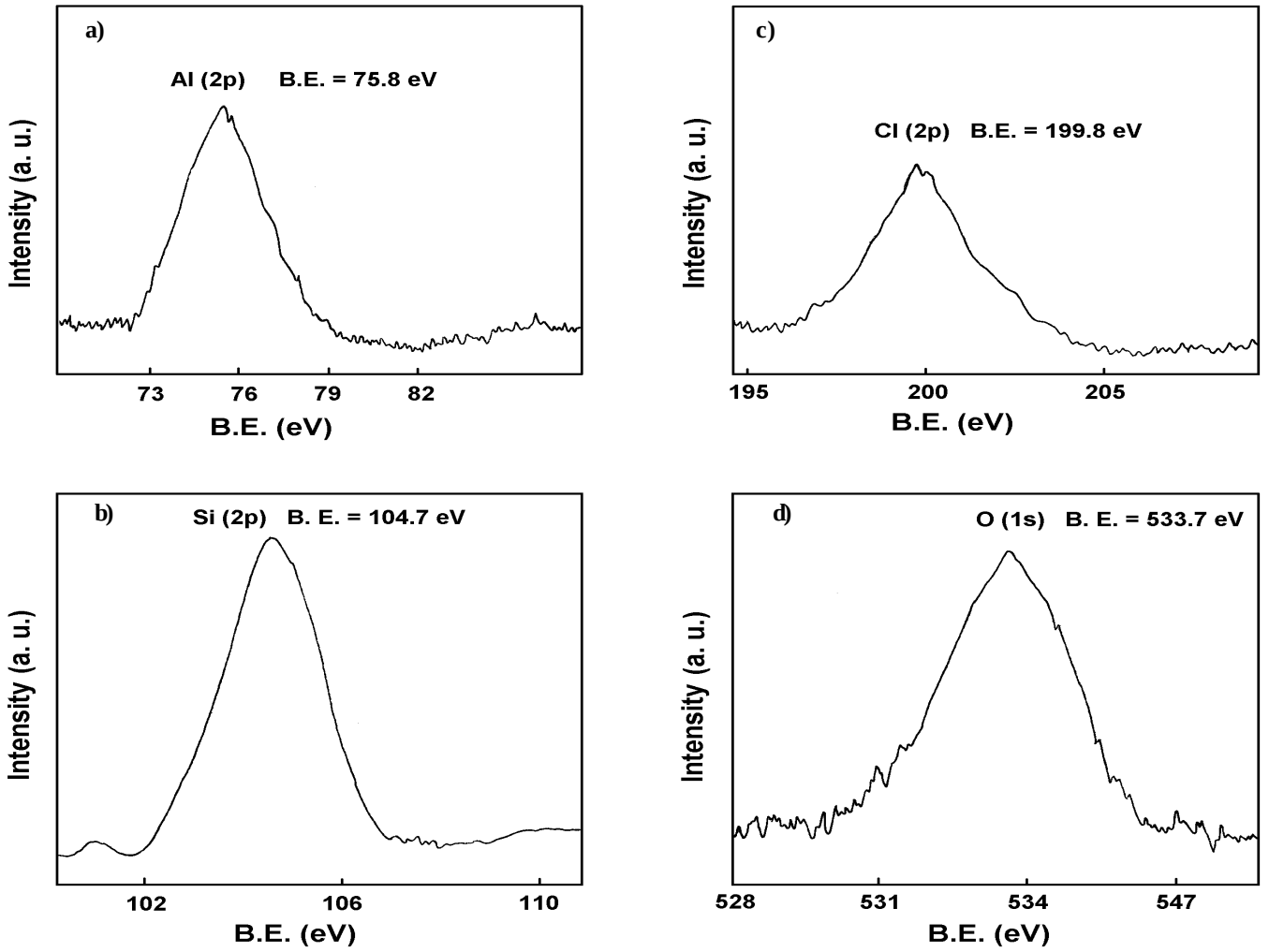

Fig. 2.3.3.3 XPS spectra of elements a) Al (2p), b) Si (2p), Cl (2p) and O (1s) in $AlCl_3$-grafted Si-MCM-41 (dried at 80^oC) obtained from using $AlCl_3$ concentration of 1.0 mmol $g^{-1}_{(Si\text{-}MCM\text{-}41)}$.

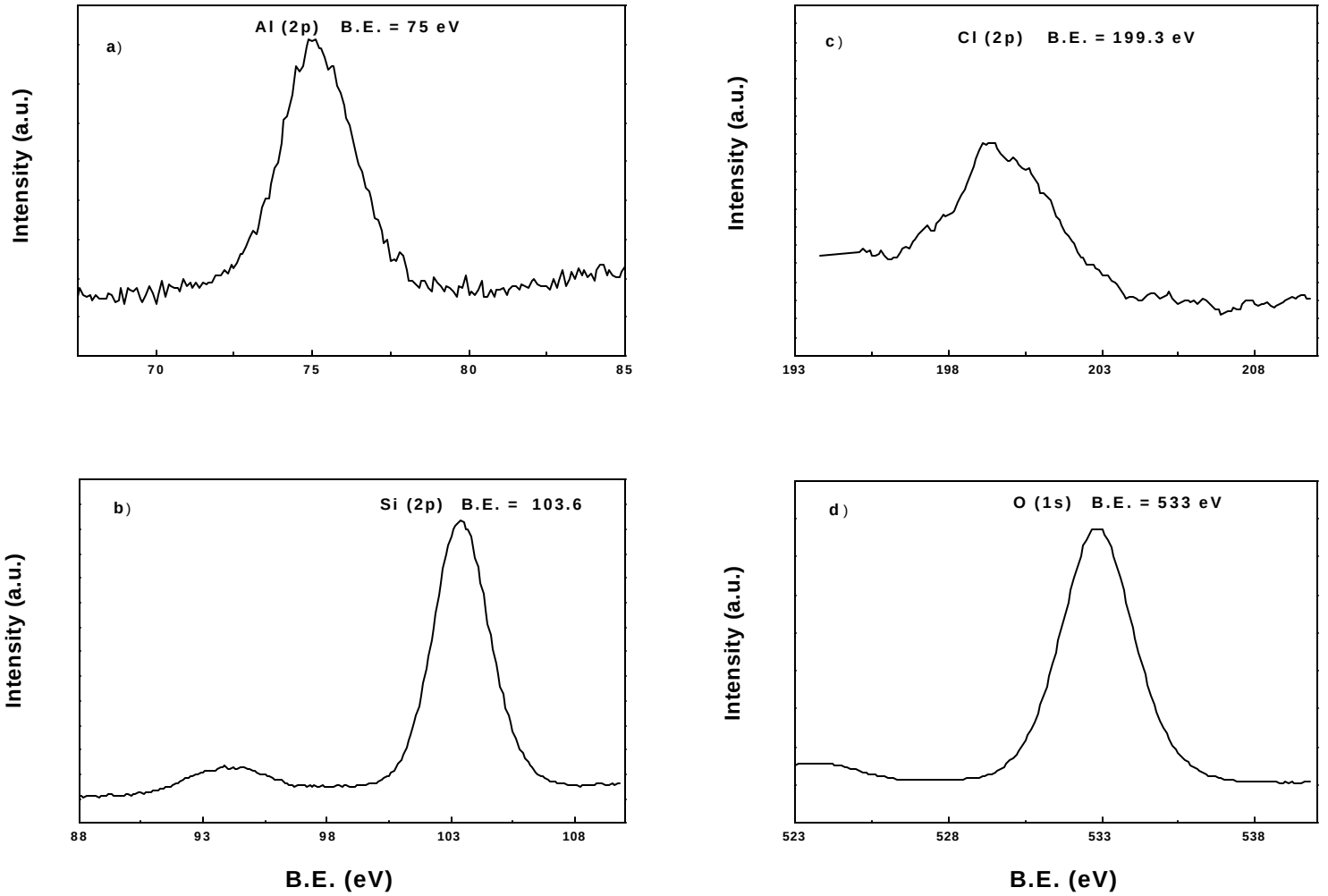

Fig. 2.3.3.4 XPS spectra of elements a) Al (2p), b) Si (2p), Cl (2p) and O (1s) in $AlCl_3$-grafted Si-MCM-41 (Calcined at 500^oC in air) obtained from using $AlCl_3$ concentration of 3.45 mmol $g^{-1}_{(Si\text{-}MCM\text{-}41)}$.

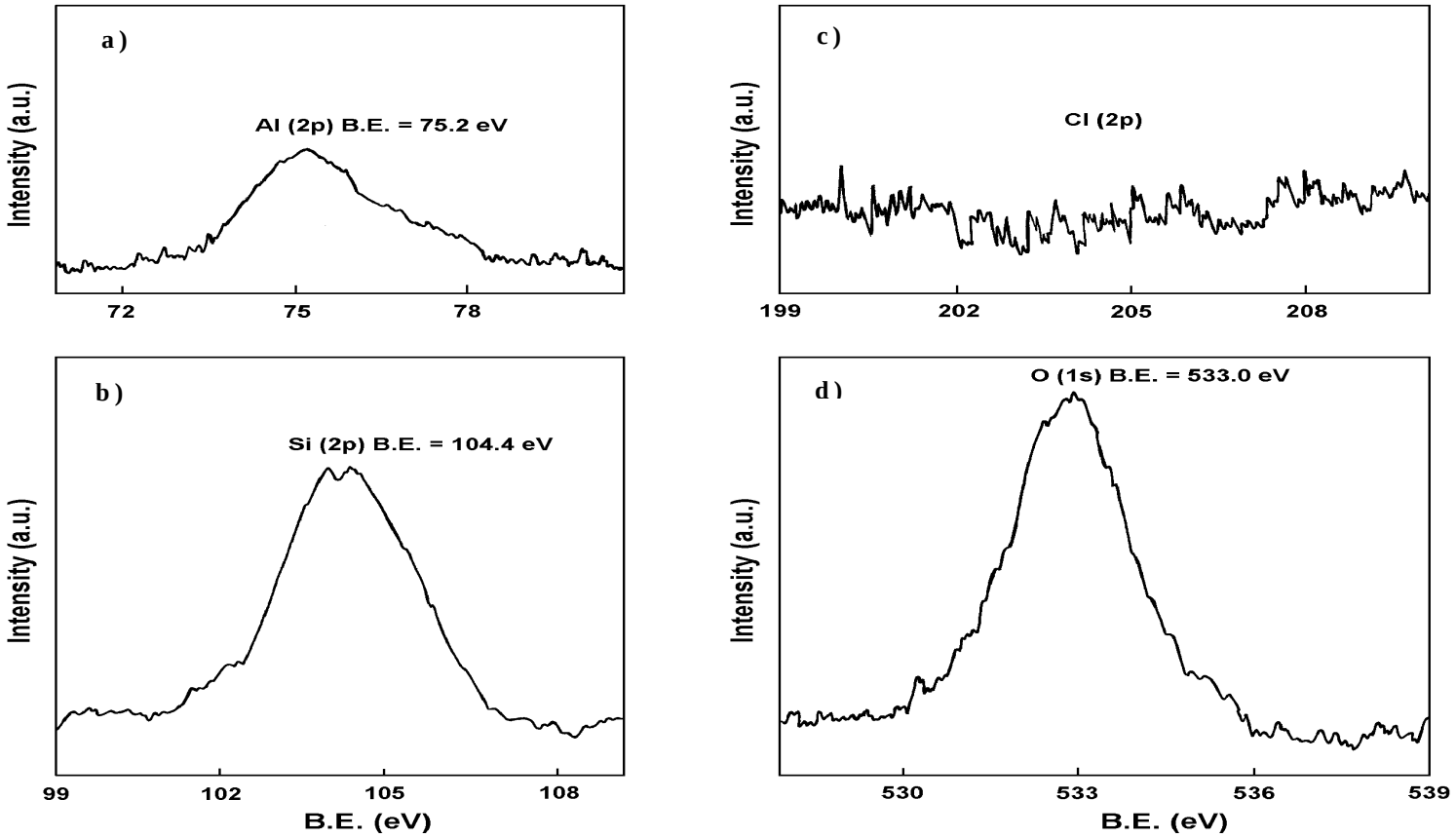

Fig. 2.3.3.5 XPS spectra of elements a) Al (2p), b) Si (2p), Cl (2p) and O (1s) in $AlCl_3$-grafted Si-MCM-41 (Calcined at 800^oC in air) obtained from using $AlCl_3$ concentration of 3.45 mmol $g^{-1}_{(Si\text{-}MCM\text{-}41)}$.

concentration of the elements (viz. Al (2p), Si (2p), Cl (2p) and O (1s)) was calculated from the XPS spectra (Figs. 2.3.3.3–2.3.3.5). The procedure is discussed in Part-I (Chapter 1.2). The XPS spectrum of the dried $AlCl_x$-grafted Si-MCM-41 (at 80°C) at higher $AlCl_3$ concentration (3.45 mmol g^{-1}) is shown in earlier Section (Section 2.3.3). This indicates the involvement of more terminal Si-OH groups from the external surface than that from the hexagonal mesoporous channels of the Si-MCM-41 in the $AlCl_3$-grafting. This is expected because of the presence of a larger number of terminal Si-OH groups at the external surface of Si-MCM-41. Also, the surface Al/Si ratio is much higher than the bulk Al/Si ratio (Table 2.3.3.1). This shows that the grafting reactions occur to a larger extent at the external surface as compared to that in the mesoporous channels. This is also expected because of the larger terminal Si-OH groups present at the external surface of Si-MCM-41. Based on the surface and bulk Cl/Al ratios, the Al containing species formed in the grafting are as follows.

For the higher $AlCl_3$ concentration (3.45 mmol. $g^{-1}_{(Si\text{-}MCM\text{-}41)}$) used in the grafting.

In the mesoporous channels: ($\equiv$Si – O)$AlCl_2$ (I) and ($\equiv$Si – O)$_2$AlCl (II)

At the external surface: ($\equiv$Si – O)$_2$AlCl (II) and ($\equiv$Si – O)$_3$Al (III)

For the lower $AlCl_3$ concentration (1.0 mmol $g^{-1}_{(Si\text{-}MCM\text{-}41)}$) used in the grafting.

In the mesoporous channels: ($\equiv$Si – O)$_2$ AlCl (II) and ($\equiv$Si – O)$_3$Al (III), II > III.

At the external surface: ($\equiv$Si – O)$_3$ Al (III) and ($\equiv$Si – O)$_2$AlCl (II), III >II.

The ^{27}Al MAS NMR spectra of the $AlCl_3$-grafted Si-MCM-41 are shown in Figs. 2.3.3.6a and 2.3.3.7a. In both the cases, two peaks, one at close to zero ppm and second at about 54 ppm, are observed. The first and second peak shows the formation of 4 coordinated (tetrahedral) and 6 coordinated (octahedral) Al, respectively, in the $AlCl_3$ grafting. The $Al_{(tetrahedral)}$ /$Al_{(octahedral)}$ ratio in the two $AlCl_3$-grafted samples is quite different; it is higher for the sample prepared using the lower concentration of $AlCl_3$ (Table 2.3.3.1).

2.3.3.2.2 Effect of Thermal Treatment Conditions

The ^{27}Al MAS NMR spectra of the $AlCl_3$ grafted Si-MCM-41 (Al/Si = 0.06 and 0.17), showing the influence of thermal treatment conditions (viz., temperature and gas atmosphere) on the relative concentration of the octahedral and tetrahedral Al, are presented in Figs. 2.3.3.6 and 2.3.3.7. The corresponding values of $Al_{(tetrahedral)}$ / $Al_{(octahedral)}$, obtained by comparing the area of the NMR peak at about 54 ppm to that at zero ppm, are included in Table 2.3.3.1. The data on the surface composition (Cl/Al and Al/Si ratios at the external surface) and strong acidity (measured in terms of the pyridine chemisorbed at 400^oC) for the thermally treated samples are also included in Table 2.3.3.1. Whereas, the influence of the thermal treatment conditions (viz., temperature and gas atmosphere) on the thermal stability of the $AlCl_3$-grafted Si-MCM-41 (Al/Si = 0.17) (measured in terms of the surface area) is shown in Fig. 2.3.3.8.

From the above results, following important observations could be made:

The thermal treatment to both the $AlCl_3$-grafted Si-MCM-41 samples at 400^oC in N_2 or at 500^oC in air causes a transformation of octahedral Al into tetrahedral Al to an appreciable extent (Table 2.3.3.1). However, at the higher temperature (800^oC) no

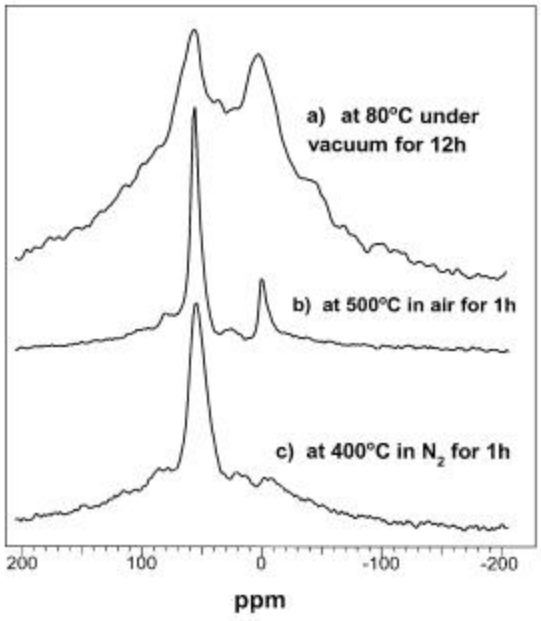

Fig. 2.3.3.6 ^{27}Al MAS NMR of the $AlCl_3$-grafted Si-MCM-41 (with Al/Si bulk ratio of 0.06) thermally treated under different conditions.

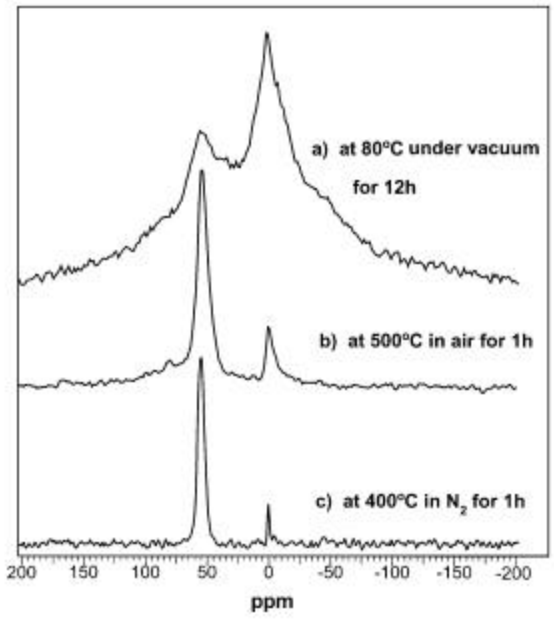

Fig. 2.3.3.7 ^{27}Al MAS NMR of the $AlCl_3$-grafted Si-MCM-41 (with Al/Si bulk ratio of 0.17) thermally treated under different conditions.

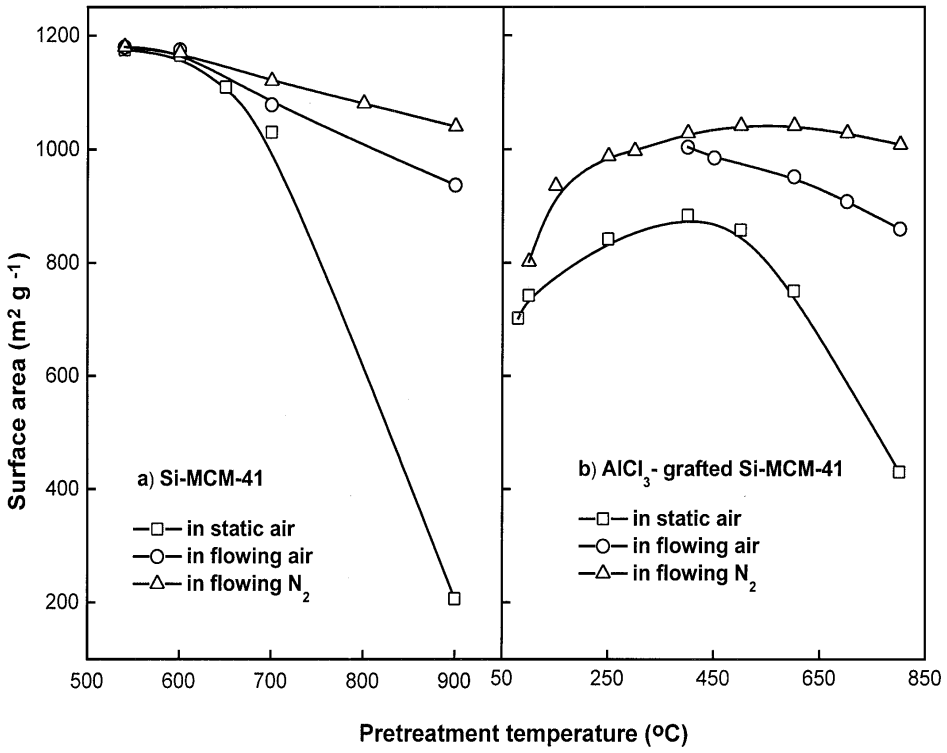

Fig. 2.3.3.8 Thermal stability of a) Si-MCM-41 and b) $AlCl_3$-grafted Si-MCM-41 (with Al/Si = 0.17) (thermal treatment under different gas atmospheres carried for 1h.

presence of tetrahedral Al is observed. The thermal treatment at 800°C (under N_2 flow) does not affect significantly the surface area but it transforms all the tetrahedral Al present in the $AlCl_3$-grafted Si-MCM-41 into octahedral Al, mostly in the form of Al_2O_3. The strong acidity, which is expected due to the presence of tetrahedral Al in zeolites[11,12] is quite consistent with the changes in the tetrahedral Al caused by the thermal treatments.

With the increase in the treatment temperature, both the bulk and surface Cl/Al ratios of the $AlCl_3$-grafted Si-MCM-41 are decreased (Table 2.3.3.1); the decrease being more pronounced in the presence of air. This is expected because of the further reaction of $AlCl_x$–species with surface hydroxyls or with the oxygen from

air, leading to the formation of AlO_x species during the thermal treatment. Also, after the high temperature (800°C) treatment, the surface Al/Si ratio is reduced drastically, indicating the migration of AlO_x species from the external surface to the mesoporous channels of the MCM-41 during the thermal treatment.

The Si-MCM-41 with or without $AlCl_3$-grafting shows the highest thermal stability in the presence of flowing N_2 and the lowest thermal stability in static air (Fig. 2.3.3.8). The observed increase in the surface area with increasing the temperature in the presence of flowing N_2 (Fig. 2.3.3.8b) is expected because of the removal of adsorbed water from the $AlCl_3$-grafted Si-MCM-41 at the higher temperatures. The presence of oxygen, particularly when it is accompanied by moisture (which is the case when the thermal treatment is given under static air), during the thermal treatment at higher temperatures (above 600°C) is detrimental to both the $AlCl_3$-grafted Si-MCM-41 and parent Si-MCM-41.

2.3.3.3 Conclusions

The surface and bulk composition (Al/Si and Cl/Al ratios) and relative concentratios of tetrahedral and octahedral Al in the $AlCl_3$-grafted Si-MCM-41 depend strongly upon the concentration of $AlCl_3$, relative to Si-MCM-41, used in the grafting. These compositional properties, and the acidity and surface area (or stability) of the $AlCl_3$-grafted Si-MCM-41 are strongly influenced by the thermal treatment conditions (viz. temperature and gas atmosphere). The thermal treatment to the $AlCl_3$-grafted Si-MCM-41, particularly at 400°C in a flow of N_2, results in the incorporation of tetrahedral Al in the MCM-41, creating strong acid sites.

2.3.3.4 References

1. Krzywicki, A.; Marczewski, M., *J. Chem. Soc., Faraday Trans.*, **76** (1980) 1311.
2. Drago, R. S.; Getty, E. E., *J. Am. Chem. Soc.* **110** (1988) 3311.
3. Getty, E. E.; Drago, R. S.; *Inorg. Chem.* **29** (1990) 1186.
4. Clark, J. H., Martin, K., Teasdale, A. J., and Barlow, J., *J. Chem. Soc., Chem. Commun.* (1995) 2037.
5. Clark, J. H.; Price, P. M.; Martin, K.; Macquarrie, D. J.; Bastock, T. W., *J. Chem. Res. (S)*, (1997) 430.
6. Price, P. M.; Clark, J. H.; Martin, K.; Macquarrie, D. J.; Bastock, T. W., *Organic Process Research & Development*, **2** (1998) 221.
7. Jun, S.; Ryoo, R., *J. Catal*. **195** (2000) 237.
8. Hu, X.; Foo, M. L.; Chuah, G. K.; Jaenicke, S., *J. Catal.*, **195** (2000) 412.
9. Chen, J., Li, Q., Xu, R., and Xiao, F., *Angew. Chem., Int. Ed. Engl.* **34**, (1995) 2694.
10. Jentys, A.; Phan, N. H.; Vinek, H., *J. Chem. Soc., Faraday Trans*., **92** (1996) 3287.
11. Haag, W. O.; Lago, R. M.; Weisz, P. B., *Nature (London)* **309** (1984) 589.
12. Weisz, P. B., *Ind. Eng. Chem. Fund.*, **25** (1986) 53.

APPENDIX

Appendix 1 Langmuir plots (p/q_r vs. p) for the adsorption of benzene on Si-MCM-41 at different temperatures.

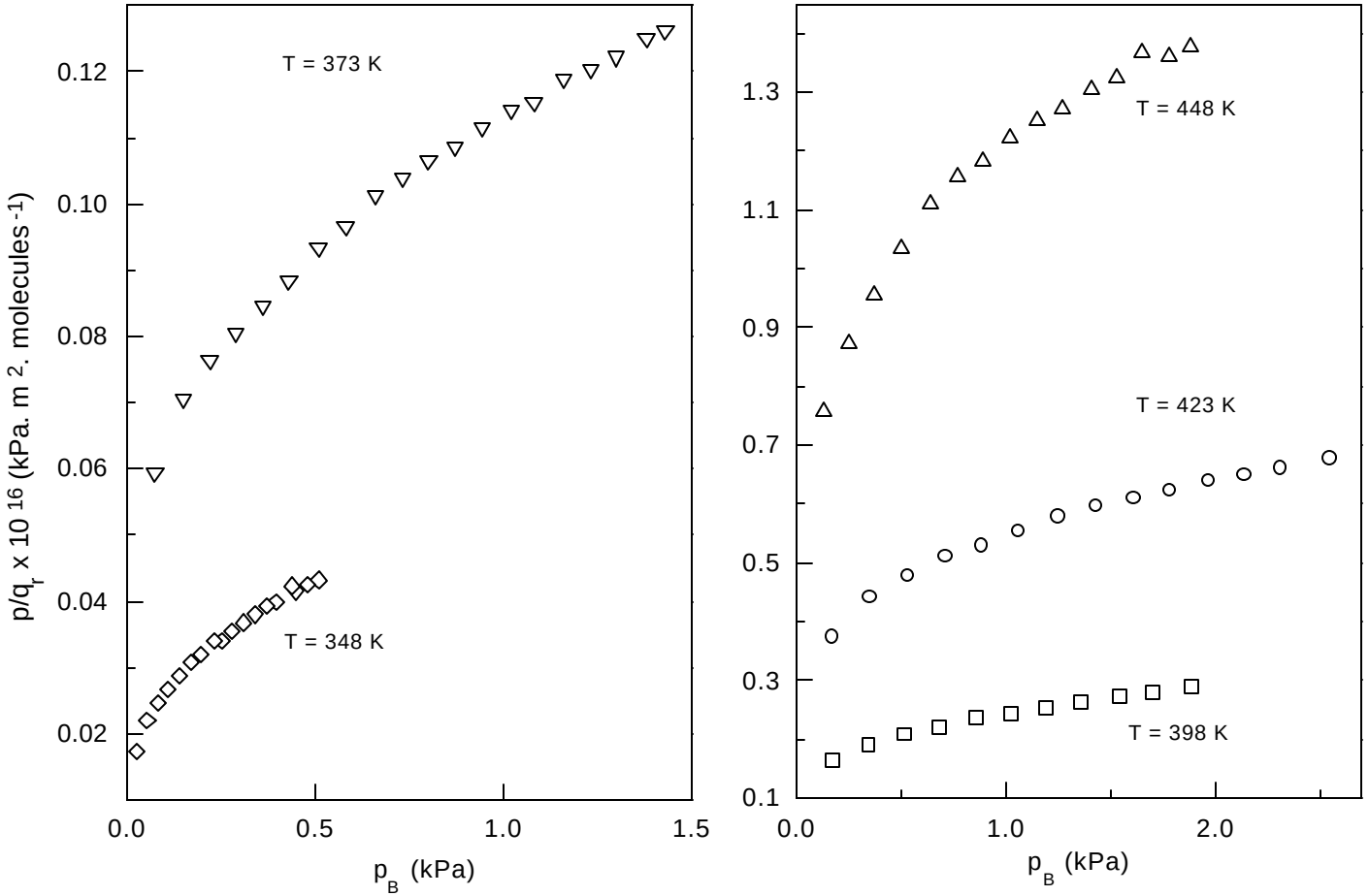

Appendix 2 Langmuir plots (p/q_r vs. p) for the adsorption of toluene on Si-MCM-41 at different temperatures

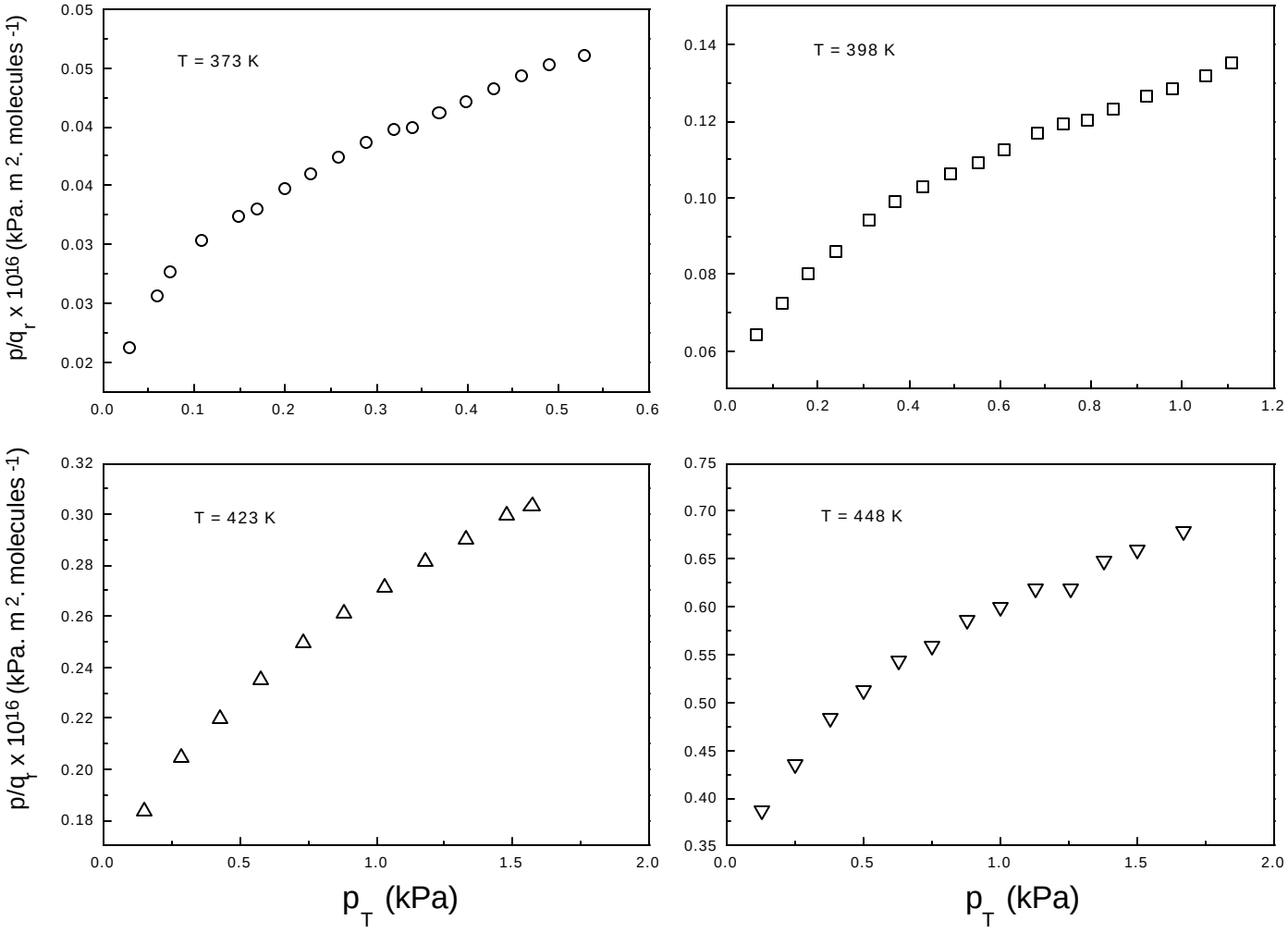

Appendix 3 Langmuir plots (p/q_r vs. p) for the adsorption of p-xylene on Si-MCM-41 at different temperatures.

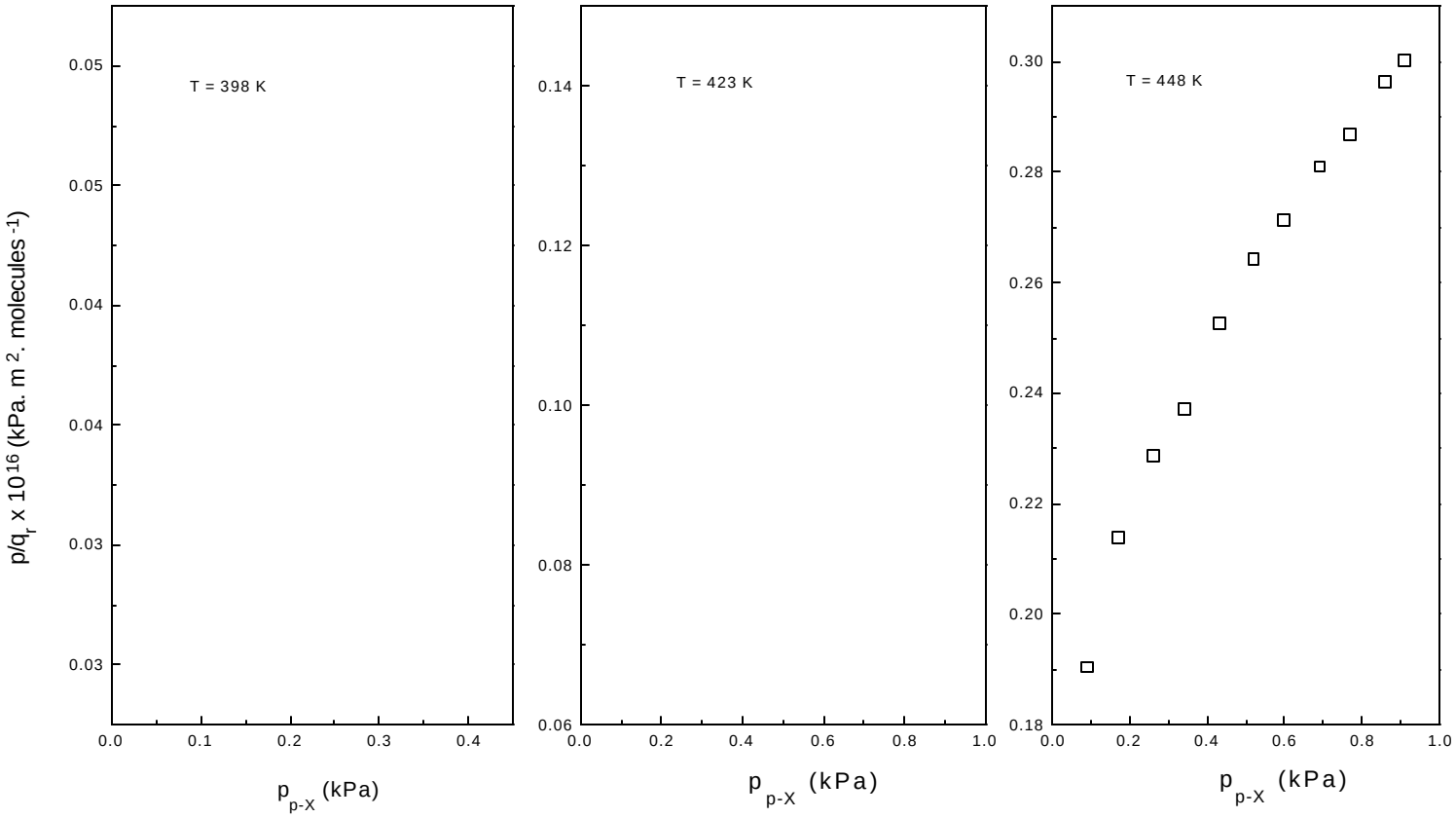

Appendix 4 Langmuir plots (p/q_r vs. p) for the adsorption of mesitylene on Si-MCM-41 at different temperatures.

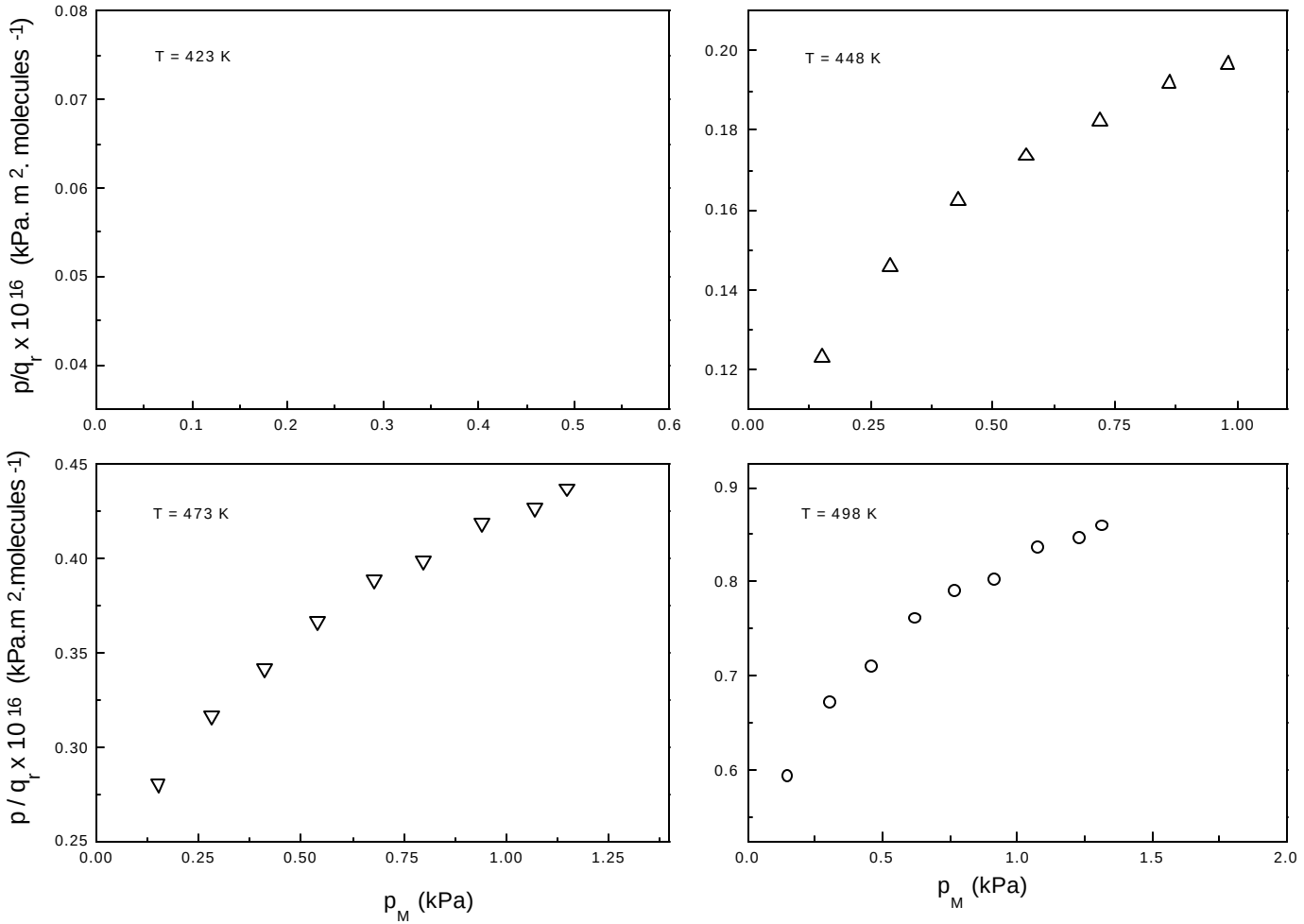

Suggestions for Further Studies

Further studies on the adsorption of aromatic hydrocarbons and other bulky compounds on modified MCM-41 may be carried out. The adsorption/separation of aromatic hydrocarbons from wastewater can be explored since this material possesses high surface area, high pore volume and narrow pore size distribution. Its applicability can also be explored for gas storage. The suitable modification and development of MCM-41 for gas storage can prove a breakthrough for solving the emission problem during the "cold start" in the automobiles. Modification of Si-MCM-41 could be done by several methods, particularly grafting using different metal chlorides that can impart several desirable characteristics to carryout various organic reactions. Grafting of MCM-41 by $GaCl_3$ $InCl_3$, $FeCl_3$, $ZnCl_2$ VCl_4, $TiCl_4$ etc. can be suitably utilized for producing highly active/selective catalysts, useful for the synthesis of various industrially important fine chemicals.

MCM-41 has tremendous potential for both as adsorbents and as catalysts (particularly for larger molecules) through suitable modification. Some applicability of this material as adsorbent and as catalyst has been explored in this thesis. But its potential as adsorbent and catalyst (after its modification) is not yet fully explored.

LIST OF PUBLICATIONS

PUBLICATIONS BASED ON THE WORK REPORTED IN THE THESIS

1. Temperature Programmed Desorption of Benzene on Mesoporous Si-MCM-41, Na.Al-Si-MCM-41 and H.Al-Si-MCM-41

   V. R. Choudhary and **K. Mantri**

   Langmuir, 16 (2000) 8024.

2. Adsorption of Aromatic Hydrocarbons on Highly Siliceous Si-MCM-41

   V. R. Choudhary and **K. Mantri**

   Langmuir, 16 (2000) 7031.

3. Temperature Programmed Desorption of Toluene, p-Xylene, Mesitylene and Naphthalene on Si-MCM-41 Molecular Sieve for Characterizing its Surface Properties and Measuring Heats of Adsorption

   V. R. Choudhary and **K. Mantri**

   Microporous and Mesoporous Mater. 40 (2000) 127.

4. Temperature Programmed Desorption of Toluene, p-Xylene, Mesitylene and Naphthalene on Na-AlSi-MCM-41 and H-AlSi-MCM-41

   V. R. Choudhary and **K. Mantri**

   Microporous and Mesoporous Mater., 46 (2001) 47.

5. Highly Selective Si-MCM-41 Supported $InCl_3$, $GaCl_3$, $FeCl_3$ and $ZnCl_2$ Catalysts for Low Temperature Esterification of tert-Butanol by Acetic Anhydride

   V. R. Choudhary, **K. Mantri** and S. K. Jana

   Microporous Mesoporous Mater., (in press).

6. Grafting of $AlCl_3$ on Si-MCM-41 for Benzylation and Benzoylation of Aromatic Compounds

   V. R. Choudhary and **K. Mantri**

   Catal. Commun. (communicated)

7. $AlCl_3$-grafted Si-MCM-41: Influence of Thermal Treatment Conditions on Surface Properties and Incorporation of Al in the Structure of MCM-41

   V. R. Choudhary and **K. Mantri**

   J. Catal. (communicated)

8. Temperature Programmed Desorption of Benzene on Highly Siliceous MCM-41

   K. Mantri and V. R. Choudhary

Golden Jubilee Catalysis Conference, NCL, Pune, January, 19-21 (1999)

9. Temperature Programmed Desorption of Aromatic Hydrocarbons on Mesoporous MCM-41.

   K. Mantri and V. R. Choudhary

   Catworkshop 2000, IICT, Hyderabad, 7-8 January (2000)**.**

10. Esterification of *tert*-Butanol with Acetic Anhydride using Si-MCM-41 Supported $InCl_3$, $GaCl_3$, $ZnCl_2$ and $FeCl_3$ Catalysts

    S. K. Jana, **K. Mantri** and V. R. Choudhary,

    15th Indian Natl. Symp. Catal. (CATSYMP-15) & 2nd Conf Indo-Pacific Catal. Association (IPCAT-2), NCL, Pune, 23-25 Jan. (2001).

PATENT FILED

A Process for the Selective Esterification of *tert*-Alcohol by an Acid Anhydride using a Reusable Solid Catalyst.

V. R. Choudhary, **K. Mantri** and Suman K. Jana (applied for U.S. and Indian patent).

PUBLICATIONS BASED ON THE WORK OTHER THAN THESIS

1. Factors Influencing Deactivation due to Coking of Ga/H-ZSM-5 Zeolite Catalyst in Propane Aromatization.

   K. Mantri, A. K. Kinage, C. Sivadinarayana and V. R. Choudhary

   Recent Trends in Catalysis, Eds. V. Murugesan; B. Arabindoo and M. Palanichamy, (1999) 389.

2. Influence of Various Catalyst Factors on Time-on-Stream Activity of Ga/H-ZSM-5 in Propane Aromatization

   V. R. Choudhary, **K. Mantri** and C. Sivadinarayana

   Ind. J. Chem. Tech. 6 (1999) 166.

3. Influence of Catalyst Binder on the Acidity and Activity/Selectivity of Ga/H-ZSM-5 in Propane aromatization.

   V. R. Choudhary, C. Sivadinarayana and **K. Mantri**

   *Proc. Ind. Acad. Sci. (Chem. Sci.)***,** 111 (1999) 615.

4. Influence of Zeolite Factors Affecting Zeolitic Acidity on the Propane Aromatization Activity and Selectivity of Ga/H-ZSM-5.

   V. R. Choudhary, **K. Mantri** and C. Sivadinarayana

   Microporous and Mesoporous Mater., 37 (2000) 1.

5. Selective Esterification of tert-Butanol by Acetic Acid Anhydride over Clay Supported $InCl_3$, $GaCl_3$, $FeCl_3$ and $ZnCl_2$ Catalysts

   V. R. Choudhary**, K. Mantri** and S. K. Jana

   Catal. Commun., 2 (2001) 57.

6. Factors Influencing Deactivation due to Coking of Ga/H-ZSM-5 Zeolite Catalyst in Propane Aromatization.

   K. Mantri, Anil K. Kinage, C. Sivadinarayana and V. R. Choudhary

   14th National Symp. on Catal., CATSYMP-98, Chennai, Dec. 16-18, (1998)**.**

7. Clayzic benzylation catalyst: role of calcination of $ZnCl_2$ impregnated Mont-K10 for the catalyst activation

   V. R. Choudhary and **Ksudiram Mantri**, ***J. Catal.*** (communicated)

8. Grafting of $GaCl_3$ on Si-MCM-41 for benzylation and benzoylation reaction of aromatic compounds

   V. R. Choudhary and **Ksudiram Mantri**, (manuscript under preparation)

9. $FeCl_3$-impregnated Mont-K10 benzylation catalyst: role of calcination of $FeCl_3$ for the catalyst activation

   V. R. Choudhary and **Ksudiram Mantri**, (manuscript under preparation)

PART–II

MCM-41 AS CATALYST AND/OR CATALYST SUPPORT

Chapter 2.1

GENERAL INTRODUCTION – LITERATURE SURVEY, OBJECTIVES AND SCOPE

Chapter 2.1

GENERAL INTRODUCTION – LITERATURE SURVEY, OBJECTIVES AND SCOPE

2.1.1 MODIFICATION OF SILICEOUS MCM-41

Pure siliceous MCM-41 (Si-MCM-41) mesoporous materials are electrically neutral, which limits their catalytic applications. In order to provide a specific catalytic activity to the chemically inert silicate framework, researchers have incorporated, in addition to Al, a variety of metals into the walls of nanostructures by either direct synthesis, ion exchange, impregnation or grafting.

2.1.1.1 Incorporation of Heteroatoms by Direct Synthesis

Trivalent cations like Al^{3+}, B^{3+}, Ga^{3+} and Fe^{3+} [1-7] can be substituted for silicon in the framework of MCM-41. The framework possesses negative charges, after substitution of silicon by trivalent cations, can be compensated by protons providing acid sites. The number of acid sites and strengths depend upon the amount and nature of the incorporated metal ions. These type of materials having acidic properties have great applications in petroleum refining processes.[8,9] After the isomorphous substitution of Si by Ti^{4+}, V^{4+}, Zr^{4+} etc.[10-14] in MCM-41, the corresponding mesoporous materials have great application in the oxidation of organic compounds.

2.1.1.2 Impregnation of Heteroatoms

Certain reactions such as aromatization and hydroisomerization are carried out on bi-functional catalysts possessing acid functionality of the molecular sieves and the hydrogenation-dehydrogenation property of the metal impregnated on the surface of

the molecular sieves. Such catalysts are prepared usually by impregnating/loading the metal (Ni, Co, Pt, Pd, W, Ga etc.) by impregnation method.

Cs impregnated MCM-41 has been reported to be a good basic catalyst for Michael addition of diethylmalonate to neopentyl glycol diacrylate and high regio selectivity was obtained in contrast to bulk cesium oxide.[15] It has been reported that sulfided Co and Mo impregnated Al-MCM-41 catalyst show higher hydrogenation and hydrocracking activities than Co-Mo/Al_2O_3 catalysts.[16] Pt impregnated MCM-41 has been used for naphthalene hydrogenation.[17]

2.1.1.3 Covalent Grafting of Heteroatoms

Variable pore diameters, large surface area materials, including amorphous metal oxides or crystalline silicate and aluminosilicate zeolites, have a long and successful history as supports in catalysis and as adsorbents in separations. Due to their smaller pore size, zeolites present some limitations for the large size compounds. Large pore (2.0 - 10.0 nm) MCM materials can now bridge the gap between the crystalline microporous zeolite to the open amorphous supports. Thus, coupling agents with small or bulky functional groups can be grafted to MCM materials while still leaving enough pore volume for chemical reactions to occur freely in the channels of MCM-41.

The versatility of the MCM materials for surface chemistry was recognized in number of papers and patents.[18,19] It has been reported that different types of terminal silanol groups, which can be functionalized by organic groups, are present in the mesoporous channels of MCM materials.[20-24] This is normally achieved through attachment of silane-coupling agents to the mesoporous walls of previously synthesized and calcined materials.[19] The silanol groups of the mesoporous supports can be functionalized by their reaction with transition metal halides, hydrides,

alkoxides, or acetates.[20-23] Surface silanol groups are very prone to react directly with the active metal species. Mesoporous materials anchored with Al-isopropoxide, $AlCl_3$, $SnCl_2$, $Zn(CH_3COO)_2$ or $Mn(CH_3COO)_2$ have high stability and catalytic activity and also ion exchange capacity.[25-29]

Aluminium chloride (an important Lewis acid catalyst) could be immobilized by its grafting on the surface of inorganic solids.[30-35] Recently, there has been a lot of research efforts focusing on the modification of purely siliceous MCM-41 via post-synthesis / covalent grafting of heteroatoms to generate materials with active sites on the inner walls of the well-ordered mesoporous framework.[25,27,36-38] The heteroatoms grafting is possible due to the presence of a high density of silanol groups[20,21] in the amorphous walls of MCM-41. Silanol groups can act as anchors for the attachment of guest species via intermolecular condensation. The post-synthesis / grafting of Al on Si-MCM-41 (using aluminium isopropoxide) has thoroughly been studied by Mokaya et al.[25,27,36,39] Al-grafted MCM-41 materials were prepared at a high Al content via aqueous or non-aqueous method,[39] using aluminum chlorohydrate or aluminum isopropoxide as Al source, respectively. In non-aqueous method dry hexane was used as a solvent. Very recently, Jun et al.[28] and Hu et al.[29] have reported the grafting of anhydrous $AlCl_3$ on Si-MCM-41 using absolute ethanol and dry benzene, respectively as solvent. The resulting catalysts showed good catalytic activity for Friedel-Crafts alkylation reactions.

One of the first examples of the deposition of active metal oxide sites on MCM-41 through the fixation of organometallic complexes on inside walls of MCM-41 was reported by Maschmeyer et al.[37] Treatment of MCM-41 with a solution of $[(C_5H_5)_2TiCl_2]$ in the presence of NEt_3 anchored the titanocene complex through oxygen atoms on the pore walls. The cyclopentadienyl ligand was removed by

calcination under a stream of O_2 and generated an epoxidation catalyst. The resulting catalyst showed good catalytic activity. Similarly, vanadium-grafted[40] and manganese-grafted[41] MCM-41 materials were derived and evaluated for their performance as oxidation catalysts.

Thomas and co-workers[42] reported the surface anchoring of the cobalt complex $[Co_3(\mu 3\text{-}O)(OAc)_5(\mu 2\text{-}OH)(py)_3]PF_6$. The resulting hybrid catalyst was studied in the oxidation of cyclohexane to cyclohexanone and cyclohexanol, and its structure was elucidated with in situ EXAFS spectroscopy.

For high dispersion of active species, a new methodology, termed as vapor grafting, was developed by Ying and Mehnert.[43] Using volatile organometallic precursors, it was possible to deposit active species in a highly dispersed and uniform fashion throughout the entire porous system of MCM-41. The Pd-grafted MCM-41 materials[38] was prepared by vacuum sublimation of $[CpPd(\eta^3\text{-}C_3H_5)]$ through the mesopore channels of MCM-41, followed by reduction under H_2. This catalyst was used as Heck catalysts for carbon - carbon coupling reaction. The highly dispersed Pd-grafted catalyst is highly effective and selective for bulky substrates and provided a less expensive and more thermally robust alternative to homogeneous Pd-complexes.

Liu et al.[44] reported an early example for the anchoring of an organometallic complex onto the porous walls of AlSi-MCM-41. They treated ion-exchanged MCM-41 with phenanthrolineiron(II) chloride and were able to immobilize the complex. The resulting material was used as oxidation catalyst for the oxidation of phenol with H_2O_2. Liu et al.[45] also reported the encapsulation of ruthenium porphyrins in modified MCM-41. In this work, the MCM-41 was treated with 3-aminopropyltriethoxysilane to provide a two electron donor anchor (NH_2 group) to

which the ruthenium porphyrin was attached. The resulting catalyst was investigated for the oxidation of olefins, giving turnover numbers that were 20-40 times higher than that for the free porphyrin.

The preparation of methylalumoxane (MAO) grafted MCM-41 for use as support for catalysts in Ziegler - Natta polymerization was reported by two different groups.[46,47] In the catalyst preparation by Tudor and O'Hare,[47] dehydrated MCM-41 material was first treated with an excess of MAO, and then with the chiral polymerization catalyst *rac*-ethenebis(indenyl)zirconium dichloride. It was found that the polypropylene produced by the resulting catalyst was fourfold higher in number averaged molecular weight and has higher isotacticity and melting point than that produced by the homogeneous catalyst.

An alternative approach in the fixation of polymerization catalysts has been developed by immobilizing zirconocene complexes that have modified cyclopentadienyl ligands through anchoring the zirconocene complexes[43] with siloxy groups present onto the walls of MCM-41. This catalyst showed remarkable reactivity for ethylene polymerization but low activity was observed for propylene polymerization.

2.1.1.4 Catalytic Applications

Because of the high surface area and porosity of MCM-41, they can be used as adsorbents for adsorption/separation, catalysts and supports for acid, base and redox catalysts including transition metal complexes. To date several mesoporous metallosilicates with significant catalytic properties have been synthesized. Some of the important reactions studied on different metallosilicate MCM-41 materials are listed in Table 2.1.1.

Table 2.1.1 Summary of the reaction studied earlier on the mesoporous MCM-41.

No.	Catalyst	Reaction	Reference
1	Al-MCM-41	n-heptane cracking	48
2	H-MCM-41	Alkylation of leucrose, isomaltulose and lactulose disaccharides	49
3	H-MCM-41	Aromatic acylation of 1-naphthol with 2,6-dimethylbenzoic acid	50
4	Zn-exchanged MCM-41	Aromatic acylation	51
5	Al-MCM-41	Cracking of n-heptane, polyethylene and vacuum gas oil	52, 53
6	Al-MCM-41	n-C-16 cracking	54
7	Al-MCM-41	Gas phase tert-butylation of phenol by tert-butyl alcohol	55,56
8	Pt/MCM-41	Hydrodesulfurization of thiophene	57
9	Pt/MCM-41	Hydrocracking and hydroisomerization process to convert wax feeds to high viscosity index lubricants	58
10	Pt/MCM-41	Hydrogenation of aromatics in diesel fuels	59
11	Al-MCM-41	Fine Chemicals synthesis by Friedel-Crafts alkylations and acylations	60-64
12	Al (Al-alkoxide) grafted Si-MCM-41	Cumene cracking	36
13	Al-MCM-41	Friedel-Crafts acylation of aromatics	65
14	Na^+, Cs^+ Al-MCM-41	Knoevenagel condensation of benzaldehyde with ethyl cynoacetate	66
15	Tetraalkylammonium hydroxide grafted-MCM-41	Knoevenagel condensations, Michael additions and aldol condensations	67

16	CsLa-oxide supported MCM-41	Michael addition of diethyl malonate to neopentyl glycol diacrylate; and isomerization of omega phenylalkanals to phenyl alkyl ketones	68,69
17	Ti-MCM-41 and Ti-HMS	Epoxidation of I-hexene using H_2O_2, epoxidation of norbornene using TBHP as oxidant	11
18	Ti-MCM-41, Ti-HMS and V-HMS	Oxidation of phenol and 2,6-di-tert-butyl phenol using H_2O_2 as oxidant	70-72
19	Cr-MCM-41	Oxidation of phenol, 1-naphthol, and aniline using H_2O_2 as oxidant	73
20	V-MCM-41	Selective oxidation of alkanes to ketones	40
21	$[Mn(bpy)_2]2+$ immobilized Al-MCM-41	Oxidation of styrene by iodosyl benzene	74
22	Ti, V, Cr, Mn, Fe, or Co containing MCM-41	Liquid phase oxidation of cyclohexane	75
23	Ti-MCM-41	Oxidation of aromatics and alcohols and epoxidation of olefins	76
24	Iron(II)-8-quinolinol/MCM-41	Phenol hydroxylation with H_2O_2	77
25	Mo-, Co-MCM-41	Oxidation of cyclooctene and aniline with aq. H_2O_2 or TBHP	78
26	Cr-MCM-41	Oxidation of 2-methylnaphthalene to 2-methylnaphthoic acid	79
27	Titanium oxide grafted MCM-41	Photo bleaching of rhodamine-6G and oxidation of α-terpineol	80
28	$[Co_3(\mu 3\text{-}O)(OAc)_5(\mu 2\text{-}OH)(py)_3]PF_6$ immobilizedMCM-41	Production of cyclohexanone from cyclohexane	42
29	Cu and Fe phthalocya-nine-MCM-41	Oxidation of n-hexane using TBHP as oxidant	81
30	$H_3PW_{12}O_{40}$/ MCM-41	Alkylation of 4-tert-butyl phenol with isobutene	82,83
31	Mo-MCM-41	Cyclohexanol and cyclohexane oxidation reactions with H_2O_2 as oxidant	84

32	Al-MCM-41 and zeolites as FCC catalysts	Comparable cracking activities for long-chain Hydrocarbons and bulky hydrocarbon molecules	85
33	Al-MCM-41 and supported MCM-41 (Review)	Various catalytic activities (cracking, hydrocracking, acidic, basic and redox reactions)	86
34	MCM-41-grafted Al-isopropoxide	Meerwein-Ponndorf-Verley reductions of ketones	87
35	Metal ion-planted MCM-41 (e.g., Mn-MCM-41)	Epoxidation of stilbene and its derivatives with tert-butyl hydroperoxide	88
36	AlSi-MCM-41 (Si/Al = 12 - 72)	Diels-Alder reaction of isoprene with different dienophiles	89
37	Transition metal incorporated MCM-41	Oxidation of cholesterol	90
38	Cu-MCM-41	Liquid phase oxidation of benzene	91
39	Co-Mo MCM-41	Hydrodesulfurization of petroleum residues	92
40	Fe^{3+} exchanged Al-HMS and Al-MCM-41	Catalytic reduction of NO with NH_3	93
41	CVD of gold nano particles on MCM-41	Low temperature oxidation of CO and H_2	94
42	Ti-substituted and Ti-grafted MCM-41	Cyclohexene oxidation with aq. H_2O_2 and tert-Butyl hydro peroxide	95
43	H-MCM-41 and H-FSM-16	vapor-phase Beckmann rearrangement of cyclohexanone oxime	96
44	Ti-MCM-41 and Ti-MCM-48	Oxidation of alkanes and alkenes	97
45	V-MCM-41 and V-MFI	Toluene gas phase oxidation to benzaldehyde and phenol	98
46	Gold deposited on titanium-based MCM-41 and other oxides	Selective oxidation of propylene	99
47	Chiral Mn (III) salen complex grafted Si-MCM-41	Epoxidation of styrene and α-methyl styrene	100, 101
48	V-MCM-41	Oxidation of benzene with H_2O_2 to phenol	102

49	Cu-ion exchanged Al-MCM-41	Selective catalytic reduction of NO with ethylene	103
50	Sn-MCM-41	Selective oxidation/epoxidation of organic compounds by aq. H_2O_2/TBHP	104
51	V-MCM-41	Oxidation of toluene and hydroxylation of benzene with H_2O_2	105
52	Perfluorinated-Ru-phthalocyanine immobilized MCM-41	Oxidation of n-hexane and cyclohexane with TBHP	106
53	Cu^{2+}-phthalocyanine and Co^{2+}-perfluoro-phthalocyanine incorporated MCM-41	Oxidation of cyclohexane	107
54	Pt/AlSi-MCM-41 (Si/Al =14 - 86)	Aromatization of cyclohexane	108
55	Au deposited on Ti-MCM-41	Epoxidation of propylene and selective oxidation of propane to acetone and of isobutane to t-butanol with a H_2-O_2 mixture under flow	109
56	Dimeric μ-oxo iron tetrasulfophthalocyanine grafted onto amino-modified silica or MCM-41	Oxidation of 2-methylnaphthalene to 2-methylnaphtho- quinone (vitamin K3) and 2,3,6-trimethylphenol to trimethylbenzoquinone	110
57	Au supported on titanosilicates	Gas phase selective oxidation of propylene to propylene oxide (PO) or propionaldehyde (PA) in the presence of H and O mix.	111
58	Vanadium(V)-supported MCM-41	Liquid-phase oxygenation of benzene	112
59	Fe and Cu complexes-immobilized MCM-41	Oxidation of cyclohexane with aq. H_2O_2	113
60	Ti-MCM-41	Hydrogen peroxide oxidation of methyl α-D-glucopyranoside, sucrose and α, α-trehalose	114
61	Pt and Pd supported MCM-41	Hydrogenation of benzene, naphthalene, phenanthrene and olefins	115-117
62	SAPO-5, SAPO-11, BEA and MCM-41	Oxidative conversion of n-heptane	118
63	V-containing MCM-41	Catalytic hydroxylation of benzene	119

64	Titanium iso-propoxide grafted M41S	Selective oxidation of 2,6-di-tert-butylphenol with H_2O_2	120
65	Cs-modified MCM-41 and MCM-48	Knoevenagel condensation of benzaldehyde with malononitrile or Et cyanoacetate	121
66	Metallophthalocyanines of iron, manganese, and cobalt anchored Si-MCM-41	Liquid phase oxidation of 2-methylnaphthalene and 2,3,6-trimethylphenol with hydrogen peroxide and t-butylhydroperoxide	122
67	Sn-O deposited Si-MCM-41	Reduction of crotonaldehyde to crotyl alcohol using propan-2-ol as the H transfer agent	123
68	VO_x/MCM-41 and VO_x/MCM-48	Partial oxidation of CH_4 to HCHO in air	124
69	Fe-MCM-41	Oxidation of sulfur dioxide to sulfuric acid	125, 126
70	Transition metal complexes encapsulated Y and MCM-41 zeolites	Liquid phase oxidation of 2-methyl naphthalene to 2-Methyl-1,4-Naphthoquinone (vitamin K_3)	127
71	NbMCM-41 modified with NH_4^+ and Cu cations	NO decomposition, reduction of NO with NH_3, hydrosulfurization of methanol, and oxidation. of thioethers with hydrogen peroxide	128
72	Guanidines encapsulated in zeolite Y and anchored to MCM-41	Aldol addition and condensation reactions of benzaldehyde and acetone	129
73	Ti-MCM-41	Epoxidation of alkenes and oxidation of sulfides	130
74	Perruthenate immobilized MCM-41	Clean oxidation of alcohols to carbonyl compounds with mol. oxygen.	131
75	V-MCM-41	Gas phase methanol oxidation	132
76	Pt and tungstophos-phoric acid supported on MCM-41	Reduction of NOx with propene in the presence of water vapor	133, 134
77	Ga_2O_3/Si-MCM-41 and In_2O_3/Si-MCM-41	Friedel-Crafts-type benzylation and acylation reactions in the presence or absence of moisture.	135
78	Cu-Impregnated MCM-41	Liquid-phase oxidation of 2,6-di-tert-butylphenol	136
79	Physically mixed CsCl with Au/Ti-MCM-41	Gas-phase epoxidation of propene using H_2 and O_2	137

80	Cu ion-exchanged Na-MCM-41	Liquid-phase oxidation of 2,6-di-tert-butylphenol.	138
81	Direct syntheses, grafting of the Al species with anhydrous $AlCl_3$ and impregnation with an aq. soln. of $AlCl_3$ on MCM-41	Friedel-Crafts alkylation of benzene, toluene, and m-xylene with benzyl alcohol	28
82	Palladium supported on Si-MCM-41 and Ti-MCM-41	Oxidative carbonylation of CO with Et-nitrite [C_2H_5ONO] to produce di-Et carbonate (DEC) and di-Et oxalate	139
83	MCM-41 doped with Cu ions	One-step process for preparation of phenol comprises oxidation of benzene or an alkyl-substituted benzene with hydrogen peroxide	140

2.1.2 OBJECTIVES AND SCOPE

It is evident from the literature survey that the mesoporous MCM-41 materials have opened up a new opportunities in the field of catalysis. Solid catalysts have been widely used in chemical industries, as they are non-corrosive, eco-friendly, easy to handle and reusable. The presence of large number of terminal Si-OH groups on the external surface or in the mesoporous channels of MCM-41 can immobilize or graft the metal chlorides.

The present Ph.D. work for this part of the thesis was undertaken with the following objectives:

1. To study the esterification of tert-butanol with acetic anhydride and dehydration of tert-butanol over Si-MCM-41 supported $InCl_3$, $GaCl_3$, $FeCl_3$ and $ZnCl_2$ catalysts.
2. To modify Si-MCM-41 by grafting of anhydrous $AlCl_3$ by a liquid phase reaction between anhydrous $AlCl_3$ and terminal Si-OH groups of

Si-MCM-41, study of kinetics of the grafting reaction, and evaluate the catalytic activity of the modified catalyst for the Friedel-Crafts type reaction.

3. To study the influence of thermal treatment conditions on surface properties and incorporation of Al in the structure of MCM-41.

2.1.3 REFERENCES

1. Tuel, A.; Gontier, S., *Chem. Mater.*, **8** (1996) 114.
2. Sayari, A.; Moudrakovaski, I.; Danumah, C.; Ratcliffe, C. I.; Ripemeester, J. A.; Preston, K. F., *J. Phys. Chem.*, **99** (1995) 16373.
3. Liu, S.; He, H.; Luan, Z.; Klinowski, J., *J. Chem. Soc., Faraday, Trans.*, **92** (1996) 2011.
4. Cheng, C.-F.; Klinowski, J., *J. Chem. Soc., Faraday Trans.*, **92** (1996) 289.
5. Cheng, C.-F.; He, H.; Zhou, W.; Klinowski, J.; Sousa, G. L. F.; Gladden, L. F.; *J. Phys. Chem.*, **100** (1996) 390.
6. Yuan, Z. Y.; Liu, S. H.; Chen, T. H.; Wang, J. Z.; Li, H. X., *J. Chem. Soc., Chem. Commun.*, (1995) 973.
7. Tuel, A., *Microporous and Mesporous Mater.*, **27** (1999) 151.
8. Casci, J. L., *Stud. Surf. Sci. Catal.*, **85** (1994) 329.
9. Sayari, A., *Chem. Mater.*, **8** (1996) 1840.
10. Kresge, C. T.; Leonowicz, M. E.; Roth, W. J.; and Vertuli, J. C., *U. S. Patent*, **5,250,282** (1993).
11. Corma, A.; Navarro, M. T.; Perez, P. J., *J. Chem. Soc., Chem. Commun.*, (1994) 147.
12. Reddy, K. M.; Moudrakovski, I. L.; Sayari, A., *J. Chem. Soc., Chem. Commun.*, (1994) 1059.
13. Luan, Z.; Xu, J.; He, H.; Klinowski, J.; Kevan, L., *J. Phys. Chem.*, **100** (1996) 19595.
14. Tuel, A.; Gontier, S.; Teissier, R., *J. Chem. Soc., Chem. Commun.*, (1996) 651.
15. Kloestra, K. R.; Bakkum, H.van, *Stud. Surf. Sci. Catal.*, **105A** (1997) 431.
16. Song, S.; Reddy, K. M., *Appl. Catal. A: General*, **176** (1999) 1.
17. Corma, A.; Martinez, A.; Martinez-Soria, V., *J. Catal.*, **148** (1997) 480.
18. Beck, J. S.; Chu, C. T.; Johnson, I. D.; Kresge, C. T.; Leonowicz, M. E.; Roth, W. J.; Vartuli, J. C., *U. S. Patent*, **5,145,816** (1992).
19. Olson, D. H.; Stuky, G. D.; Vartuli, J. C., *U. S. Patent*, **5,364,797** (1994).
20. Chen, J.; Li, Q.; Xu, R.; Xiao, F., *Angew. Chem. Int. Ed. Engl.*, **34** (1995) 2694.
21. Jentys, A.; Pham, N. H.; Vinek, H., *J. Chem. Soc., Faraday Trans.*, **92** (1996) 3287.

22. Mercier, L.; Pinnavaia, T. J., *Adv. Mater.*, **9** (1997) 500.
23. Cauvel, A.; Renard, G.; Brunel, D., *J. Org. Chem.*, **62** (1997) 749.
24. Zhao, X. S.; Lu, G. Q.; Whittaker, A. K.; Millar, G. J.; Zhu, H. Y., *J. Phys. Chem. B*, **101** (1997) 6525.
25. Ryoo, R; Jun, S.; Kim, J. M.; Kim, M. J., *J. Chem. Soc., Chem. Commun*., (1997) 2225.
26. Chen, L. Y.; Ping, Z.; Chuah, G. K.; Jaenicke, S.; Simon, G., *Microporous and Mesoporous Mater*., **27** (1999) 231.
27. Mokaya, R.; Jones, W., *Chem. Commun*., (1997) 2185.
28. Jun, S.; Ryoo, R., *J. Catal*., **195** (2000) 237
29. Hu, X.; Foo, M. L.; Chuah, G. K.; Jaenicke, S., *J. Catal*., **195** (2000) 412
30. Krzywicki, A.; Marczewski, M., *J. Chem. Soc., Faraday Trans.*, **76** (1980) 1311.
31. Drago, R. S.; Getty, E. E., *J. Am. Chem. Soc*., **110** (1988) 3311.
32. Getty, E. E.; Drago, R. S., *Inorg. Chem.*, **29** (1990) 1186.
33. Clark, J. H.; Martin, K.; Teasdale, A. J.; Barlow, J., *J. Chem. Soc., Chem. Commun.*, (1995) 2037.
34. Clark, J. H.; Price, P. M.; Martin, K.; Macquarrie, D. J.; Bastock; T. W., *J. Chem. Res. (S)*, (1997) 430.
35. Price, P. M.; Clark, J. H.; Martin, K.; Macquarrie; D. J.; Bastock, T. W., *Organic Process Research & Development*, **2** (1998) 221.
36. Mokaya, R.; Jones, W., *Phys. Chem. Chem. Phys*., **1** (1999) 207.
37. Maschmeyer, T.; Rey, F.; Sankar, G.; Thomas, J. M., *Nature*, **378** (1995) 159.
38. Mehnert, C. P.; Ying, J. Y., *Chem. Commun*., (1997) 2215.
39. Mokaya, R., *J. Catal*., **186** (1999) 470.
40. Neumann, R.; Khenkin, A. M., *Chem. Commun*. (1996) 2643.
41. Burch, R. Cruise, N.; Gleeson, D.;Tsang, S. C., *Chem. Commun*., (1996) 951.
42. Maschmeyer, T.; Oldroyd, R. D.; Sankar, G.; Thomas, J. M.; Shannon, Ian J.; Klepetko, J. A.; Masters, A. F.; Beattie, James K.; Catlow, C. Richard A., *Angew. Chem., Int. Ed. Engl*., **36** (1997) 1639.
43. Ying, J. Y.; Mehnert, C. P.; Wong, M. S., *Angew. Chem. Int. Ed. Engl.*, **38** (1999) 56.
44. Liu, C.; Ye, X.; Wu, Y., *Catal. Lett*., **36** (1996) 263.
45. Liu, C. -J.; Li, S.-G.; Pang, W.-Q.; Che, C.-M., *Chem. Commun*., (1997) 65.

46. Ko, Y. S.; Han, T. K.; Park, J. W.; Woo, S. I., *Macromol. Rapid Commun.*, **17** (1996) 749.
47. Tudor, J.; O'Hare, D., *Chem. Commun.* (1997) 603.
48. Aufdembrink, B. A.; Chester, A. W.; Herbst, J. A.; Kresge, C. T., *U. S. Patent*, **5,258,114** (1993).
49. de Goede, A. T. J. W.; van der Leij; van der Heijden, A. M.; van Rantwijk, F.; van Bakkum, H., *PCT Int. Appl.*, **WO 96 136640** (1996).
50. Van Bakkum, H.; Hoefnagel, A. J.; van Koten, M. A.; Gunnewegh, E. A.; Vogt, A. H. G.; Kouwenhoven, *Stud. Surf. Sci. Catal.*, **83** (1994) 379.
51. Gunnewegh, E. A.; Gopie, S. S.; van Bakkum, H., *J. Mol. Catal.*, **106** (1996) 151.
52. Aguado, J.; Serrano, D. P.; Romero, M. D.; Escola, J. M., *J. Chem. Soc., Chem. Commun.*, (1996) 725.
53. Corma, A., Grande, M. S.; Gonzalez-Alfero, V.; Orchilles, A. V., *J. Catal.*, **159** (1996) 375.
54. Chen, X. Y.; Huang, L. M.; Ding, G. Z.; Li, Q. Z., *Catal. Lett.*, **44** (1997) 123.
55. Badamali, S. K.; Saktivel, A.; Selvam, P., *Catal. Today*, **63** (2000) 291.
56. Saktivel, A. Badamali, S. K.; Selvam, P., *Microporous and Mesoporous Mater.*, **39** (2000) 457.
57. Sugioka, M.; Morishita, S.; Kurosaka, T.; Seino, A.; Nakagawa, M.; Namba, S., *Stud. Surf. Sci. Catal.*, **125** (1999) 531.
58. Marler, D. O.; Mazzone, D. N., *U. S. Patent*, **5,288,359** (1994).
59. Corma, A.; Martinez, A.; Martinez-Soria, V., *J. Catal.*, **169** (1997) 480.
60. Armengol, E.; Cano, M. L.; Corma, A.; Gracia, H.; Navarro, M. T., *J. Chem. Soc., Chem. Commun.*, (1995) 519.
61. Ermengol, E.; Corma, A.; Garcia, H.; Primo, J., *Appl. Catal. A. General*, **126** (1995) 391.
62. Ermengol, E.; Corma, A.; Garcia, H.; Primo, J., *Appl. Catal. A. General*, **149** (1997) 411.
63. Le, Q. N., *U. S. Patent*, **5,191,134** (1993)
64. Kloestra, K. R.; Van Bekkum, H., *J. Chem. Res (S)* **1** (1995) 26.
65. Spagnol, M.; Gilbert, L.; Alby, D., "The Roots of Organic Development", Desmurs, J. R.; Ratton, S., Eds., *Elsevier: New York* (1996) 29.

66. Kloestra, K. R.; Van Bakkum, H., *J. Chem. Soc., Chem. Commun*., (1995) 1005.

67. Rodriguez, I.; Iborra, S.; Corma, A.; Rey, F.; Jorda, J. L., *Chem. Commun*. (Cambridge), (1999) 593.

68. Kloestra, K. R.; Van Bakkum, H., *Stud. Surf. Sci. Catal*., **105** (1997) 431.

69. Kloestra, K. R.; Van Bakkum, H., *Catal. Lett*., **47** (1997) 235.

70. Reddy, J. S.; Dicko, A.; Sayari, A., *Chem. Ind.*, **69** (1997) 405.

71. Reddy, J. S.; Sayari, A., *J. Chem. Soc., Chem. Commun.*, (1995) 2231.

72. Zhang, W.; Frola, M.; Wang, J.; Tanev, P. T.; Wong, J.; Pinnavaia, T. J., *J. Am. Chem. Soc*., **118** (1996) 9164.

73. Ulagappon, N.; Rao, C. N. R., *J. Chem. Soc., Chem. Commun*., (1996) 1047.

74. Kim, S.-Su; Zhang, W.; Pinnavaia, T.J., *Catal. Lett.*, **43** (1997) 149.

75. Carvalho, W. A.; Varaldo, P. B.; Wallau, Martin; Schuchardt, Ulf, *Zeolites*, **18** (1997), 408.

76. Reddy, J. Sudhakar; Dicko, Awa; Sayari, Abdelhamid, *Chem. Ind*. (Dekker), **69** (1997) 405.

77. Liu, C.; Shan, Y.; Yang, X.; Ye, X.; Wu, Yue, *J. Catal*., **168** (1997) 35.

78. Ayyappan, S.; Ulagappan, N., *Proc. - Indian Acad. Sci., Chem. Sci.*, **108** (1996), 505.

79. Das, T. K.; Chaudhari, K.; Nandanan, E.; Chandwadkar, A.J.; Sudalai, A.; Ravindranathan, T.; Sivasanker, S., *Tetrahedron Lett.*, **38** (1997) 3631.

80. Aronson, B. J.; Blanford, C. F.; Stein, A., *Chem. Mater*., **9** (1997) 2842.

81. Ernst, S.; Glaser, R.; Selle, M., *Stud. Surf. Sci. Catal.*, **105 A** (1997) 69.

82. Kozheunikov, I. V.; Sinnema, A.; Jansen, R. J. J.; Pamin, K.; Van Bakuum, H., *Catal. Lett*., **30** (1995) 241.

83. Kozheunikov, I. V.; Kloestra, K. R.; Sinnema, A.; Zandberzen, H. W.; Van Bakuum, H., *J. Mol. Catal. A*. **114** (1996) 287.

84. Rana, R. K.; Viswanathan, B., *Catal. Lett*., **52** (1998) 25.

85. Koch, H.; Reschetilowski, W., *Microporous and Mesoporous Mater*., **25** (1998) 127.

86. Corma, A.; Kumar, D., *Stud. Surf. Sci. Catal*., **117** (1998) 201.

87. Anwander, R.; Gerstberger, G.; Palm, C.; Groeger, O.; Engelhardt, G., *Chem. Commun.* (1998) 1811.

88. Yonemitsu, M.; Tanaka, Y.; Iwamoto, M., *J. Catal*., **178** (1998) 207.

89. Genske, D.; Bornholdt, K.; Lechert, H., *Stud. Surf. Sci. Catal*., **117** (1998) 421.

90. Vercruysse, K. A.; Klingeleers, D. M.; Colling, T.; Jacobs, P. A., *Stud. Surf. Sci. Catal*., **117** (1998) 469.

91. Okamura, J.; Nishiyama, S.; Tsuruya, S.; Masai, M., *J. Mol. Catal.A: Chem.*, **135** (1998) 133.

92. Reddy, K. M.; Wei, B.; Song, C., *Catal. Today*, **43** (1998) 261.

93. Yang, R. T.; Pinnavaia, T. J.; Li, W.; Zhang, W., *J. Catal*., **172** (1997) 488.

94. Okumura, M.; T., S.; Iwamoto, M.; Haruta, M., *Chem. Lett*., (1998) 315.

95. Chen, L. Y.; Chuah, G. K.; Jaenicke, S., *Catal. Lett.*, **50** (1998) 107.

96. Dai, L.-Xin; Koyama, K.; Tatsumi, T., *Catal. Lett.*, **53** (1998) 211.

97. Tatsumi, T.; Koyano, Keiko A.; Igarashi, N., *Chem. Commun.* (Cambridge), (1998) 325.

98. Centi, G.; Fazzini, F.; Canesson, L.; Tuel, A., *Stud. Surf. Sci. Catal*., **110** (1997) 893.

99. Haruta, M.; Uphade, B. S.; Tsubota, S.; Miyamoto, A., *Res. Chem. Intermed*., **24** (1998) 329.

100. Kim, G.-J.; Shin, Ji-H., *Tetrahedron Lett.*, **40** (1999) 6827

101. Kim, G.-J., *React. Kinet. Catal. Lett.*, **67** (1999) 295.

102. Chen, Yu-W.; Lu, Yi-H., *Ind. Eng. Chem. Res*., **38** (1999) 1893

103. Long, R. Q.; Yang, R. T. *Ind. Eng. Chem. Res.*, **38** (1999) 873

104. Chaudhari, K.; Das, T. K.; Rajmohon, P. R.; Lazar, K.; Sivasanker, S.; Chandwadkar, A. J., *J. Catal*. **183** (1999) 281.

105. Chatterjee, M.; Iwasaki, T.; Hayashi, H.; Onodera, Y.; Ebina, T.; Nagase, T., *Chem. Mater*., **11** (1999) 1368.

106. Ernst, S.; Selle, M., *Microporous and Mesoporous Mater*., **27** (1999) 355.

107. Armengol, E.; Corma, A.; Fornes, V.; Garcia, H.; Primo, J., *Appl. Catal., A*, **181** (1999) 305

108. Chaudhari, K.; Das, T. K.; Chandwadkar, A. J.; Sivasanker, S., *J. Catal.*, **186** (1999) 81

109. Kalvachev, Y. A.; Hayashi, T.; Tsubota, S.; Haruta, M., *J. Catal.*, **186** (1999) 228.

110. Sorokin, A. B.; Tuel, A., *New J. Chem.*, **23** (1999) 473.

111. Uphade, B. S.; Tsubota, S.; Hayashi, T.; Haruta, M., *Chem. Lett*., (1998) 1277.

112. Ishida, M.-aki; M., Y.; Hamada, R.; Nishiyama, S.; Tsuruya, S.; Masai, M., *J. Chem. Soc., Perkin Trans.*, **2** (1999) 847.
113. Carvalho, Wagner Alves; Wallau, Martin; Schuchardt, Ulf. *J. Mol. Catal. A: Chem.*, **144** (1999) 91
114. Mombarg, E. J. M.; Osnabrug, S. J. M.; Van Rantwijk, F.; Van Bekkum, H., *Stud. Surf. Sci. Catal*., **108** (1997) 385.
115. Armor, J. N., *Appl. Catal.*, **112** (1994) N21.
116. Reddy, K. M.; Song, C., *Catal. Today*, **31** (1996) 137.
117. Inui, T.; Kim, J. B.; Seno, M., *Catal. Lett*., **29** (1994) 271.
118. Stoylkova, T. Y.; Chanev, C. D.; Lechert, H. T.; Bezouhanova, C. P., *Appl. Catal., A*, **203** (2000) 121.
119. Lee, C. W.; Lee, W. J.; Park, Y. K.; Park, S.-E., *Catal. Today*, **61** (2000) 137.
120. Kang, K. K.; Byun, C. S.; Ahn, W. S., *Stud. Surf. Sci. Catal*. **129** (2000) 335.
121. Ernst, S.; Bongers, T.; Casel, C.; Munsch, S., *Stud. Surf. Sci. Catal.*, **125** (1999) 367.
122. Sorokin, A. B.; Tuel, A., *Catal. Today*, **57** (2000) 45.
123. Burch, R.; Caps, V.; Gleeson, D.; Nishiyama, S.; Tsang, S. C., *Appl. Catal., A*, **194-195** (2000) 297.
124. Berndt, H.; Martin, A.; Bruckner, A.; Schreier, E.; Muller, D.; Kosslick, H.; Wolf, G.-U.; Lucke, B., *J. Catal.*, **191** (2000) 384.
125. Wingen, A.; Anastasieviec, D.; Hollnagel, A.; Werner, D.; Schuth, F., *Stud. Surf. Sci. Catal*., **130C** (2000) 3065.
126. Wingen, A.; Anastasievic, N.; Hollnagel, A.; Werner, D.; Schuth, F., *J. Catal.*, **193** (2000) 248.
127. Murthy, K. V. V. S. B. S. R.; Srinivas, N.; Kulkarni, S. J.; Raghavan, K. V., *Proc. Int. Zeolite Conf., 12th, Meeting Date 1998*, **2** (1999) 893.
128. Ziolek, M.; Sobczak, I.; Nowak, I.; Decyk, P.; Lewandowska, A.; Kujawa, J., *Microporous and Mesoporous Mater.*, **35-36** (2000) 195.
129. Sercheli, R.; Vargas, R. M.; Sheldon, R. A.; Schuchardt, U., *J. Mol. Catal. A: Chem.*, **148** (1999) 173.
130. Khenkin, A. M.; Neumann, R., *Catal. Lett*., **68** (2000) 109.
131. Bleloch, A.; Johnson, B. F. G.; Ley, S. V.; Price, A. J.; Shephard, D. S.; Thomas, A. W., *Chem. Commun*. (Cambridge), (1999) 1907.

132. Lim, S.; Haller, G. L., *Appl. Catal., A*, **188** (1999) 277.

133. Jentys, A.; Schiesser, W.; Vinek, H., *Catal. Today*, **59** (2000) 313.

134. Jentys, A.; Schiesser, W.; Vinek, H., *Stud. Surf. Sci. Catal*., **130B** (2000) 1523.

135. Choudhary, V. R.; Jana, S. K.; Kiran, B. P., *J. Catal*., **192** (2000) 257

136. Fujiyama, H.; Kohara, I.; Iwai, K.; Nishiyama, S.; Tsuruya, S.; Masai, M., *J. Catal*., **188** (1999) 417

137. Uphade, B. S.; Okumura, M.; Tsubota, S.; Haruta, M., *Appl. Catal., A*, **190** (2000) 43.

138. Kohara, I.; Fujiyama, H.; Iwai, K.; Nishiyama, S.; Tsuruya, S., *J. Mol. Catal. A: Chem*., **153** (2000) 93.

139. Zhen, Jiang Xuan; Hua, Su Yue; Hua, Chien Shu., *Catal. Lett*., **69** (2000) 153.

140. Cheng, S.; Chou, B., *U.S. patent*, **61,80836** (2001) 10 pp.